Chapter 6

Membrane Physiology

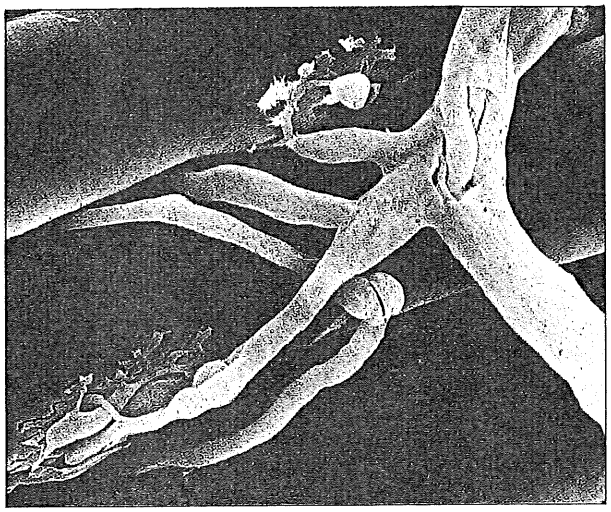

Scanning electron micrograph of a motor nerve and two end-plates on adjacent muscle fibers. *(Photo courtesy of D. W. Fawcett/Desaki & Venara/ Photo Researchers, Inc.)*

Chapter Outline

The **plasma membrane** is the interface between the internal cytoplasmic environment and the extracellular environment. This cell membrane must limit the exchange of many solutes, often against immense concentration gradients that favor exchange between the cytoplasm and external medium. At the same time, it must allow ready transport of many nutrients and waste products into and out of the cell; consequently, there are often specific membrane transport systems for passive or active exchange.

Cells have a complex internal system of interconnected membrane spaces, membrane-bound vesicles, and organelles (Figure 6–1). Mitochondria and lysosomes are examples of membrane-bound organelles. In fact, most of the total membrane content of a cell is intracellular, not the surface plasma membrane. For example, a single liver cell of a rat (Weiner et al. 1968) has an approximate surface area of 2000 μ^2 and volume of 5100 μ^3. The 1100 or so mitochondria make up 20% of the cytoplasmic volume (995 μ^3) and have membrane areas of 7470 μ^2 (outer membrane) and 39600 μ^2 (inner membrane). Endoplasmic reticulum also has an extensive surface area of 17000 μ^2 (smooth ER) and 30400 μ^2 (rough ER). The nucleus is about 4% of the cellular volume and has a surface area of about 200 μ^2.

The functions of the membranous structures in a typical animal cell include protein synthesis, transport, formation of storage vesicles, release of

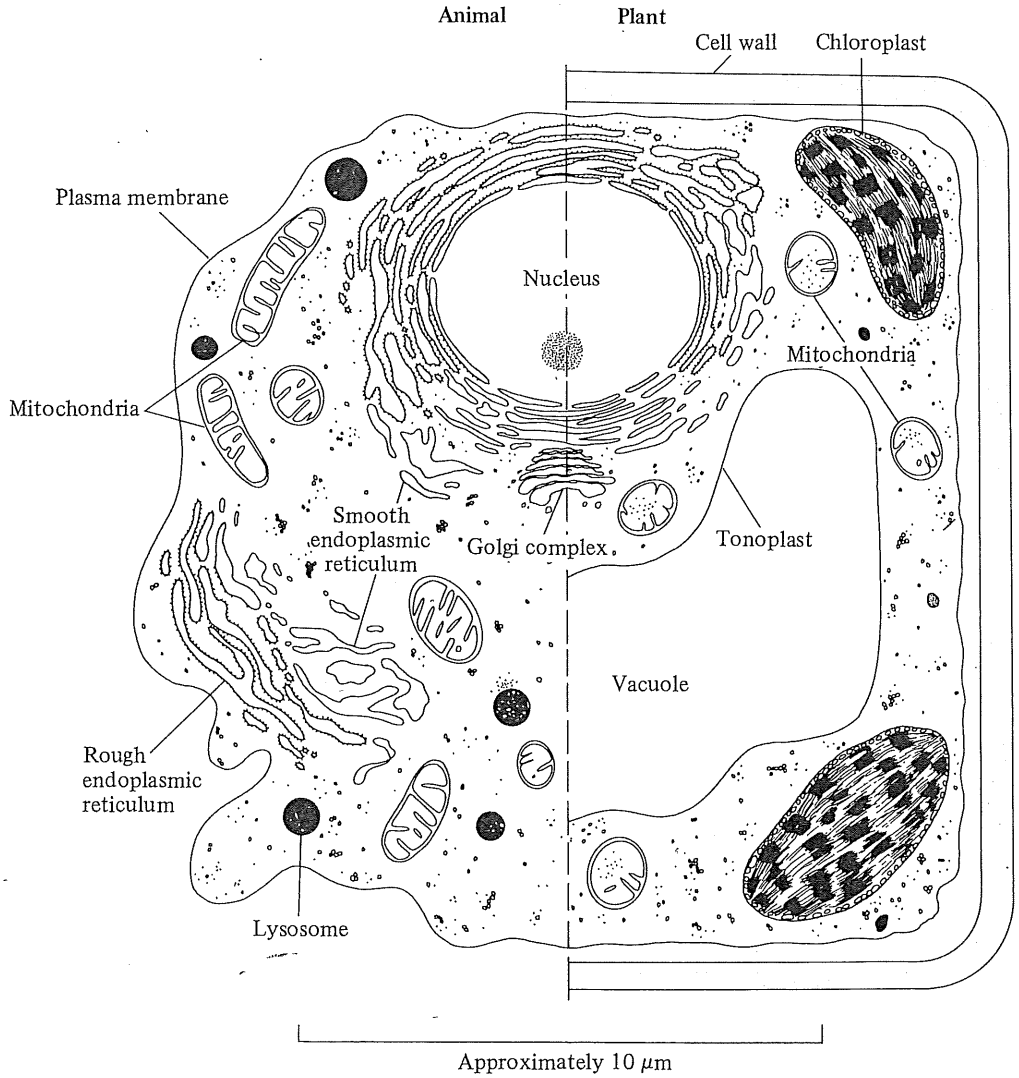

FIGURE 6–1 Diagrammatic illustration of the membranous structures and organelles of an animal cell (left) and a plant cell (right). *(From Finean, Coleman, and Michell.)*

TABLE 6–1

Membrane structures of animal cells and their primary functions. *(Modified from Fawcett, 1986; Lockwood 1978).*

Plasma Membrane	Barrier between intracellular and extracellular fluids, controls passive and active transport of many solutes, and has electrically excitable properties in many cells.
Nuclear Envelope	Double membrane barrier separating the nucleus from the remainder of the cytoplasm; is perforated by large pores to allow diffusional exchange.
Mitochondria	Membrane-bound organelles that synthesize ATP from $NADH^+$ and $FADH_2$; they have their own DNA and are self-replicating.
Rough Endoplasmic Reticulum	Membrane-lined reticulum of spaces containing ribosomes; the site of protein synthesis.
Smooth Endoplasmic Reticulum	Membrane-lined reticulum continuous with rough ER; the site of steroid metabolism; acts as transport route for movement of products of rough ER to Golgi apparatus.
Golgi Complex	Membrane-lined spaces continuous with rough and smooth ER; concentrates, modifies, and packages secretory products into membrane-bound vesicles for secretion.
Lysosomes	Membrane-bound vesicles containing hydrolytic enzymes at acid pH for intracellular breakdown of materials engulfed by phagocytosis or pinocytosis for removal of damaged cell organelles and destruction of engulfed bacteria.
Peroxisomes	Small spherical membrane-bound vesicles containing enzymes that synthesize hydrogen peroxide; may be involved in uric acid metabolism.
Phagosomes	Membrane-bound vesicles containing particulate material engulfed from the outside of the cell by phagocytosis.
Pinocytotic Vesicles	Small membrane-bound vesicles containing materials absorbed into the plasma membrane to form a vesicle.

materials by exocytosis, uptake of materials by phagocytosis, and mitochondrial ATP synthesis (Table 6–1). The nuclear membrane, endoplasmic reticulum, and Golgi complex are examples of interconnected membranous spaces with different functions. Plant cells are similar to animal cells except for their stiff cell wall, the often large vacuole bounded by the tonoplast membrane, and the photosynthetic organelles (chloroplasts).

Membrane Structure

The existence and important role of the plasma membrane was recognized in the late nineteenth century, and the basic **lipid bilayer** structure of membranes was deduced early in the twentieth century. The amount of lipid that could be extracted from, for example, a red blood cell could be reconstituted as a lipid monolayer with an area that was about twice that of the original red cell. The conclusion of such experiments was that the plasma membrane was a bilayer of lipid molecules; this is clearly evident in electron micrographs of cell membranes (Figure 6–2A). The structural model of the plasma membrane structure, proposed by Danielli and Davson (1935), was a bilayer of lipid molecules, with the hydrophobic portions ("water-avoiding," i.e., not water soluble) oriented towards the inside of the lipid bilayer and the hydrophilic portions ("water-loving," i.e., water soluble) forming the outer surfaces in contact with either the cytoplasmic or extracellular fluids. They further speculated that there was a protein coating at the aqueous surfaces, some of which penetrated through the lipid bilayer, since this was consistent with the observations of facilitated transport of various solutes.

Subsequent studies of plasma and also various intracellular membranes have variously modified Danielli and Davson's basic lipid-bilayer model into more complex models (Figure 6–2B). The "fluid-mosaic" model (Singer and Nicholson, 1972) represents the membrane as a disorderly, fluid-like lipid bilayer that contains complex proteins with hydrophobic regions located deep within the lipid hydrocarbon zone and the polar regions at the surface. There are ordered aggregates of both protein and lipid called domains covering the membrane surface. The outer surface of the plasma membrane contains many glycoproteins, proteins with short (about 10 monosaccharide residues) polysaccharides. These carbohydrates "bristle" from the cell surface and may assist in keeping apart adjacent cells since they

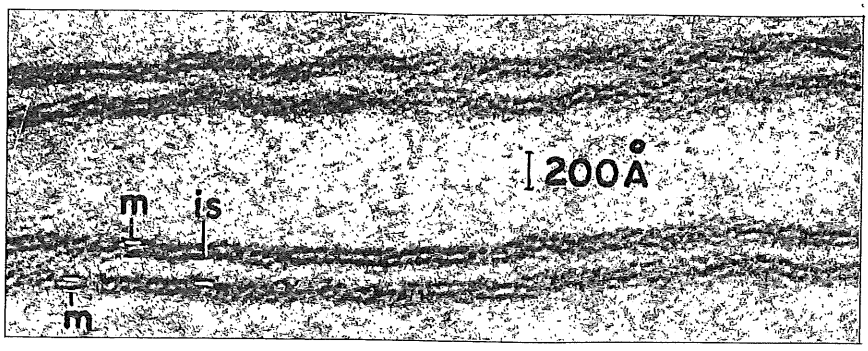

A

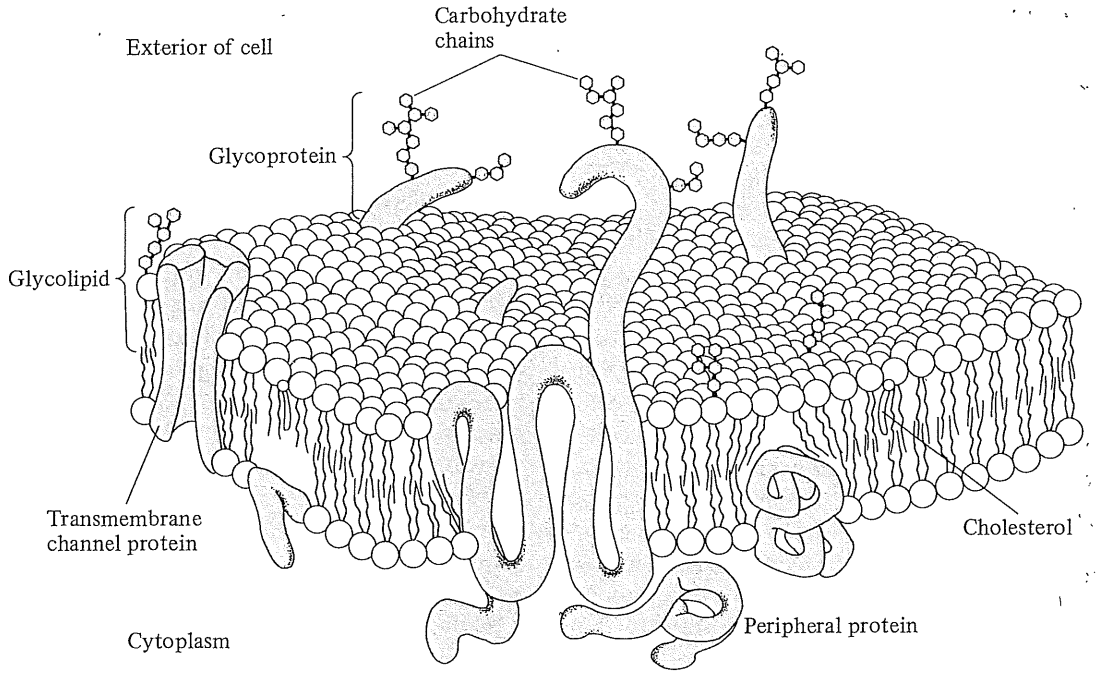

B

FIGURE 6–2 **(A)** An electron micrograph of a cell membrane (four separate membranes are shown, labelled M) shows the 10 nm thick, double layer of dark lines representing the hydrophilic lipid heads and the intervening space of hydrophobic tails. **(B)** A schematic representation of the fluid-mosaic model of a cell membrane showing the lipid constituents and their arrangement as the bilayer portion of the membrane and the protein constituents of the membrane.

are negatively charged. The inner surface of the membrane has other loosely associated proteins and microfilaments and microtubules that provide lateral movement of the membrane domains (Nicholson 1976).

About 25 to 50% of the membrane dry weight is lipid, mostly compound lipids such as glycerophosphatides (phosphatidyl choline, phosphatidyl ethanolamine, phosphatidyl serine, phosphatidyl inositol), sphingolipids (which resemble glycerophosphatides but contain a nitrogenous base, sphingosine, instead of glycerol), and cholesterol (Lockwood 1978). The polar ends of these lipids are arranged on the aqueous sides of the lipid bilayer. The cholesterol, which is found mainly in the outer layer of the bilayer, most likely interacts structurally with the phospholipids, such as phosphatidyl ethanolamine (Figure 6–2B). The local concentration of

particular lipids can create zones of greater or lesser mobility. There is also considerable variation in specific lipid constituents between membranes of different types of cells and membranes of different parts of cells. For example, the myelin sheath of some nerve cells has a higher sphingolipid content and lower glycerophosphatide content than the mitochondrial membrane and is rich in saturated, long-chain fatty acids.

Changes in the specific lipid constituents of membranes are an important aspect of thermal acclimation by membranes (see Chapter 5). The chain length and extent of saturation of the lipids determine the melting point, or phase transition temperature, of the membrane. Short chains and low saturation decrease the phase transition temperature. Cholesterol has the interesting property of decreasing the molecular mobility of membrane constituents in the liquid phase, but increasing their mobility in the solid phase. Consequently, the presence of high levels of cholesterol in a membrane "blurs" the temperature transition between the liquid ("melted") phase and solid ("frozen") phase.

Membrane-associated proteins are often enzymes but many have a structural, rather than a catalytic, function. Many proteins bridge, or span, the lipid bilayer (Figure 6–2B). The acetylcholine (ACh) receptor is a good example of a structural protein in a membrane. It usually is a dimer of two pentameric subunits, joined by a disulfide bridge and associated proteins on the intracellular side of the membrane. The pentameric subunit consists of four glycopeptides. The ACh receptor has two binding sites for ACh and the transmembrane bridging portion forms a gated ionic pore through the lipid bilayer; the gate opens to allow cation flux when two acetylcholine molecules are bound to the receptor portion (see below). Other examples of bridging proteins that function as specific transport channels are the proton-pumping bacteriorhodopsin proteins found in the purple membrane of certain halophytic bacteria, plasma membrane connexons for intercellular transport, ATP synthetase, and cytochrome oxidase. Many other examples of specific transport systems will be described below. For example, the Na^+-K^+ ATPase enzyme is a characteristic constituent of all plasma membranes and is of vital importance in maintaining the intracellular-extracellular Na^+ and K^+ concentration gradients. Another important enzyme links carbohydrates with protein to form glycoproteins, which often form a 5 to 7 nm thick bristling coat over the cell surface. Blood group factors are one class of glycoproteins; other glycoproteins are released from the plasma membrane and become components of serum proteins, cartilage, mucus, and the vitreous humor of the vertebrate eye.

Membrane Permeation

The plasma membrane influences the passage of all solutes and water that enter or leave the cell. It must be selectively permeable, allowing ready passage of certain molecules, such as O_2, CO_2, glucose, NH_3, and urea, yet impeding the loss of important intracellular solutes, such as K^+, ATP, amino acids, and proteins.

An artificial pure lipid bilayer is the simplest model of plasma membrane transport. Solutes that are lipid soluble will be able to dissolve into, hence pass through, the lipid bilayer; they will have a high permeability. Solutes that are not lipid soluble will not traverse the lipid bilayer. Oxygen, for example, is quite lipid soluble and passes relatively freely through a hexadecanol membrane. However, O_2 is about 100 × more permeable to a plasma membrane than to simple lipid bilayers. This is probably because the close packing of lipids in the plasma membrane is partly disrupted by other large, "awkwardly shaped" molecules, thus providing pores, or gaps. The random thermal motion of the lipids would also create temporary pores large enough for transport of small molecules, such as O_2, CO_2, and water. It is therefore important to examine properties of membrane permeation with a realistic model of, or an actual, plasma membrane, and appreciate that there are a variety of mechanisms for membrane permeation (Figure 6–3).

Diffusion

The passive permeability of a lipid membrane varies for different solutes; it depends on the **permeability coefficient** (*P*). The permeability of a solute should be proportional to its lipid solubility, or **partition coefficient** (*K*). The partition coefficient is the ratio of the solubility of a solute in a solvent (e.g., olive oil or ether) to the solubility in water. There is a strong correlation between the permeability coefficient and the partition coefficient, and a strong influence of molecular weight on *P*. Lipid-soluble solutes are passively permeable to cell membranes because they dissolve into the membrane lipid bilayer. Their passage through cell membranes is essentially a diffusional process, described by Fick's first law of diffusion. Some small water-soluble solutes may also diffuse through small pores in the cell membrane, but most water-soluble solutes are too large for this.

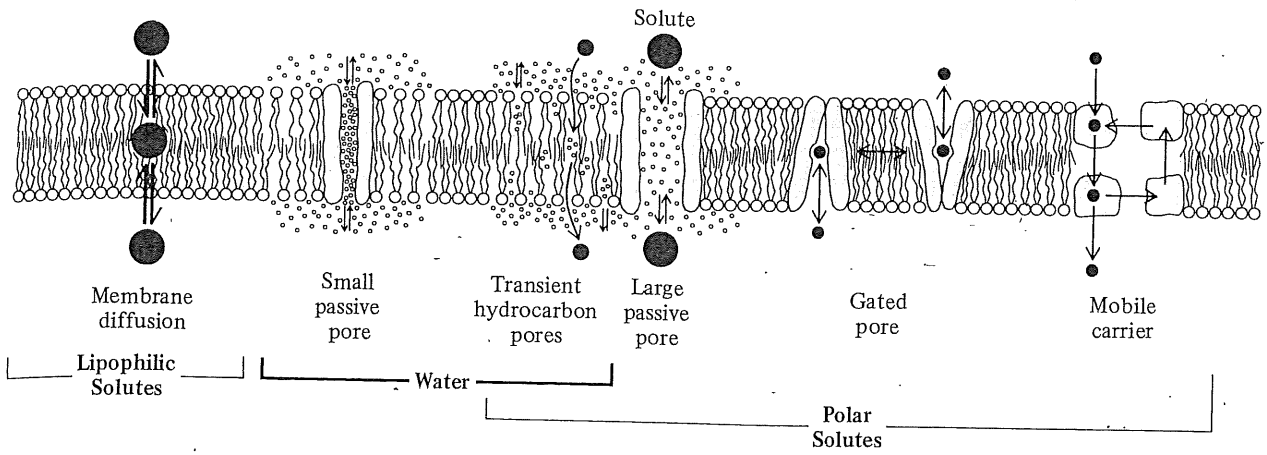

FIGURE 6–3 Possible mechanisms for permeation of cell membranes by water, lipophilic solutes, and polar solutes (e.g., ions). Lipophilic solutes can diffuse directly through the membrane because they are lipid soluble. Water may permeate through the spaces between hydrophobic lipid molecules, specific water pores, or other pores; polar solutes may permeate through the lipid bilayer but are more likely to permeate through specific pores, gated pores, or "ferryboat" mobile carriers.

The passive permeation of lipid-soluble solutes through cell membranes depends on their partition coefficient. It is relatively straightforward to rearrange Fick's first law of diffusion to a form that includes the partition coefficient and the diffusion coefficient of the membrane for the solute (D_m; $cm^2\ sec^{-1}$);

$$J_m = D_m K A_m (C_{m2} - C_{m1})/\Delta x_m$$
$$= P_m A_m (C_{m2} - C_{m1}) \qquad (6.1a)$$

where J_m is the net transmembrane flux (mol sec^{-1}), A_m is the membrane surface area (cm^2), C_m is the solute concentration on each side of the membrane (mol cm^{-3}), and Δx_m is the thickness of the membrane (cm). The membrane diffusion coefficient, partition coefficient, and membrane thickness can be consolidated into a single coefficient, the permeability (P_m; cm sec^{-1}), i.e.,

$$P_m = D_m K/\Delta x_m \qquad (6.1b)$$

The membrane permeability should be directly proportional to the partition coefficient and the membrane diffusion coefficient, and inversely proportional to the membrane thickness. The diffusion coefficient also depends on other variables, including the molecular weight of the solute; in general, $D \propto \sqrt{1/\text{MWt}}$. Thus, P and P/K should also depend on the molecular weight. Such an inverse dependence of P/K on MWt is observed for many membranes.

The permeability of solutes is not well correlated with their partition coefficient if there are specific transport mechanisms, either passive or active. Small nonlipophilic molecules, such as water and urea, may also diffuse through the plasma membrane pores. In theory, pores of diameter $\approx$ 0.8 nm form when the hydrocarbon tails of membrane lipids or a cholesterol molecule are temporarily displaced by random thermal motion; this would allow passage of water (<0.2 nm), urea (0.2 nm), hydrated Na^+ (0.56 nm), and K^+ (0.38 nm), but not Ca^{2+} (0.96 nm) or Mg^{2+} (1 nm). Because of specific transport mechanisms, many other polar solutes have a permeability higher than predicted by their K and molecular weight (see below).

There can be a flow of water through a membrane's transient hydrocarbon or protein pores due to a hydrostatic pressure difference or osmotic concentration difference; this hydraulic water flow is called **bulk flow**. There is a fundamental difference at the molecular level between the permeability coefficient of water for diffusional and hydraulic flow. The hydraulic permeability (P_f, or filtration permeability) is generally higher than the diffusional permeability (P_d; Sha'afi 1981). Bulk water movement thus "enhances" the rate of diffusion of water across a membrane; it also enhances the rate of exchange of other small solutes, such as urea, which are drawn along by the water flow. This enhancement of solute flux by bulk water flow is

solvent drag. The incorporation of cholesterol into membranes generally decreases their diffusional permeability to water; remember that cholesterol also generally decreases molecular mobility of the liquid membrane phase.

Many polar solutes are transported by specific membrane pores, and so their permeability is not dependent on their partition coefficient or molecular weight. Some permeation might occur through the same thermally formed hydrocarbon pores that allow water exchange, but the observation that water and small polar solute flux can be experimentally disassociated suggests that "water pores" are too small for the larger polar solutes and that there must be specific larger diameter pores. Urea has a low partition coefficient ($K_{ether} < 0.003$) but is highly permeable to most, although not all, biological membranes. There appear to be specific urea transport pores in at least some membranes. For example, the urea permeability of toad urinary bladder and the mammalian nephron can be increased by antidiuretic hormone (as is water permeability), but there appear to be different pores for water (smaller diameter and more of them) and urea (larger diameter and fewer of them).

Ions are another category of small polar molecules that can be passively transported across membranes through membrane pores or specific ion channels, e.g., Na^+, K^+, Cl^-, and Ca^{2+}. For ions, the combined electrical and chemical driving forces, the **electrochemical gradient**, drives diffusion. This is significant because most membranes generally have a resting membrane potential of about -90 mV, which favors ion flux even in the absence of a concentration gradient. Specific mediated-transport mechanisms for ions will be further discussed below.

Mediated Transport

The permeation mechanisms discussed so far are driven by diffusion; the flux is proportional to the permeability and the concentration or electrochemical gradient. However, membrane permeation of many solutes is not explained by simple diffusion; the permeation flux may be much faster than predicted, may be a nonlinear function of the concentration difference, may be inhibited by chemical analogs or reagents that alter protein structure, may become saturated, and may occur against a concentration gradient. Transport of many solutes is mediated by specific membrane proteins, in a fashion resembling enzyme-substrate interactions; this is **mediated transport**.

In **facilitated diffusion**, the flux is mediated transport but is passive and in the direction down the electrochemical gradient, i.e., "downhill" from a high concentration to a low concentration. In contrast, **active transport** is mediated transport but is an "uphill" flux against an electrochemical gradient, i.e., from a low to a high concentration.

The basic concept of mediated transport is simple. A protein carrier molecule binds the solute molecule, then a conformational alteration of the protein-solute complex translocates the solute across the membrane; the solute then separates from the carrier on the opposite side of the membrane (West 1983). The essential features of such a mediated-transport mechanism are:

1. there is a transport protein with a solute-specific binding site,
2. the binding site alternates in location from one side of the membrane to the other, and
3. the kinetic events of transition from one state to the other have specific rate constants.

The characteristic properties of such a system are:

1. the rate of flux is greater than predicted by a solute's partition coefficient, size, or molecular weight;
2. transport becomes saturated at high solute concentrations;
3. chemically or sterically similar solutes can competitively inhibit the flux; and
4. reagents that interfere with the protein carrier can noncompetitively inhibit solute flux.

Some facilitated exchange systems have more complex properties, including exchange diffusion and countertransport (see below).

Mediated transport can involve a mobile intramembrane carrier, i.e., is **mobile carrier-mediated**, or a transmembrane pore that has a closing mechanism, i.e., a **gated channel-mediated** pore (Figure 6–3). In practice, the end result is the same for carrier-mediated and channel-mediated transport, and it is experimentally difficult to distinguish between the two mechanisms. However, there are well-established examples of both types of mediated transport and some solutes may be transported by a combination of both mechanisms.

Channel-mediated transport resembles the kinetics of a simple Michaelis-Menten enzymatic reaction (Chapter 3)

$$C + S_i \rightleftharpoons CS \rightleftharpoons C + S_o \qquad (6.2a)$$

where C is the channel protein, S_i is the substrate on the inside of the membrane, and S_o is the substrate translocated to the outside. The "enzyme reaction" is the translocation of the substrate from one side to the other, rather than a chemical reac-

tion. The flux (J) is related in a hyperbolic fashion to substrate concentration ([S]).

$$J = \frac{V_{max}[S]}{K_t + [S]} \qquad (6.2b)$$

where V_{max} is the maximal velocity, K_t is analogous to the Michaelis-Menten constant, and [S] is the substrate concentration.

Mobile carrier-mediated transport is more complex; the carrier is located alternately at each side of the membrane and may bind or release the solute. There are eight possible "reactions" (each with a specific rate constant, a, b, c, . . . , g, h) for the mobile carrier and the solute (Figure 6–4A). If there is no substrate on the inside ($S_i = 0$), then the rate of flux (J) is related to the total carrier concentration

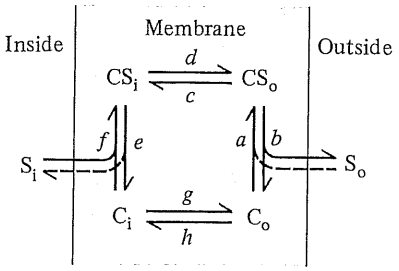

A. Mobile Carrier Transport System

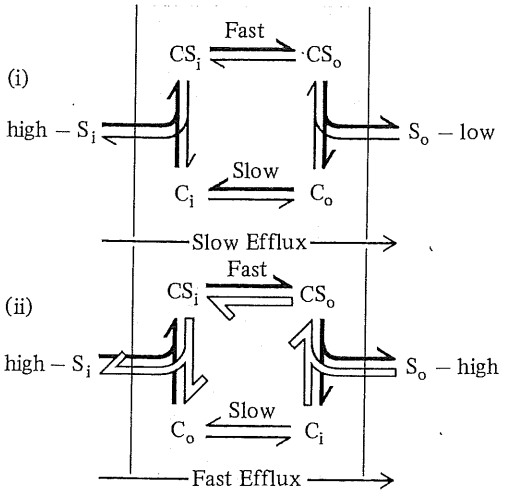

B. Exchange Diffusion

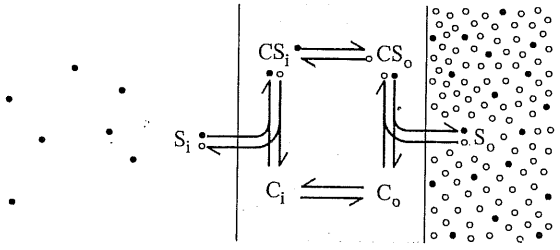

C. Counter Transport of •

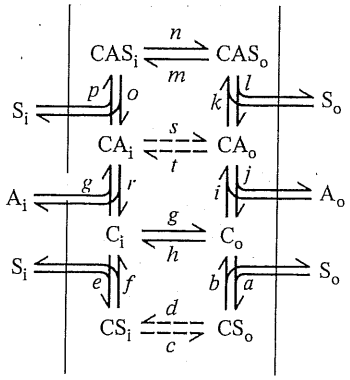

D. Cotransport

FIGURE 6–4 **(A)** General scheme for a mobile carrier transport system in the cell membrane; C represents the carrier molecule and S the substrate molecule, and i and o the two sides of the membrane. There are eight rate constants for the various reversible reactions (a–h) that can occur during transport of the substrate. **(B)** Exchange diffusion can transport a substrate faster from one side (e.g., inside, i) of a membrane to the other side (e.g., outside, o) if there is a higher concentration on the outside because there is a higher concentration of the transport intermediate CS_o, which is rapidly transported across the membrane to become CS_i. Solid arrows indicate the preferential efflux route; open arrows indicate the influx route. **(C)** Countertransport can produce a transient, passive, "uphill" transport of an isotopic or chemical analog (•) of a solute (o) from side i to side o. **(D)** Cotransport by a mobile carrier membrane transport system; the mobile carrier binds two substrates, S and A. There are 20 different rate constants (a–t) but some (*s, t; c, d*) are unimportant (or else the system would not be cotransport).

(C_t), the outside concentration (S_o), and the eight reaction constants as follows.

$$J = \frac{C_t[S_o]aceg/(a(ce + cg + dg + eg))}{[S_o] + (h + g)(bd + be + ce)/(a(ce + cg + dg + eg))} \quad (6.3)$$

This equation resembles the Michaelis-Menten hyperbolic kinetic equation (see Equation 6.2b).

The rate constant for the mobile carrier moving from one side of the membrane to the other may be equal to the rate constant for carrier-solute movement in the same direction (i.e., $d = g$, $c = h$) but this need not be so. In fact, the rate constants can differ by a factor of 10 to 100 ×, e.g., the loaded carrier may reorient faster than the unloaded carrier. The rate of efflux ($J_{i\rightarrow o}$) may be low even if the internal concentration (S_i) is high and the external concentration (S_o) is low because the rate of reorientation of the unloaded carrier from the outside to the inside is slow (Figure 6–4Bi). The rate of efflux will increase if the concentration of solute on the outside is high because of the faster reorientation of the carrier-solute complex towards the inside (Figure 6–4Bii). The influx $J_{o\rightarrow i}$ also increases at high $[S_o]$. The unidirectional flux of a solute can thus depend on the unidirectional flux in the opposite direction if there is an asymmetry in the rate constants; this is **exchange diffusion**.

Countertransport is passive transport against a concentration gradient; it can occur if there is an asymmetry in concentrations of a solute and a similar solute (or radioisotope) that is also transported (Figure 6–4C). Let us assume that there is a very high concentration of solute (S) on the outside and none on the inside, and there is a low concentration of the analog (A) on the inside and a higher concentration on the outside (i.e., $0 = S_i < A_i < A_o << S_o$). The carrier system will preferentially transport S inwards (since $S_o >> A_o$ and will competitively inhibit inward transport of A) and preferentially transport A outwards (since $A_i > S_i = 0$). There is an efflux of A even though $A_o > A_i$. Remember that the carrier cannot distinguish A from S, although we can. This passive uphill transport of A is a transient phenomenon that will cease when the concentrations of A and S come to equilibrium across the membrane. The occurrence of countertransport can be used as a criterion to distinguish between pore exchange and mobile carrier exchange, since it would not occur for a gated-pore transport mechanism.

Cotransport of two solutes (S and S′) is considerably more complex than mediated transport of one solute. There are 20 possible reactions and rate constants for cotransport (Figure 6–4D), although four (c, d, s, t) must be insignificant by definition, since for cotransport both S and S′ are required for transport. There are two possible routes from C to CSS′

$$C + S \rightarrow CS + S' \rightarrow CSS'$$

and

$$C + S' \rightarrow CS' + S \rightarrow CS'S$$

The cotransport is said to be ordered if there is a required sequence for the formation of CSS′ and is random if either pathway to CSS′ occurs. The Na^+-K^+ ATPase enzyme/ion pump is one example of a cotransport system; another is the Na^+-linked active transport of amino acids and some monosaccharides across the intestinal mucosa. These examples will be further discussed below.

Facilitated Diffusion. Facilitated diffusion is a mediated, "downhill" transport process that is better described by a hyperbolic flux concentration relationship (Equation 6.2b) than by Fick's first law of diffusion. A typical example of the flux concentration relationship showing saturation kinetics is observed for the facilitated uptake of galactose by the human erythrocyte (Figure 6–5A).

Facilitated transport mechanisms include both mobile carrier and gated pore models. This variation in transport mechanism is well exemplified by ionophores, compounds of bacterial origin that function as ion-selective pores when introduced into a membrane. These ionophores are heterogeneous in terms of their specific molecular structure, but all are characterized by a folded structure that has a hydrophobic exterior and an interior lined by oxygen atoms that can bind cations. Valinomycin is a mobile carrier ionophore that is highly specific for K^+ rather than Na^+ (by a preference of over 10,000 to 1); this high specificity is remarkable considering the similar sizes of hydrated K^+ and Na^+ ions (see below). Valinomycin clearly is a mobile carrier, requiring normal membrane fluidity (Figure 6–5B). In contrast, gramicidin is a channel ionophore. Its protein chain appears to form a spiral (about 3 nm long and 0.4 nm diameter) that spans the hydrophobic portion of the membrane and forms a water-filled, ion-conducting pore that allows the permeation of water and many small ions. Gramicidin is not as discriminating for solutes as is valinomycin.

The glucose carrier of the human erythrocyte membrane is another example of a facilitated diffusion system but is somewhat intermediate between a mobile carrier and a gated pore model. The carrier

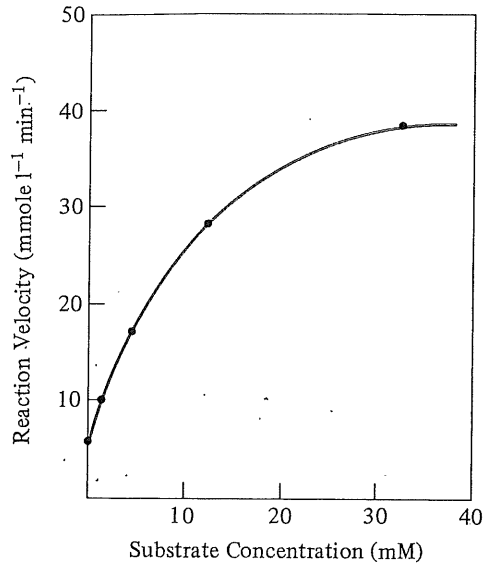

A

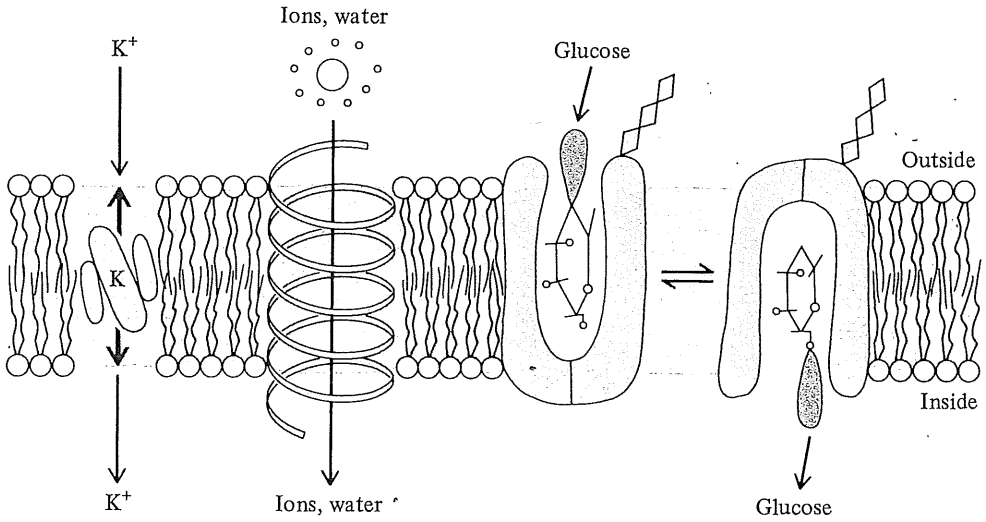

B

FIGURE 6–5 **(A)** Example of carrier-mediated transport showing the nonlinear relationship between transport rate (J; mmole l^{-1} cells^{-1} min^{-1}) and intracellular substrate concentration ([S]; mM), and saturation kinetics for the human red blood cell. **(B)** Schematic representation of a mobile ionophore (valinomycin), a channel (pore-forming) ionophore (gramicidin), and a somewhat intermediate membrane transport system, the gated pore glucose carrier. *(Data from Ginsburg and Stein, 1975; modified from West 1983; Harrison and Lunt 1980.)*

is asymmetric in that a carbohydrate moiety is located on the outside of the membrane; it therefore is not a freely mobile carrier. However, the active site for glucose binding appears to be alternately exposed to the outside and inside membrane surfaces, and in this sense it is like a mobile carrier (Figure 6–5B).

Active Transport. Active transport mechanisms move solutes against an electrochemical gradient (i.e., "uphill") and require the expenditure of metabolic energy. It is a primary active transport system if the free energy change for the uphill solute transport by the carrier is provided directly by the metabolic energy stores (e.g., ATP). It is a secondary active transport system if the free energy change is provided by other energy sources, such as ion electrochemical gradients.

Probably the best understood primary active transport mechanism is the Na^+-K^+ ATPase (Na^+ pump) of animal plasma membranes. The Na^+-K^+ pump generally transports 3 Na^+ out and 2 K^+ in, per ATP hydrolyzed. The net transport of one positive charge out per ATP hydrolyzed means that

the pump establishes an electrical gradient, i.e., it is **electrogenic**. Sometimes there is a 1:1 ratio of Na^+ to K^+ transport (e.g., 2 Na^+:2 K^+ or 3 Na^+:3 K^+ per ATP) and the pump is **electroneutral**. However, the 1:1 rather than 3:2 ratio of Na^+:K^+ transport may be a consequence of the membrane being leaky to Na^+, allowing some of the extruded Na^+ to reenter the cell and giving the impression of no net charge transfer by the pump. The Na^+-K^+ ATPase is a tetramer, $\alpha_2\beta_2$, of α-subunits (molecular weight about 10^5) and β-subunits (molecular weight about 5 10^4). The larger subunits span the plasma membrane from the inside to outside surfaces; the binding sites for ATP and Na^+ are located on the inside, and for K^+ on the outside. Ouabain, a cardiac glycoside that is a specific reversible inhibitor of the Na^+-K^+ ATPase, binds to the outside of the plasma membrane. There appear to be two forms of the Na^+-K^+ ATPase enzyme, E_1 and E_2, that differ significantly in binding properties. The chemical events that occur in the Na^+-K^+ transport cycle are fairly well understood (Figure 6–6) although the details of translocation process across the membrane are not. The two slowest steps are the interconversion of E_1 and E_2, i.e., $E_1 \rightarrow E_2$ and $E_2 \rightarrow E_1$; these are suspected to be the actual translocation processes.

Secondary active transport uses other forms of energy, such as electrochemical gradients, to provide free energy for active transport. The halophytic bacterium *Halobacterium halobium* has a unique light-driven proton pump, bacteriorhodopsin, which transports H^+ ions out of the bacterium; the energy is derived from illumination. This proton pump can supplement or even replace the respiratory chain proton pumps during anoxia. In animal cells, the electrochemical gradient for secondary active transport is most commonly the Na^+ gradient (it can be a H^+ gradient in plant and bacterial cells; Nobel 1983).

The Na^+-linked uptake of amino acids and some monosaccharides (glucose, galactose) by the epithelial cells of the intestine, or integument, of certain marine invertebrates is an example of secondary active transport (Figure 6–7). The Na^+ pump is located on the serosal membrane of the epithelium (blood side) and actively transports Na^+ from inside the epithelial cell into the body fluids. The low intracellular (Na^+) and negative intracellular charge provide a substantial electrochemical gradient for Na^+ influx into the epithelial cells. A "facilitated diffusion" type of transport mechanism binds an amino acid (or monosaccharide) and an Na^+ at the same time; this is a **symport**. Alanine-Na^+ cotransport is a typical example. Alanine will slowly diffuse into an epithelial cell in the absence of Na^+ until the intracellular and luminal concentrations are equal. The presence of Na^+ increases the rate

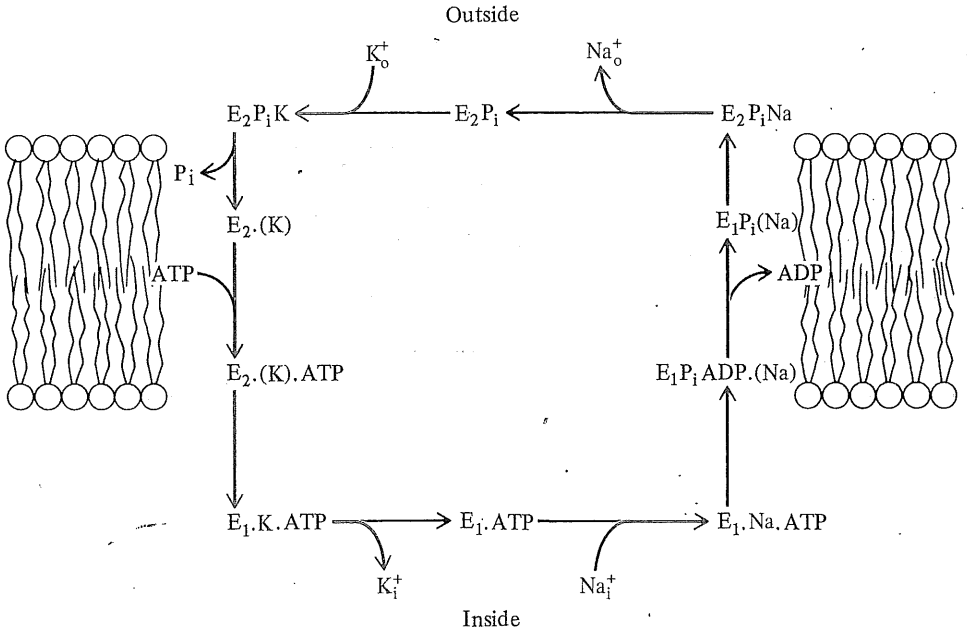

FIGURE 6–6 Proposed movement of the Na^+-K^+ ATPase (E_1 and E_2) to exchange Na^+ and K^+ across the cell membrane and the role of ATP hydrolysis. *(Modified from Karlish, Yates, and Glynn 1978.)*

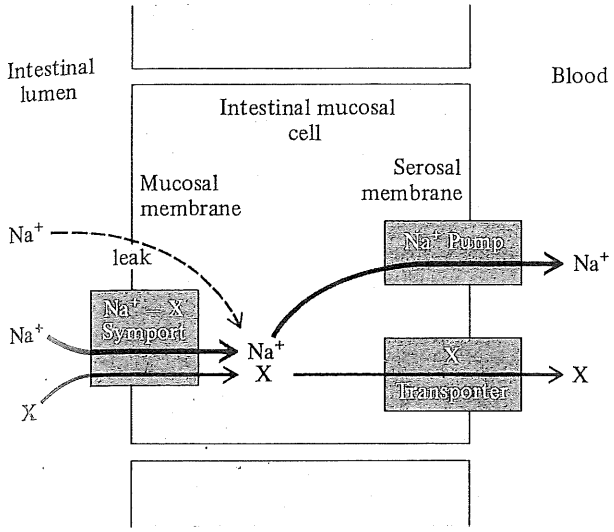

FIGURE 6–7 Cotransport of solute "X" (e.g., glucose, amino acids) and sodium by the intestinal mucosal cell across the lumen membrane by a symport carrier molecule, then separate transport across the mucosal membrane by the Na^+ pump and a transport protein for "X." *(Modified from Harrison and Lunt 1980.)*

of uptake, and the internal alanine concentration approaches ten times that of the luminal concentration, i.e., there is rapid "uphill" transport of alanine driven by the Na^+ gradient. The Lineweaver-Burk plot for alanine transport, with and without Na^+, indicates that transport is independent of the $[Na^+]$ at infinite [alanine], but the absence of Na^+ decreases the affinity of the transport system (K_t, which is analagous to the Michaelis-Menten constant for enzymatic reactions, K_m). The absence of Na^+ is effectively acting as a competitive inhibitor of transport.

Water can diffuse across membranes via small pores and there can also be a bulk flow of water due to either a hydrostatic pressure difference or an osmotic concentration difference (see Chapter 16). Water flow can be osmotically linked to active transport of solutes, especially Na^+, through establishment of local osmotic gradients (see Chapter 16). No specific carrier for active transport of water has yet been identified, although active transport of water has occasionally been hypothesized.

Dynamics of Semipermeable Membranes

Biological membranes vary greatly in their permeability to different solutes, i.e., they are complex **semipermeable membranes**. The semipermeability of biological membranes has far-reaching consequences (Donnan 1927). Consider two water compartments separated by a semipermeable membrane (Figure 6–8A). If a solute, for example KCl, is added to one compartment (side 1), then $[K^+]_1 > [K^+]_2 = 0$ and $[Cl^-]_1 > [Cl^-]_2 = 0$. If the membrane is freely permeable to both K^+ and Cl^-, then both ions will diffuse from side 1 to side 2 until $[K^+]_1 = [K^+]_2 = [Cl^-]_1 = [Cl^-]_2$. The addition of potassium-proteinate to side 1 and KCl to side 2 so that $[K^+]_1 = [K^+]_2$ produces a complex situation if the membrane is permeable to K^+ and Cl^- but not Pr^- (Figure 6–8B). The Pr^- cannot diffuse from side 1 to 2 despite its concentration difference, and K^+ would not be expected to diffuse because the concentrations are the same. The Cl^- concentration is higher on side 2 and it is not in equilibrium; it will diffuse from side 2 to side 1. However, Cl^- will not continue to diffuse until $[Cl^-]_1 = [Cl^-]_2$ because movement of Cl^- from side 2 to side 1 establishes a charge imbalance, making side 2 negative and side 1 positive. The negative charge on side 1 will repel Cl^- from side 2 to side 1, and will also influence the distribution of K^+ ions even though the $[K^+]$ was initially in concentration equilibrium across the membrane. K^+ will be electrically attracted towards side 1 (−) and repelled from side 2 (+). The Pr^- distribution is unaffected because it is impermeable. When the K^+ and Cl^- ions come to equilibrium, there will be (1) a concentration gradient for K^+, Cl^- (and Pr^-) across the membrane; (2) a net positive charge on side 2 and a negative charge on side 1; and (3) a higher osmotic concentration on side 1 than side 2. This equilibrium distribution of permeable and impermeable ions across a semipermeable membrane is called a **Donnan equilibrium**.

The magnitude of the electrical gradient across a semipermeable membrane due to a Donnan equilibrium can be calculated using the Nernst equation

$$E_m = \frac{RT}{zF} \ln \frac{C_2}{C_1} = \frac{2.303RT}{zF} \log_{10} \frac{C_2}{C_1} \qquad (6.4)$$

where E_m is the membrane potential (volts), R is the gas constant, T is the temperature (°K), z is the charge on the ion (e.g., +1 for Na^+ and K^+, −1 for Cl^-, +2 for Ca^{2+}), F is Faraday's constant, and C_1 and C_2 are the ion concentrations on each side of the membrane. The value of RT/F is about 0.025 volt at T = 20° C, or 58 mV if we use $\log_{10}$ rather than natural log (ln). But, in the above example, do we use $[K^+]_1$ and $[K^+]_2$ or $[Cl^-]_1$ and $[Cl^-]_2$ to calculate E_m? We can use either, because both ions are distributed at equilibrium across the membrane. Therefore,

$$E_m = \frac{RT}{(+1)F} \ln \frac{[K^+]_2}{[K^+]_1} = \frac{RT}{(-1)F} \ln \frac{[Cl^-]_2}{[Cl^-]_1} \qquad (6.5a)$$

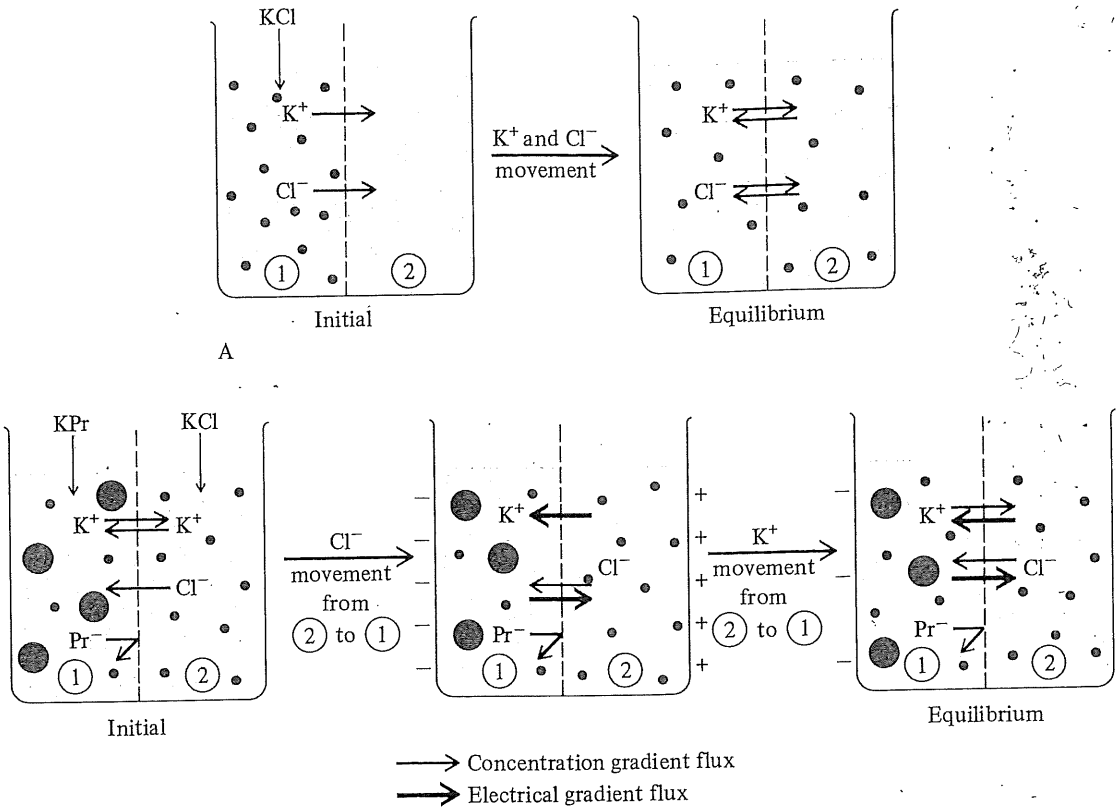

FIGURE 6–8 **(A)** Distribution of KCl solution added to one side (1) of a permeable membrane; there are equal concentrations of K^+ and Cl^- on each side of the membrane at equilibrium. **(B)** Donnan distribution of potassium proteinate solution and equal concentration of KCl added across a semipermeable membrane (permeable to K^+ and Cl^- but not Pr^-). At equilibrium, there is a concentration gradient (thin arrows) for K^+ and Cl^- balanced by an electrical gradient (thick arrows).

Rearranging this equation yields the characteristic reciprocal distribution of the cation and anion for a Donnan equilibrium.

$$\frac{[K^+]_2}{[K^+]_1} = \frac{[Cl^-]_1}{[Cl^-]_2} \quad \text{or} \quad [K^+]_2[Cl^-]_2 = [K^+]_1[Cl^-]_1 \tag{6.5b}$$

Electroneutrality must also be maintained on each side of the membrane (although there is a small charge imbalance due to the membrane potential; see below) and so

$$[Pr^-]_1 + [Cl^-]_1 = [K^+]_1 \quad \text{and} \quad [Cl^-]_2 = [K^+]_2 \tag{6.5c}$$

The magnitude of the Donnan potential can be estimated from Equations 6.5a, 6.5b, and 6.5c. Let us assume that the intracellular fluid has a protein concentration of 40 mEq l^{-1}, a K^+ concentration of 140 mEq l^{-1}, and a Cl^- concentration of 100 mEq l^{-1} (these values are realistic for most cells, but we will unrealistically ignore Na^+). If the outside $[Pr^-]$ is 0, then $[Cl^-]_o = [K^+]_o = 118$ mEq l^{-1}. The E_m due to the Donnan equilibrium can now be calculated as $RT/F \ln [K^+]_i/[K^+]_o = -4.2$ mV.

Resting Membrane Potentials

Electrical potentials, of the order of a few millivolts (mV) to over 100 mV, commonly occur across cell membranes. The resting membrane potential (E_m) remains constant for many types of cells but alters dramatically for excitable (irritable) cells, such as sensory, nerve, and muscle. Essentially three mechanisms contribute to these potentials: (1) the electrogenic ion pump, (2) the Donnan equilibrium, and (3) diffusion potentials.

The electrogenic Na^+-K^+ pump exchanges 3 Na^+ for 2 K^+ per ATP hydrolyzed. There is thus a net transfer of 1 + charge, and this contributes to the normal membrane potential. However, it is not the immediate cause of the normal membrane potential, as is apparent when the Na^+-K^+ pump is poisoned by specific blockers, such as ouabain. There is little or no effect of ouabain on E_m (although the E_m ultimately declines to 0 as the Na^+ and K^+ concentration gradients dissipate; see below).

A Donnan equilibrium contributes a small membrane potential because the intracellular fluid has a higher protein (Pr^-) concentration than the extracellular fluid. The Donnan potential is generally not responsible for the resting E_m.

The third and most important mechanism contributing to the E_m is the existence of marked diffusion potentials for various ions across the membrane; these occur because there are large ionic concentration differences for ions that are permeable across the membrane.

Diffusion Potentials

There are three important aspects to the electrical contribution of ions to membrane potentials: (1) ion mobility, (2) selective ion permeability, and (3) ion concentration gradients.

Ion Mobility. All ions are not equally mobile in solution. Ions experience frictional forces when in motion, and these frictional forces retard their movement. The magnitude of the frictional force depends on the size of the ion, and so mobility (u) is a strong function of size. The absolute ion mobility is defined as the average velocity (cm sec^{-1}) in an electrical field of 1 V cm^{-1}. Perhaps contrary to expectation, the ions of smaller atomic radius have lower mobilities (Table 6–2). This is because ions are generally covered with a surface "hydration layer" of water molecules, attracted by the charge density of the ion. Larger ions have a lower charge density (because they have a greater surface area) and therefore have a thinner hydration layer and a smaller hydrated radius. It is possible to estimate the hydrated radius and number of water-of-hydration molecules in the hydration layer, e.g., Li^+, 0.06 nm hydrated radius, 6-12 H_2O; Na^+, 0.095 nm radius, 4.5 H_2O; K^+, 0.133 nm radius, 3 H_2O. The water of hydration is in a dynamic exchange with other water molecules, and so the hydrated ion should not be thought of as a fixed volume sphere with a central ion and peripheral hydration layer. The diffusion coefficient is directly proportional to mobility.

$$D = RTu/F$$

Ionic Permeability. The electrical properties of cell membranes depend on the selective (and often changing) permeabilities of the membrane to different ions. There are many specific ion channels, or pores, that make the cell membrane highly but selectively permeable to ions. For example, there are Na^+ channels, K^+ channels, Ca^{2+} channels, Cl^- channels, etc. These channels are usually very selective. The Na^+ channel is quite specific for Na^+; it is considerably less permeable to similar ions such as K^+, Rb^+, and Cs^+ (Table 6–3). The K^+ channel is highly specific for K^+ and relatively impermeable to Na^+ and Li^+. The selective permeability of channels is not just due to molecular weight and size, but also to hydrated radius and

TABLE 6–2

Mobility (u; μ sec^{-1} per Volt cm^{-1}) and diffusion coefficient (D; cm sec^{-1}; = RTu/F) for various important ions are dependent on atomic mass and hydrated ionic radius (r_{hyd}, nm). Values are for 25° C. *(Data from Hille 1984; Davis, Gailey, and Whitten 1984.)*

	Atomic Mass	Hydrated Radius r_{hyd}	Mobility u	Diffusion Coefficient D
Ca^{2+}	40.08	0.099	$3.08\ 10^{-4}$	$0.79\ 10^{-5}$
Li^+	6.94	0.060	$4.01\ 10^{-4}$	$1.03\ 10^{-5}$
SO_4^{2-}	96.06		$4.15\ 10^{-4}$	$1.06\ 10^{-5}$
Na^+	22.99	0.095	$5.19\ 10^{-4}$	$1.33\ 10^{-5}$
K^+	39.10	0.133	$7.62\ 10^{-4}$	$1.96\ 10^{-5}$
Cl^-	35.45	0.181	$7.92\ 10^{-4}$	$2.03\ 10^{-5}$
I^-	126.90	0.216	$7.96\ 10^{-4}$	$2.04\ 10^{-5}$
Br^-	79.90	0.195	$8.09\ 10^{-4}$	$2.08\ 10^{-5}$

TABLE 6–3

Relative permeabilities of sodium and potassium channels in an excitable cell membrane of a frog axon to various ions.

	Na^+ Channel P/P_{Na}	K^+ Channel P/P_k
Li^+	0.930	<0.018
Na^+	1.000	<0.010
Th^+	0.330	2.30
K^+	0.086	1.000
NH_4^+	0.160	0.13
Rb^+	<0.012	0.91
Cs^+	<0.013	<0.077

charge. Some ion channels are relatively nonselective, e.g., are general cation or anion channels.

What is the structure of such an ion pore, and how can it be so selective for particular ions? The pore has a specific transmembrane protein structure that has a selectivity filter at some point along its length (Figure 6–9A). The selectivity filter discriminates between ions mainly on hydrated size and charge. The differing hydrated radii of various ions are one important aspect to ion selectivity. Pores may also have a gating mechanism that can, by conformational change, open or close the pore to ion flow. A sensor, which may be voltage sensitive, controls the gating mechanism.

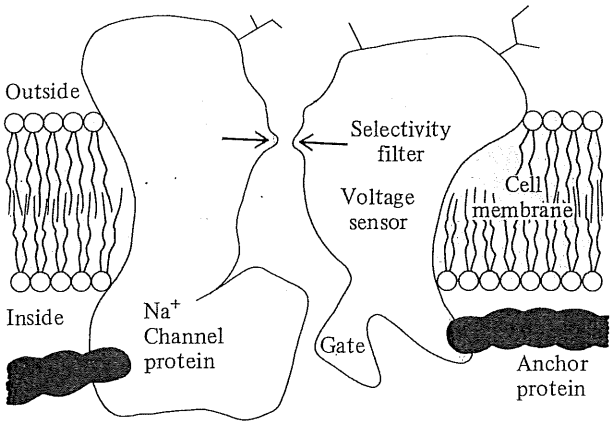

A

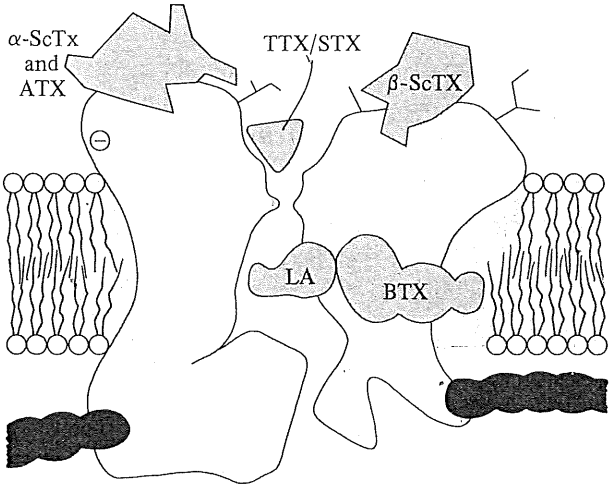

B

FIGURE 6–9 **(A)** Diagrammatic representation of an ionic channel with typical properties of selectivity (due to a size or charge-dependent selectivity filter) and a gating mechanism that is voltage dependent; a sensor portion of the protein channel acts as the sensor that monitors the transmembrane potential and alters the gating mechanism accordingly. **(B)** Tetrodotoxin (TTX) and saxitoxin (STX) are highly specific blockers of sodium channels; both bind to the external opening of the channel. Other toxins, such as batrachatoxin (BTX), scorpion toxins (α- and ß-ScTX), and anemone toxins (ATX) bind to other parts of the Na^+ channel and increase Na^+ conductance. LA, local anesthetic. *(Modified from Albuquerque, Daly, and Warnick* 1988.)

The identification of specific ion channels was aided greatly by the discovery of highly specific channel blocking agents. For example, tetrodotoxin (TTX), which is obtained from puffer fish and other fish of the Order Tetraodontiformes, and saxitoxin (STX) from the dinoflagellates *Gonyaulax*, specifically block the Na^+ channel when applied to the outside of the membrane (Figure 6–9B). Other agents also affect the Na^+ channel permeability. Various scorpion and anemone toxins (ScTX and ATX) prevent Na^+ channel inactivation. Batrachatoxin (BTX) from poison-arrow frogs increases Na^+ channel permeability.

Ionic Concentration Differences. In general, the intracellular fluid has a lower Na and Cl^- concentration and a higher K^+ concentration than the extracellular fluid. Ion gradients are summarized for frog and insect muscle in Table 6–4. The intracellular K^+ concentrations are about 10 to 60 × higher than the extracellular concentrations, whereas intracellu-

TABLE 6–4

Intracellular and extracellular ion concentrations for frog and insect muscle.

	$[\ ]_{inside}$	$[\ ]_{outside}$	$[\ ]_i / [\ ]_o$
Frog Muscle[1]	*Muscle Cell*	*Plasma*	
K^+	124	2.3	55
Na^+	10	109	0.092
Cl^-	1.5	77.5	0.019
Ca^{2+}	4.9[3]	2.1[3]	—
Insect Muscle[2]	*Muscle Cell*	*Hemolymph*	
K^+	86	11	7.6
Na^+	22	117	0.19
Ca^{2+}	3.4[3]	3.6[3]	—

[1] *(From Conway 1957.)*
[2] *(From Natochin and Parnova 1987.)*
[3] The total intracellular calcium concentration is given; the cytoplasmic calcium ion activity is considerably lower due to sequestration of calcium in sarcoplasmic reticulum and it is not meaningful to calculate the $[\ ]_i / [\ ]_o$ from these values.

lar Na^+ and Cl^- concentrations are only 0.02 to 0.30 × the extracellular values. There are similar differences for concentrations of other ions across the cell membrane.

Equilibrium Potentials

There are marked ionic concentration differences across cell membranes. The ultimate cause of these ion concentration gradients is the Na^+-K^+ ATPase, but it is irrelevant in this respect whether the pump is electrogenic or neutral. There are concentration gradients for many ions, K^+, Na^+, Cl^-, Ca^{2+}, Mg^{2+}, etc., but let us initially consider K^+ because it is normally quite permeable (so is Cl^- but why we needn't consider Cl^- here will be explained below).

Consider a selectively permeable membrane (permeable to K^+ but not Cl^-) separating a 1.0 M KCl solution (side 1) from a 0.1 M KCl solution (side 2; Figure 6–10A). K^+ ions tend to diffuse down their concentration gradient from the 1 M side to the 0.1 M side, thereby establishing a positive electrical potential on the 0.1 M side and a negative potential on the 1 M side. The K^+ ions will not continue to diffuse until the K^+ concentrations are equal on either side of the membrane because the establishment of an electrical potential causes K^+ movement from side 1 to side 2. At equilibrium, the magnitude of the membrane potential due to K^+ movement can be calculated from the Nernst equation

$$E_m = \frac{RT}{zF} \ln \frac{C_2}{C_1} = 0.058 \log_{10} \frac{0.1}{1.0} = -58 \text{ mV} \quad (6.6)$$

at 20° C. Which side of the membrane is negative and which is positive is indicated from the calculated sign of E_m if we remember that the potential of side 1 relative to side 2 is calculated if the concentration ratio is C_2/C_1 as above; side 1 had the high $[K^+]$ and its potential was negative with respect to side 2. If we had used the concentration ratio of C_1/C_2 or considered anion flux ($z = -1$), then we would calculate the potential of side 2 relative to side 1, as +58 mV. If in doubt about the polarity of the

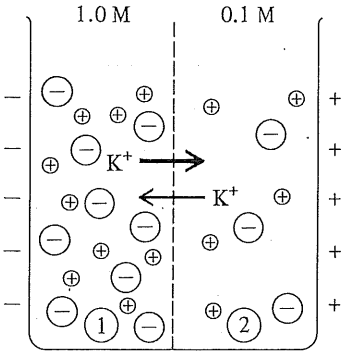

$$E_m = \frac{RT}{ZF} \ln \frac{C_2}{C_1} = -58 \text{ mV}$$

A

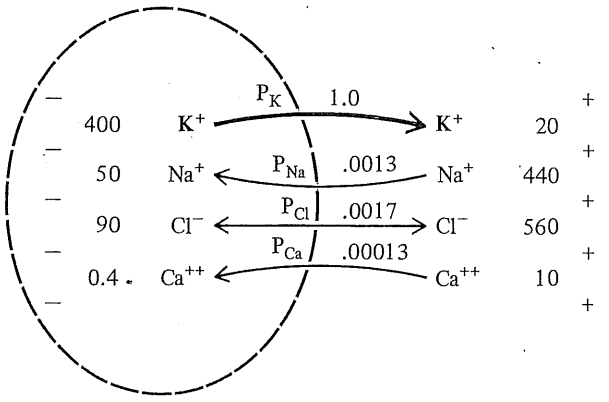

$$E_m = \frac{RT}{F} \ln \frac{[K^+]_o P_K + [Na^+]_o P_{Na} + [Cl^-]_{in} P_{Cl} + [Ca^{++}]_o^{\frac{1}{2}} P_{Ca}}{[K^+]_{in} P_K + [Na^+]_{in} P_{Na} + [Cl^-]_o P_{Cl} + [Ca^{++}]_{in}^{\frac{1}{2}} P_{Ca}} = -68 \text{ mV}$$

B

FIGURE 6–10 **(A)** Establishment of a membrane potential (E_m) due to passive distribution of potassium ions across a semipermeable membrane (permeable to K^+ but not Cl^-). The concentration-driven flux of K^+ (thin arrow) from the side with a concentration of 1.0 M KCl towards the side with a concentration of 0.1 M KCl is countered at equilibrium by an electrical-driven flux (thick arrow). The magnitude of the E_m can be calculated using the Nernst equation (at 20° C)

$$E_m = \frac{RT}{zF} \ln \frac{[K^+]_2}{[K^+]_1} = 58.2 \log_{10} \frac{[K^+]_2}{[K^+]_1} \text{mV}$$

(B) Establishment of a membrane potential across a cell membrane by passive distribution of ion species with differing permeabilities. The membrane potential can be calculated from the concentration differences and permeabilities for all ion species using the Goldman-Hodgkin-Katz equation; the greatest contribution to resting E_m is by K^+ (shown in bold) because of its high permeability. Concentration and permeability values are for the giant squid axon.

calculated membrane potential, just consider the direction of movement and charge for the permeable ion to determine which side is positive and which is negative.

What would happen if the membrane was permeable to both K^+ and Cl^-? Both ions would diffuse from side 1 to side 2, and at equilibrium their concentrations would be equal on either side of the membrane and there would be no membrane potential. However, it is of interest to consider in passing what happens during the equilibration process as well as at the equilibrium state. If the membrane was equally permeable to both K^+ and Cl^-, then we might expect no electrical potential to develop across the membrane. However, Cl^- ions have a higher mobility than K^+ ions ($7.92\ 10^{-8}$ and $7.62\ 10^{-8}$ cm^2 volt^{-1} sec^{-1} respectively), and so Cl^- ions diffuse more rapidly from side 1 to side 2 than do K^+ ions. This temporarily establishes a small electrical potential, negative on side 2 and positive on side 1. The magnitude of the transient membrane potential is calculated as

$$E_m = \frac{RT}{F}\frac{u^+ - u^-}{u^+ + u^-}\ln\frac{C_2}{C_1} \qquad (6.7a)$$

where u is the mobility of the + and − charged ions; for our example from above, side 1 is +1.1 mV with respect to side 2.

$$E_m = 58\,\frac{(7.62 - 7.92)}{(7.62 + 7.92)}\log_{10}\frac{0.1}{1.0} = +1.1\text{ mV} \qquad (6.7b)$$

What if we had used NaCl rather than KCl? Na^+ has a lower mobility than K^+ and Cl^-, of $5.19\ 10^{-8}$, and so the transient E_m is 12.1 mV, not 1.1 mV. The NaCl diffusion potential is much greater than the KCl diffusion potential. This is partly the reason for filling microelectrodes with a KCl solution rather than NaCl or some other solution; the small KCl diffusion potential that exists across the microelectrode tip due to differing ionic permeabilities doesn't affect the measurement of the membrane potential as much as would the higher NaCl diffusion potential.

The membrane potential calculated from the internal and external K^+ concentrations and Nernst equation (Equation 6.6) is called the **potassium equilibrium potential** (E_K), because it is the E_m if only the distribution of K^+ ions across the membrane contributes to the membrane potential. The value of E_K is readily calculated for the mammalian muscle cell as −98 mV (Table 6–5). The potassium equilibrium potential is approximately equal to the resting E_m because the potassium permeability is much greater than that of the other ions at rest, and as a first approximation K^+ is the only ion contributing to the E_m.

TABLE 6–5

Intracellular ([ ]$_i$) and extracellular ([ ]$_o$) concentrations and equilibrium potentials for major ions of mammalian skeletal muscle. *(Data from Hille 1984.)*

	[ ]$_o$	[ ]$_i$	[ ]$_o$/[ ]$_i$	E_{eq}[1]
Na^+	145	12	12	+67 mV
K^+	4	155	0.026	−98 mV
Cl^-	123	4.2	30	−90 mV
Ca^{2+}	1.5	$<10^{-7}$	>15000	+128 mV

[1] $E_{eq} = \frac{RT}{zF}\ln\frac{[\,]_o}{[\,]_i} = 61.54\log_{10}\frac{[\,]_o}{[\,]_i}$ mV at 37° C.

If Na^+ had been the more important ion, then the E_m would be closely approximated by the **sodium equilibrium potential** (E_{Na} = +67 mV). The resting membrane potential is not close to the sodium equilibrium potential, but the membrane potential of excitable cells does approach the E_{Na} during an action potential (see below).

We can similarly calculate the **chloride equilibrium potential** (E_{Cl}) as −90 mV. The chloride equilibrium potential, like the potassium equilibrium potential, is close to the resting membrane potential. This is because chloride is passively distributed across the membrane. The intracellular-extracellular ratio of Cl^- is not due to active transport but to passive distribution in response to the normal E_m; the intracellular potential is negative, so the intracellular chloride concentration is low. This is why chloride can be omitted from the Goldman-Hodgkin-Katz equation without serious error. In some cells, P_{Cl} is fairly low whereas it is high in other cells.

An equilibrium potential can be calculated for any other ion present in biological systems. For example, the calcium equilibrium potential (E_{Ca}) is +128 mV.

Goldman-Hodgkin-Katz Potential

Animal cells are not such simple systems as K^+Cl^- solutions; many other ions are present, especially Na^+. Fortunately, it is relatively easy to extend the Nernst equation to a more complex form that can describe the electrical potential across biological membranes. All we need to appreciate is that (1) any + charged ion is equivalent to any other + charged ion, electrically speaking, i.e., Na^+ is electrically equivalent to K^+, and (2) the contribution of any ion species to the membrane potential depends not only on its charge, but also on its

permeability, i.e., freely permeable ions will readily diffuse down their concentration gradient and contribute to E_m, whereas impermeable ions will not diffuse across the membrane and cannot contribute to the E_m. The net contribution of any ion species (X) by movement in one direction across a membrane is therefore equal to the product of its concentration on that side and its permeability, i.e., $[X].P_X$. The Goldman-Hodgkin-Katz equation calculates the E_m from all species of ion present by taking into account for each ion its concentration on each side of the membrane and its permeability; the general form is as follows.

$$E_m = \frac{RT}{F} \ln \frac{[K^+]_o.P_K + [Na^+]_o.P_{Na} + [Cl^-]_i.P_{Cl} + [Ca^{2+}]_o^{\frac{1}{2}}.P_{Ca} + \ldots}{[K^+]_i.P_K + [Na^+]_i.P_{Na} + [Cl^-]_o.P_{Cl} + [Ca^{2+}]_i^{\frac{1}{2}}.P_{Ca} + \ldots} \quad (6.8a)$$

Figure 6–10B shows this concept diagrammatically for four of the major ions: K^+, Na^+, Cl^-, and Ca^{2+}. The extracellular, or outside, concentration of ions is placed in the numerator by convention so that the calculated potential is that of the inside relative to the outside. Note that for anions the outside concentration is in the denominator. The charge term z must be incorporated into the log term. Hence, the $[Ca^{2+}]$ term is raised to the power $1/z$, i.e., 1/2; the power terms for Na^+ and K^+ are omitted for clarity since $1/z$ is 1. For Cl^-, $z = -1$ and so the $[Cl^-]_i$ is in the numerator and $[Cl^-]_o$ is in the denominator. Fortunately, this equation can be greatly simplified to

$$E_m = \frac{RT}{F} \ln \frac{[K^+]_o.P_K + [Na^+]_o.P_{Na}}{[K^+]_i.P_K + [Na^+]_i.P_{Na}} \quad (6.8b)$$

This is possible because many ions (e.g., Ca^{2+}) are not very permeable, and Cl^- can generally be ignored (even though it may be fairly permeable) because it is passively distributed across the membrane and its permeability remains constant (see below). Furthermore, K^+ is normally much more permeable than Na^+, and so a further simplification is possible.

$$E_m = \frac{RT}{F} \ln \frac{[K^+]_o}{[K^+]_i} \quad (6.8c)$$

How well does the measured E_m conform to the value calculated from the above equations? Very well, in fact! Table 6–6 summarizes ion concentrations and permeabilities for squid giant axons, and shows that the measured E_m of −68 mV is closely matched by the calculated E_m from Equation 6.8a (−74 mV) and Equation 6.8b (−74 mV). The most simplified form of the Goldman-Hodgkin-Katz equation (Equation 6.8c; −74 mV) also closely estimates the E_m.

TABLE 6–6

Intracellular and extracellular ionic concentrations (mEq l^{-1}), and relative membrane permeabilities for the squid giant axon. These data are used to calculate the resting membrane potential using the Goldman-Hodgkin-Katz equation using all four ions, the simplified equation for only Na^+ and K^+, and only K^+ (i.e., the potassium equilibrium potential). The equilibrium potentials for each ion are calculated using the Nernst equation. Values are calculated at 15° C assuming $\frac{RT}{F} \log_{10} = 57.17$. *(Data from Curtis and Cole 1942; Hodgkin 1958; Meves and Vogel 1973).*

	$[\ ]_i$	$[\ ]_o$	Relative P
Na^+	50	440	0.0013
K^+	400	20	1.0
Cl^-	90	560	0.0017
Ca^{2+}	0.4	10	0.00013

Goldman-Hodgkin-Katz Equation

$$E_m = \frac{RT}{F} \ln \frac{[K^+]_o P_K + [Na^+]_o P_{Na} + [Cl^-]_i P_{Cl} + [Ca^{2+}]_o^{\frac{1}{2}} P_{Ca}}{[K^+]_i P_K + [Na^+]_i P_{Na} + [Cl^-]_o P_{Cl} + [Ca^{2+}]_i^{\frac{1}{2}} P_{Ca}} = -73.6 \text{ mV}$$

Short version of Goldman-Hodgkin-Katz Equation

$$E_m = \frac{RT}{F} \ln \frac{[K^+]_o P_K + [Na^+]_o P_{Na}}{[K^+]_i P_K + [Na^+]_o P_{Na}} = -73.7 \text{ mV}$$

Equilibrium Potentials

$$E_K = \frac{RT}{F} \ln \frac{[K^+]_o}{[K^+]_i} = -74.4 \text{ mV}$$

$$E_{Na} = \frac{RT}{F} \ln \frac{[Na^+]_o}{[Na^+]_i} = +54.0 \text{ mV}$$

$$E_{Cl} = \frac{RT}{F} \ln \frac{[Cl^-]_i}{[Cl^-]_o} = -45.4 \text{ mV}$$

$$E_{Ca} = \frac{RT}{2F} \ln \frac{[Ca^{2+}]_o}{[Ca^{2+}]_i} = +40.0 \text{ mV}$$

Actual $E_m = -68$ mV

Further experimental evidence for the applicability of the Goldman-Hodgkin-Katz equation is the close match between measured and calculated E_m when the external $[K^+]$ and $[Na^+]$ are altered from their normal values (Figure 6–11). The internal $[K^+]_i$ is assumed to remain constant at 140 mEq l^{-1}, but the external $[K^+]_o$ and $[Na^+]_o$ concentrations can be readily manipulated by changing the bathing medium; the E_m can be calculated using either Equation 6.8b or Equation 6.8c, by assuming $P_K = 1.0$ and $P_{Na} = 0.01$ (the denominator term $[Na^+]_i.P_{Na}$ is totally ignored because both $[Na^+]_i$ and P_{Na} are small). There is a close correspondence between measured E_m and calculated E_m using Equation

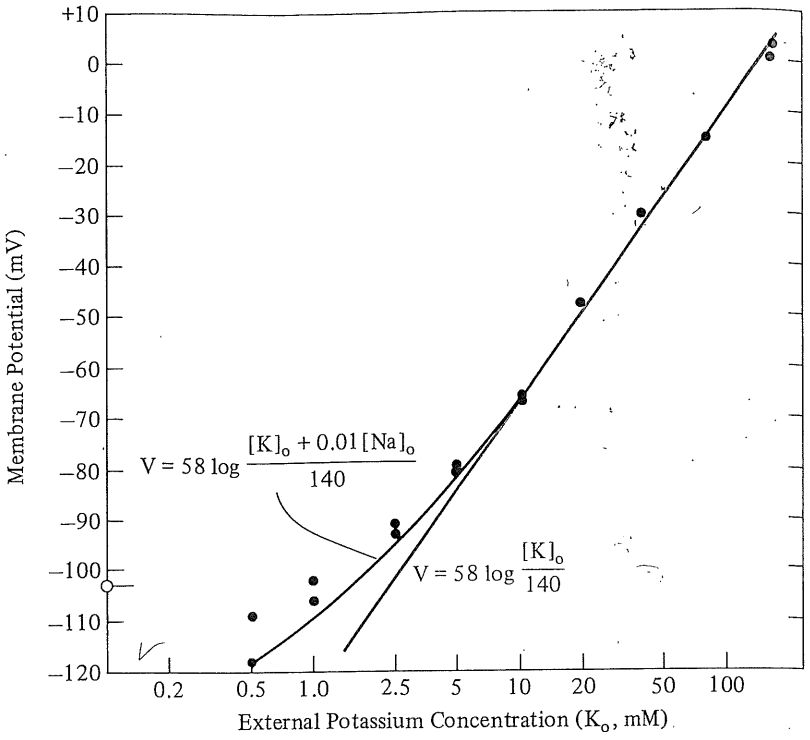

FIGURE 6–11 The predominant role of K^+ distribution across a muscle cell membrane in determining the membrane potential is apparent from experimental manipulation of the extracellular K^+ concentration ($[K^+]_o$), from the normal value of about 5 mM to as low as 0.5 mM and over 100 mM. The measured E_m is approximately calculated using the Nernst equation for K^+ distribution (color line); the deviation of actual E_m from estimated E_m at low $[K^+]_o$ is due to the relatively greater importance of the Na^+ distribution even though the sodium permeability is lower than the potassium permeability. The measured E_m is closely estimated by the Goldman-Hodgkin-Katz equation accounting for K^+ and Na^+ concentrations, assuming a ratio of permeabilities of 1:0.01 (K^+:Na^+) and an internal $[Na^+]$ of 0 (black line). *(Modified from Hodgkin and Horowicz 1959.)*

6.8B, and a good fit using Equation 6.8C, except at the lowest $[K^+]_o$ where the contribution of $[Na^+]$ becomes significant.

Conductance, Current, and Capacitance

The complex biological membrane can be represented as a simple electrical circuit that has equivalent electrical properties as the membrane. The membrane is essentially a low-voltage battery that establishes an electrical potential; the ion-specific pores of the membrane are pathways for electrical flow equivalent to resistors (or conductors; conductance = 1/resistance); the lipid bilayer portion of the membrane is a capacitor, keeping electrical charges separated on either side of the membrane. Such an electrical analog of the cell membrane is shown in Figure 6–12, superimposed over a representation of the structure of a membrane. We have already discussed the origin of the membrane potential (the "battery").

The membrane conductance (g; mho cm^{-2}) is the electrical analog of membrane permeability. The units for conductance are the inverse of resistance, since $g = 1/R$; if the membrane resistance to electrical flow is measured in ohms cm^{-2}, then g has units of ohm^{-1} cm^2, or mho cm^2. The terms "permeability" and "conductance" are not identical in meaning although they are related. Conductance depends on the permeability and driving force for movement. A low permeability means that conductance is low, but a high permeability does not necessarily mean that the conductance is high. Ions will only move across a membrane if they are present and if there is a driving force, regardless of their permeability. For example, a membrane might have a high permeability to lithium (Li^+) through Na^+ channels, but the Li^+ conductance would be low because Li^+ ions are not present in biological fluids.

Ohm's law summarizes the relationship between voltage difference (E), resistance (R), conductance (g), and current (I) for an electrical resistor.

$$I = E/R \quad \text{and} \quad I = Eg \tag{6.9a}$$

The relationship is not as simple for biological membranes because current flow across a membrane, due to any particular ion species, depends on both the ionic conductance (g) and the electrochemical gradient (E). There is no current flow when the E_m is equal to the equilibrium potential of that that ion, but there is current flow if $E_m = 0$ mV and $E_{eq} \neq 0$. The electrical potential that drives the current flow of an ion is therefore not E_m but $E_m - E_{eq}$. The relationship between current flow, conductance, and E_m is different for each ion species, depending on their equilibrium potential.

$$\begin{aligned} I_K &= g_K(E_m - E_K) \\ I_{Na} &= g_{Na}(E_m - E_{Na}) \\ I_{Cl} &= g_{Cl}(E_m - E_{Cl}) \end{aligned} \tag{6.9b}$$

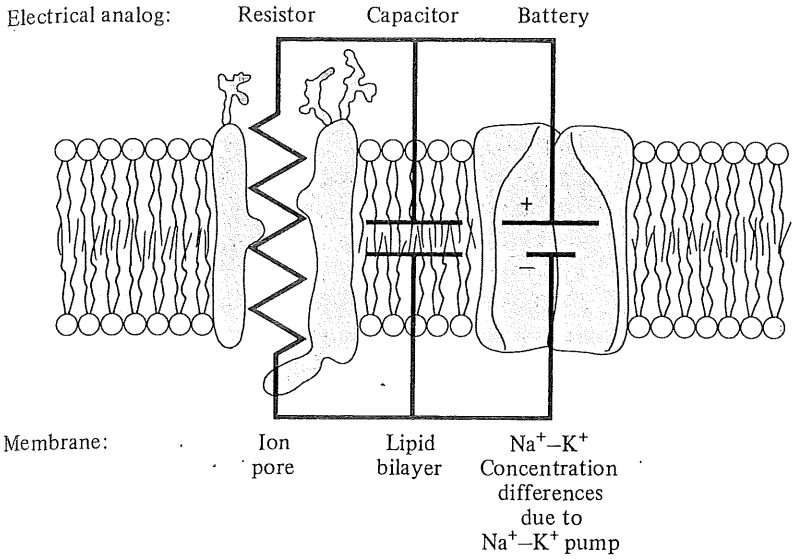

FIGURE 6–12 The basic electrical analog model of a cell membrane consists of an electrochemical gradient equivalent to an electrical potential (or battery) due to the Na^+/K^+ concentration differences across the membrane, a capacitor (due to the membrane lipid bilayer), and a resistor (ion-specific pores allow ion flow and are the membrane "resistors").

Current flow is low if conductance (and permeability) is low and/or the electrical gradient is low.

Capacitance (C; Farads) is a measure of how much charge (Q; Coulombs) can be maintained across an insulating gap at a certain voltage (E; Volts). A 1 farad capacitor can separate 1 coulomb of charge (1 coulomb = 6.24 10^{18} charges) with a 1 volt difference. The capacitance of two parallel plates depends on their separation distance (d), area of the plates (A), and the dielectric constant of the medium separating the plates (k)

$$C = Q/E = k\epsilon_o A/d \qquad (6.10)$$

where ϵ_o is the permittivity of free space (8.85 10^{-12} C V^{-1} m^{-1}). For example, a 1 cm^2 capacitor separated by 10 nm of air (k = 1) has a capacitance of about 0.09 μF.

The lipid bilayer of biological membranes is an effective capacitor because it separates charged ions across a very thin gap (about 10 nm) and has a high-dielectric constant (k = 10). The capacitance of cell membranes is generally about 1 μF cm^{-2}. Cell membranes sustain a high-voltage gradient, e.g., 100 mV/10 nm is equivalent to 10^7 V m^{-1}. This exceeds the dielectric strength (the maximum voltage gradient without electrical breakdown) of air (3 10^6 V m^{-1}).

The capacitance of membranes is important because it contributes an additional transient current whenever there is a change in membrane potential. Whenever a capacitor charges or discharges, there is a transient current flow until the voltage reaches the new equilibrium value. The capacitor-discharge current depends on the rate of voltage change ($\Delta E/\Delta t$)

$$I = C\Delta E/\Delta t \qquad (6.11a)$$

The voltage across a discharging capacitor declines in an exponential manner over time

$$E = E_0 e^{-t/RC} \qquad (6.11b)$$

where E is the instantaneous voltage, E_0 is the initial voltage, t is time, C is the capacitance, and R is the resistance discharging the capacitor. The exponential discharge of such a resistance-capacitance (RC) circuit is shown in Figure 6–13A. The values of R and C determine the rate of discharge; a high time constant ($\tau = RC$) confers a low rate of charge or discharge. The voltage decays to $1/e$ (0.367) of the initial E_0 after 1 time constant (RC seconds); the voltage further decreases to $1/e$ of the value after each successive time constant.

Membranes, although more complex in structure than an electrical capacitor, behave similarly; the value of R_mC_m for a cell membrane is the **membrane time constant**, τ_m. For biological membranes, τ_m varies from about 10 μsec to 1 sec, corresponding to an R_m of 10 to 10^6 Ω cm^2. An example of the measurement of the membrane parameters, τ_m, C_m, and R_m, for a protozoan (*Paramecium*) is shown in Figure 6–13B. Injection of a current (I_m) into the protozoan causes an exponential change in E_m, with a time constant of about 60 msec. Since C is approximately 1 μF cm^{-2} then R must be about 60000 Ω cm^2. A current of about 0.23 nA results in a voltage change of about 23 mV, hence the membrane resistance is about 10^8 Ω. The membrane area of *Paramecium* is therefore about 6 10^{-4} cm^2.

The net current flow across a membrane is the sum of all ionic currents and any charging or discharging current flow if there is a change in membrane potential.

$$I_{total} = \Sigma I_{ion} + C_{membrane}\,\Delta E/\Delta t \qquad (6.12)$$

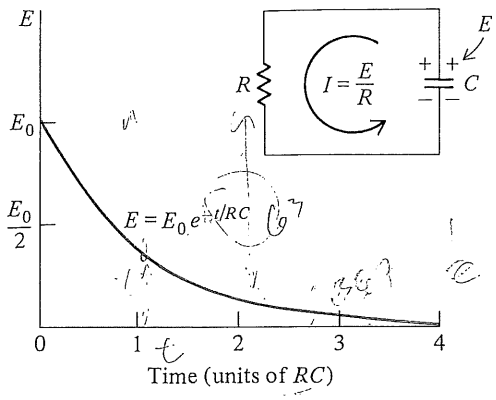

A

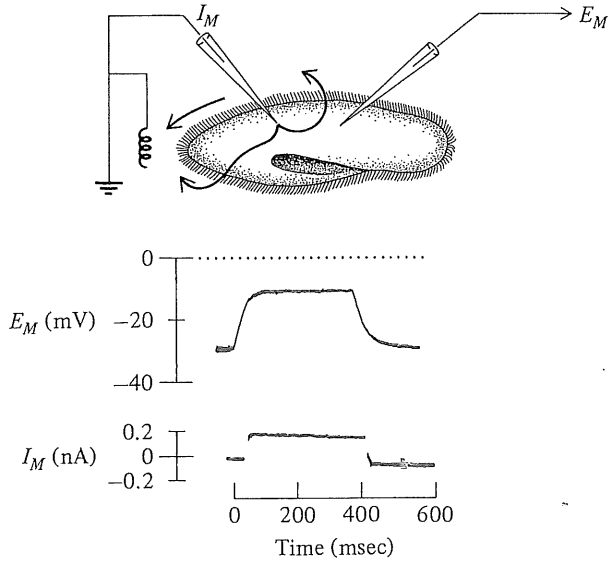

B

FIGURE 6–13 **(A)** An *RC* circuit (above) is a simple electrical analog showing the exponential nature of capacitor (*C*) discharging through a resistance (*R*). The magnitude of the current flow (*I*) depends on the voltage across the capacitor (*E*). The direction of the "conventional" current is indicated (i.e., direction of flow of + charges). The capacitor discharges in an exponential fashion (below) as the initial electrical potential across the *RC* circuit (E_o) declines to zero, with a time course dependent on the values for *R* and *C*; the value of *E* is 36.7% of E_o after one time constant (*RC*). **(B)** The cell membrane of the protozoan *Paramecium* acts as an *RC* circuit, showing exponential charging and discharging when an exogenous current is injected across the cell membrane. The membrane time constant τ_m is estimated to be about 60 msec, and the membrane resistance about 10^8 Ω since an injected current of 0.23 namp causes a change in E_m of 23 mV. *(From Hille 1984; Kung and Eckert 1972.)*

If the membrane voltage is held constant (i.e., "clamped" at a specified value by an external electrical circuit), then $\Delta E/\Delta t = 0$ and any measured current is an ionic flux current rather than a capacitance current, i.e., voltage clamping a membrane enables the direct measurement of ionic current. A voltage clamp only works if the time constant for the clamping circuit is considerably shorter than the membrane time constant.

Only a small number of ions are involved with cell electrical phenomena. Consider a cell membrane permeable to K^+ but not Cl^-, with $R_m = 1000\ \Omega\ cm^{-2}$; $C_m = 1\ \mu F\ cm^{-2}$; $\tau_m = 1$ msec. If we add two KCl solutions with a concentration ratio of 1:52 across the membrane, then the membrane potential increases exponentially over time from 0 to 100 mV ($E_m = RT/F \ln(1/52) = 100$ mV) with a time constant of 1 msec. The system reaches equilibrium after only a few msec and the amount of charge now distributed across the membrane is equal to 10^{-7} coulomb cm^{-2} ($Q = E.C_m = 0.1 \cdot 1\ \mu F\ cm^{-2} = 10^{-7}$ coulomb cm^{-2}). How many K^+ ions moved? The number is *Q*/*F*, or 10^{-12} moles $K^+\ cm^{-2}$. This is such a tiny amount of K^+ that it would hardly affect the original concentration of K^+ on either side of the membrane. Thus, significant electrical potentials can be generated very rapidly by the movement of only a few ions through a few membrane pores. The actual effect on ionic concentration of such an ionic flux through a membrane to establish a membrane potential depends on the ratio of membrane surface to cytoplasmic volume. For a 1000 μ diameter giant squid axon, a K^+ flux of 10^{-12} moles cm^{-2} alters the K^+ concentrations by only about $1/10^5$. For a tiny cell dendrite, e.g., 0.1 μ diameter, the surface-to-volume ratio is about 10^4 times higher and the K^+ flux might alter the K^+ concentrations significantly, by 10% or so.

Excitable Cell Membranes

All cell membranes have an electrical potential because there is an ionic concentration gradient across membranes. The membrane potential is stable in some cells but often transiently increases, forming an **action potential** in excitable cells (primarily sensory, nerve, and muscle cells).

Action Potentials

The cell membrane is essentially an electrical circuit with a capacitance and parallel resistances for the flow of each ion, e.g., K^+, Na^+, and Cl^-. The most important ions are, as we shall see, Na^+ and K^+,

and their resistances are variable. In addition, each ionic resistance is in series with the equilibrium potential of each ion. For example, there is no current flow due to potassium ions if $E_m = E_K$; the E_m for no K current flow is not 0 mV!

The resting membrane potential is approximately equal to the potassium equilibrium potential. Let us now consider what happens if K^+ is not the most permeable ion. If Cl^- becomes the most permeable ion, then the rather uninteresting effect is to shift the E_m towards the E_{Cl}, which is very similar to the resting E_m. However, what if Na^+ became the most permeable ion? The sodium equilibrium potential is very different (about +65 mV) from the resting E_m, E_K, and E_{Cl}. Thus, increasing Na^+ conductance (g_{Na}) by 1000 × would dramatically shift the E_m from −90 mV to +65 mV (Figure 6–14a). This change in E_m from resting E_m towards 0 mV and positive mV values (i.e., towards E_{Na}) is **depolarization**. If the g_{Na} returns to normal, then the E_m returns to resting E_m; this is **repolarization**. The membrane potential becomes even more negative than resting E_m (moves towards E_K) if the K^+ conductance is increased; this is **hyperpolarization**. This rather simplistic analysis of depolarization and hyperpolarization in response to increases in g_{Na} and g_K conductance is actually quite similar to the events during an action potential.

An action potential is a rapid, transient (about 1 to 2 msec) depolarization of the cell membrane potential, followed by a rapid repolarization and transient hyperpolarization (Figure 6–14B). The action potential transfers information from one cell (e.g., a sensory cell or neuron) to another (e.g., a neuron or effector cell). The mechanisms for information exchange will be detailed more thoroughly in Chapter 7. Here, it is sufficient to note that all action potentials are essentially identical and information is transferred by the frequency of action potential firing, rather than by the specific shape or amplitude. This information transfer is more like digital information in a computer (i.e., "On"–"Off", or "0"–"1" information) rather than analog voltage information (i.e., any voltage within a continuous range, such as from 0 to 5 volts).

Action potentials are initiated by the depolarization of a resting membrane. There can be many causes of an initial depolarization. For sensory cells, the depolarizing stimulus may be photons of light, heat, sound, movement, etc. For nerve cells, it may be an action potential in a sensory cell or another nerve cell. For muscle or secretory cells, it is usually an action potential in a nerve cell. If the depolarization reaches or exceeds a critical E_m, called the **threshold**, then an action potential occurs

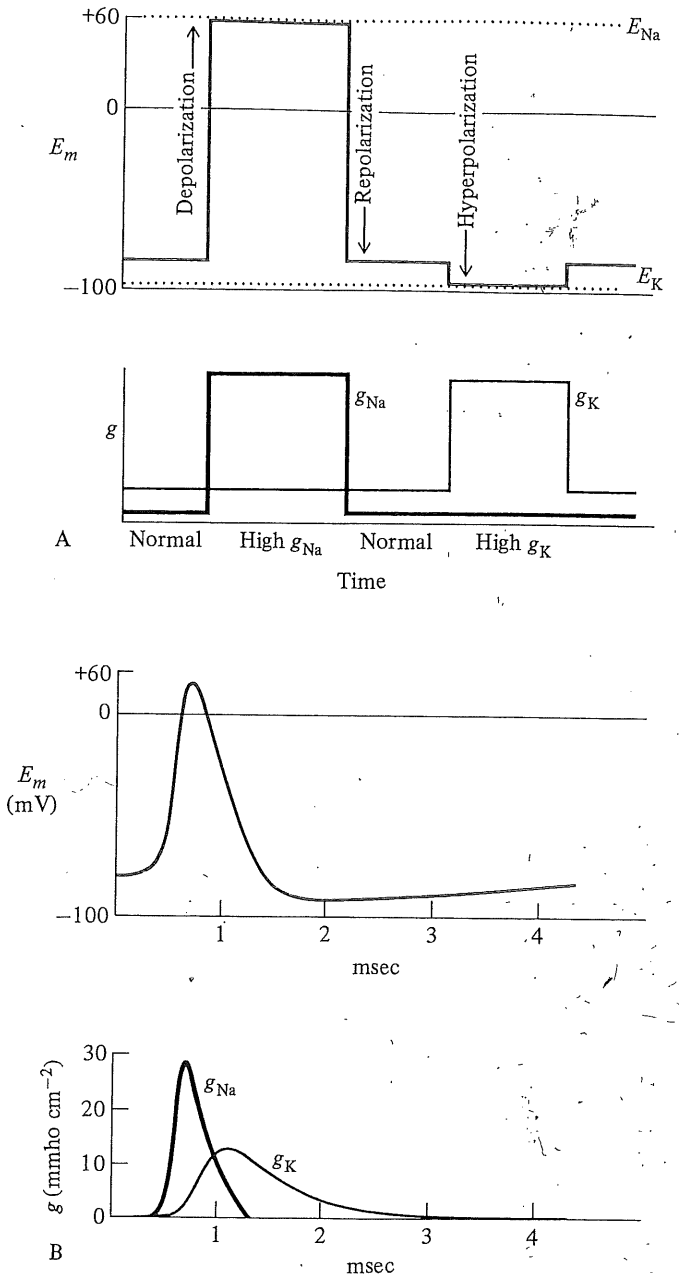

FIGURE 6–14 **(A)** A simple model of changes in membrane conductance (g) that alter the membrane potential. A transient increase in Na^+ permeability depolarizes the E_m towards the sodium equilibrium potential (E_{Na}); a subsequent transient increase in potassium permeability hyperpolarizes the E_m towards E_K. The actual changes in E_m and g_{Na}/g_K are much more complex (see part B). **(B)** Changes in membrane conductance (mmho cm^{-2}) to sodium (g_{Na}) and potassium (g_K during a nerve action potential, and the change in cell membrane potential (E_m; mV) due to ionic conductance changes.

(see below). If the depolarization does not reach threshold (is subthreshold), then an action potential will not be initiated; the E_m will return to the normal resting value. An action potential is "all-or-none"; it either occurs or it doesn't. There is (normally) no such thing as a "small" action potential or a "big" action potential.

The mechanism for an action potential is a change in ionic conductance, in particular Na^+ conductance (g_{Na}). The membrane potential E_m affects the sodium permeability of the cell membrane; the sodium permeability is **voltage dependent** (Figure 6–15). There is also a voltage dependence of the potassium permeability; the magnitude of the change is similar for K^+ but the change occurs considerably more slowly. The voltage-dependent increase in Na^+ conductance is responsible for initiating an action potential. An increase in Na^+ conductance causes the E_m to move towards E_{Na}; this change in E_m will itself further increase g_{Na}. If depolarization reaches threshold, there is a rapid progressive opening of all Na^+ channels such that Na^+ conductance increases to about 1000 × resting; this exceeds the resting potassium conductance by about 100 ×. This positive feedback between depolarization and increased g_{Na} results in a rapid and maximal increase in E_m and g_{Na}. The E_m approaches the sodium equilibrium potential since $g_{Na} >> g_K$, but rapidly repolarizes because the Na^+ channels automatically close and g_{Na} declines. The E_m at any point during an action potential can be approximately calculated from the instantaneous g_{Na} and g_K values using the short version of the Goldman-Hodgkin-Katz equation (Equation 6.8b). A rapid rise then fall in g_{Na} would cause a fairly symmetrical action potential, but in practice the action potential is followed by a short period of hyperpolarization due to a delayed increase of potassium permeability. Supplement 6–1 (page 248) summarizes the model of an action potential proposed by Hodgkin and Huxley.

There is a similar voltage dependence of K^+ conductance on E_m and also a feedback cycle for K^+ conductance. However, the K^+ cycle is a negative feedback or stabilizing cycle. Depolarization increases g_K causing K^+ efflux from the cell, and the K^+ efflux repolarizes the E_m. One role of the increase in K^+ conductance and hyperpolarization after the action potential spike is to return the E_m to normal and to stabilize it from further changes. This, and the property of the Na^+ channels to temporarily remain inactivated after activation, ex-

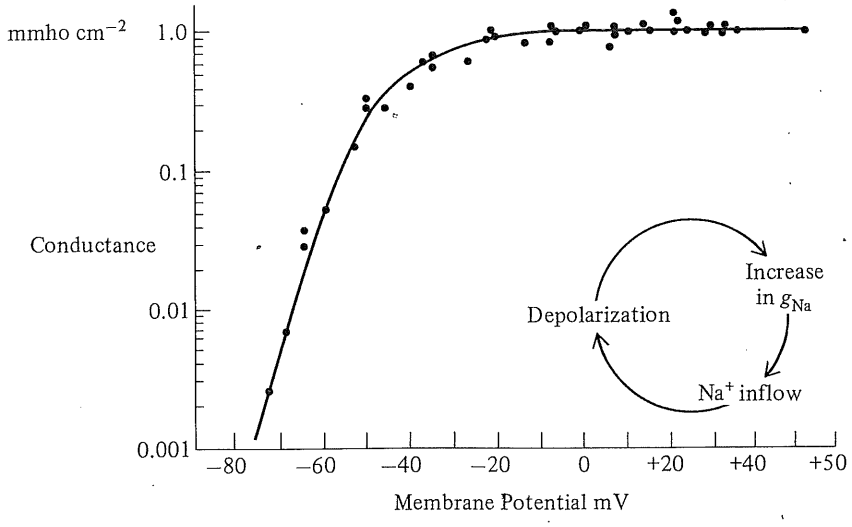

FIGURE 6–15 The ionic conductance of the giant squid axon for Na^+ (and K^+) is highly voltage dependent; g_{Na} increases from about 0.002 for the resting membrane to 1.0 mmho cm^{-2} for a membrane depolarization of 120 mV, and g_K increases from 0.02 to 1.0 mho cm^{-2}. The rate of change in conductance (mmho cm^{-2} sec^{-1}) is about 15 times faster for g_{NA} than g_K; the change in g_K is therefore limited during an action potential by the rapid repolarization (after about 0.5 to 1.0 msec). The voltage dependence of the g_{Na} leads to a positive-feedback relationship between membrane potential and g_{Na} (whereas the voltage dependence of g_K is a negative-feedback, stabilizing effect). *(Modified from Hodgkin and Huxley 1952.)*

plains the inability of a membrane to support a second action potential during, or soon after, a previous action potential. This period when a membrane cannot be stimulated to support an action potential is called the **absolute refractory period.**

The extracellular fluids of most animals contain high levels of Na^+ and low levels of K^+. However, many of the "higher" insects, especially phytophagous insects that consume copious amounts of plant material, have remarkably different extracellular ion concentrations than other insects; the extracellular K^+ and Mg^{2+} concentration is high, and the Na^+ level is low (Florkin and Jeuniaux 1974; Treherne and Maddrell 1967; Mullins 1985). This perhaps reflects the low Na^+ and high K^+ levels and high ingestion rates of food. These unusual extracellular ion concentrations would have dramatic implications for the electrical properties of excitable cells, both resting membrane potential and action potential spikes. For example, the stick insect *Carausius* has a higher extracellular $[K^+]$ than $[Na^+]$ (Table 6–7). The resting E_m estimated as the potassium equilibrium potential for hemolymph-intracellular fluid is -70 mV, whereas the actual value is -25 mV. The calculated peak E (i.e., E_{Na}) for an action potential is -37 mV; this is more negative than the resting E_m! Either the hemolymph and/or intracellular Na^+ and K^+ concentrations used to calculate these E_m's are incorrect, or there is a fundamentally different mechanism for action potential initiation and propagation in phytophagous insects, or the extracellular fluid around the nerve cells has a different composition from hemolymph.

The nerve cord of the stick insect is surrounded by a sheath of fat-body cells, which forms an extraneural space between the axons and the hemolymph (Figure 6–16). The fluid in this extraneural space has a higher Na^+ and K^+ than hemolymph because of ionoregulation by the fat-body cell membranes. The E_K calculated using the extraneural and intracellular K^+ concentrations is -38 mV, which is considerably closer to the observed E_m than the value of -70 mV obtained using the hemolymph concentration. The peak E_m during an action potential (E_{Na}) is calculated to be $+23$ mV, which is

TABLE 6–7

Estimated intracellular and extracellular ionic concentrations (mM) for the stick insect at 18° C, and potassium and sodium equilibrium potentials calculated using the ratio of hemolymph:intracellular concentration and nerve cord fluid:intracellular fluid. The resting E_m is more closely calculated from the nerve cord fluid:intracellular K^+ concentrations and action potential spike from the nerve cord fluid:hemolymph Na^+ concentrations. *(Data from Treherne 1965; Treherne and Maddrell 1967.)*

	Hemolymph (*H*)	Extracellular (in sheath around nerve cord) (*E*)	Intracellular (neuron) (*I*)
Na^+	20.1	212.4	86.3
K^+	33.7	124.5	555.8
Ca^{2+}	6.4	2.2	61.8
Mg^{2+}	61.8	117.4	10.7
	H/I [1]	*E/I* [2]	
E_K	−70.4	−37.6	Resting E_m = −25 mV
E_{Na}	−36.6	+22.6	Peak E_m +59 mV

[1] $E_m = 57.8 \log_{10}$ Hemolymph/Intracellular
[2] $E_m = 57.8 \log_{10}$ Extracellular/Intracellular

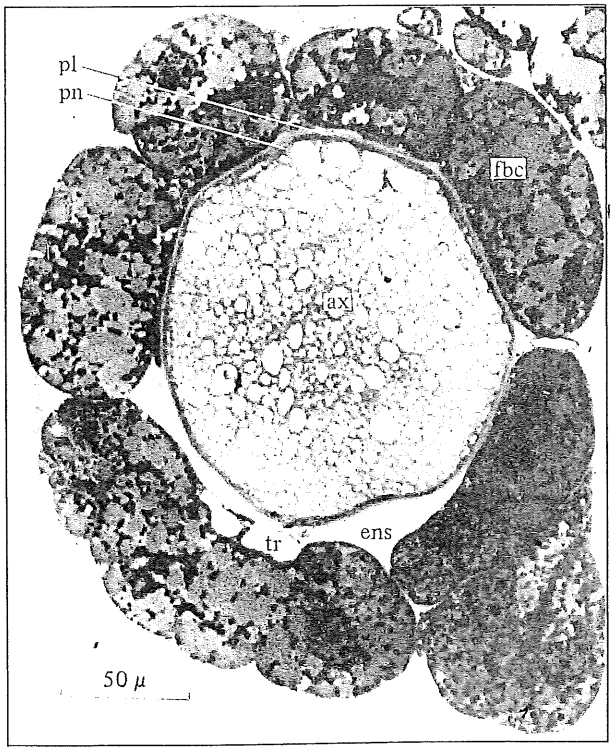

FIGURE 6–16 A sheath of fat-body cells (*fbc*) surrounds the interganglionic nerve connective between thoracic ganglia of the stick insect, leaving only a narrow connection to the extraneural space (*ens*); *ax*, axons; *pl*, acellular nerve cord perilemma; *pn*, cellular perineurial layer surrounding the nerve cord; *tr*, trachea. *(From Treherne and Maddrell 1967.)*

closer to the observed +59 mV than is −37 mV, the E_{Na} calculated from hemolymph concentrations. Thus, consideration of the composition of the extraneural fluid better explains the electrical properties of the muscle cells of this phytophagous insect.

Role of Ion Channels. There are many different types of ion channels (Table 6–8). Na^+ channels are relatively less diverse than K^+ and Ca^{2+} channels and have only one major function—to initiate rapid depolarization of the transmembrane potential of excitable cells. Their ion selectivity is relatively constant ($Na^+ = Li^+ > K^+$), and the pharmacology of various receptor sites of the Na^+ channel is constant (there is an external TTX/STX receptor, an external polypeptide receptor, a hydrophobic receptor, and an internal receptor for local anesthetics). Potassium channels are much more diverse,

TABLE 6–8

Properties of various ion channels for excitable cell membranes that exhibit voltage-dependent permeability change.

Channel	Properties	Role	Blocker
Sodium			
I_{Na}	Rapidly activated by depolarization with voltage-dependent activation and inactivation.	Current responsible for action potential, e.g., nerve, muscle membranes.	TTX[1]
Potassium			
Delayed rectifier $I_{K(V)}$	Delayed activation by depolarization.	Rapidly repolarizes membrane after an action potential.	Ca^{2+} TEA[2]
Fast transient $I_{K(A)}$	Activated by depolarization, inactivated by prolonged depolarization; inactivation removed by hyperpolarization.	Repetitive pacemakers.	Low TEA[2]
Calcium Activated $I_{K(Ca)}$	Voltage-dependent and activated by intracellular Ca^{2+}; higher conductance than other K channels.	Terminates Ca^{2+} entry into cells; causes long hyperpolarizing pauses, e.g., bursting pacemakers.	Apamin TEA[2] Cs^+
Inward rectifying $I_{K(X_1)}$ $I_{K(K_2)}$	Inactivated by depolarization; activated by hyperpolarization.	Decreases K conductance during prolonged depolarization for energy economy and to maximize I_{Na}, e.g., cardiac muscle.	Cs^+ TEA[2] Rb^+
Calcium			
I_{Ca}	Activated by strong depolarization; low current; slow and incomplete inactivation with prolonged depolarization; intracellular Ca^{2+}-dependent inactivation.	Regulation of intracellular Ca^{2+} for control of a variety of cellular functions, i.e., secretion, muscle contraction, ionic gating.	Verapamil Nifedipine D-600
Chloride			
I_{Cl}	Some are weakly voltage dependent ("background" channels) or strongly voltage dependent.	"Background" channels stabilize resting E_m.	Anthracene-9-carboxylic acid Thiocyanate

[1] TTX = tetrodotoxin.
[2] TEA = tetraethylammonium.

functioning in many different roles: some open rapidly, some slowly, most open if the E_m becomes less negative, but some open if it becomes more negative. They can help stabilize the resting membrane potential, make the E_m more negative, or produce a plateau potential (see below). There are four main types of K channels: (1) delayed rectifiers, (2) Ca^{2+}-dependent K channels, (3) A channels, and (4) inward rectifier channels. These are defined mainly by their gating characteristics, and their functions will be described below. Chloride channels generally lack voltage dependence, and simply stabilize the resting cell membrane potential, although some giant algae apparently have Cl^- channels that initiate action potentials. Many synaptic membranes also have Cl^- channels. Ca^{2+} channels are found in all excitable cells; they close more slowly than Na^+ channels, and therefore they can produce long-term depolarization. They also have the essential role of transducing membrane depolarization into nonelectrical events, such as glandular secretion, vesicle exocytosis, and muscle contraction.

Sodium channels. The single most important event during an action potential is the initial rapid increase in Na^+ conductance. The activation gating mechanism for the Na^+ channel is voltage dependent, i.e., the g_{Na} depends on E_m. An increase in g_{Na} further depolarizes the membrane, increasing g_{Na}. Thus, a positive-feedback cycle is initiated once the depolarization reaches some critical E_m and g_{Na}; there follows a rapid and complete activation of all Na^+ channels. This critical E_m is the threshold value.

An equally important property of the Na^+ channels is inactivation. Once an Na^+ channel is activated, it is automatically inactivated soon afterward by a mechanism that is essentially independent of the activating mechanism.

Potassium channels. There are a number of different K^+ channels that confer a variety of different properties to cell membranes (Table 6–8). The different K^+ channels stabilize the E_m, ensure that the length of an action potential is kept short, terminate periods of rapid action potential initiation, vary the rate of repetitive action potential occurrence, or lower the excitability of the cell membrane.

Probably the two most important properties of action potentials are a high velocity of spread (this will be described in detail below) and rapid inactivation to assure a short action potential duration. The latter property requires a rapid inactivation of the Na^+ channels and a rapid increase in potassium permeability; this latter role is performed by the rapidly activating, **delayed rectifying K^+ channel**, which provides the $I_{K(V)}$ current. Despite their daunting name, the function of these K^+ channels is fairly straightforward; their current flow is voltage dependent, i.e., rectified. Any electrical circuit where resistance and conductance vary with voltage is a rectifying circuit; the Na^+ channel is also rectified. It is easier for K^+ ions to move out through the cell membrane than in, and so the new E_m is more rapidly reached after a depolarizing stimulus than after a repolarizing stimulus.

Neural information is generally encoded by the frequency of action potentials, which is quantitatively related to the stimulus intensity (see Chapter 7). However, axon membranes generally will not produce a chain of action potentials whose rate is proportional to the magnitude of a stimulus current, i.e., they will not encode voltage information into action potential frequency information. The information encoding membrane, located elsewhere in the neuron, has **fast transient K^+ channels**, or A channels (providing the $I_{K(A)}$ current). The A channels can encode a sustained depolarizing stimulus into a sustained rate of action potentials. They are inactivated at the end of an action potential, but are "primed" by the hyperpolarization to open when the membrane repolarizes to the normal E_m. The $I_{K(A)}$ current opposes the depolarizing stimulus current and temporarily keeps E_m at the normal resting value. The A channels then automatically close, and the depolarizing stimulus now depolarizes the membrane and initiates an action potential. This cycle is repeated for as long as the stimulus current is maintained.

Bursting pacemakers of mollusks fire with a complex pattern of alternating bursts of firing and quiescent periods (Figure 6–17). These bursts of firing are due to the influx of Ca^{2+} from the external medium. The Ca^{2+} influx exceeds the rate at which it can be pumped out of the neuron, and so the intracellular Ca^{2+} concentration rises until eventually it activates Ca^{2+}-dependent K^+ channels. The resultant $I_{K(Ca)}$ hyperpolarizes the neuron, inhibits further action potentials, and allows the Ca^{2+} to be pumped out of the neuron. The cycle of burst activity begins again as the intracellular Ca^{2+} concentration falls.

The **inward rectifying K^+ channel** has been identified in many types of cells, including vertebrate cardiac muscle fibers, frog skeletal muscle, starfish and tunicate eggs, and the electric organ of electric eels. There are at least two types of inward rectifying K^+ channels in cardiac muscle that differ in their E_m range for activation. K_2 channels close if E_m is -90 to -60 mV and inactivate slowly (the halftime is about 3 sec). X_1 channels close if E_m is -50 to

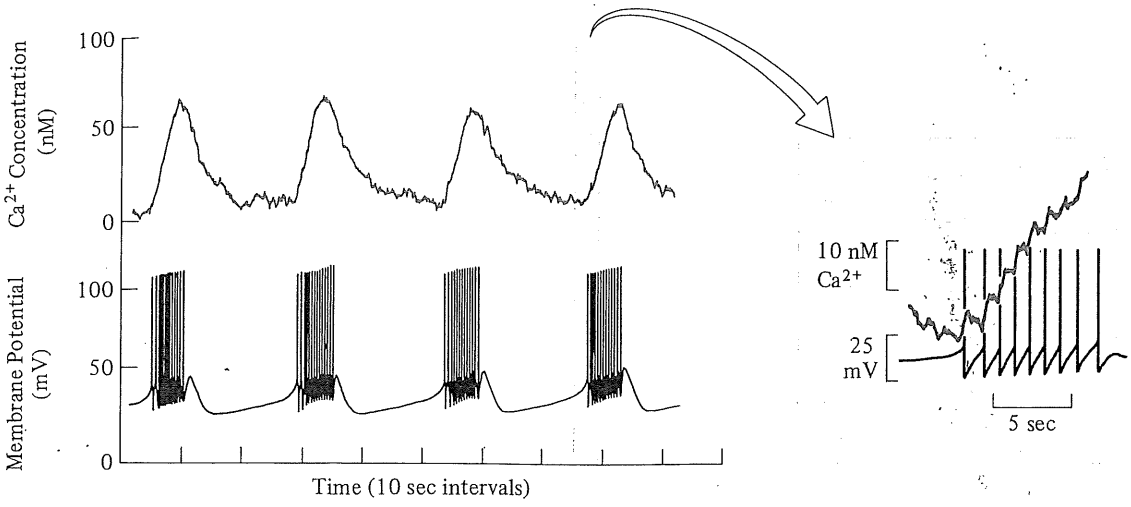

FIGURE 6–17 Bursting pacemaker of the sea hare *Aplysia* exhibits periods of repetitive action potentials interspersed with quiescent periods (lower trace). There is an increase in intracellular Ca^{2+} concentration with each action potential (upper trace), until the intracellular Ca^{2+} concentration becomes sufficiently high to open calcium-dependent potassium channels; the $I_{K(Ca)}$ hyperpolarizes the membrane and inhibits further action potentials and Ca^{2+} influx. *(From Gorman and Thomas 1978.)*

+10 mV, and inactivate faster. Vertebrate cardiac muscle cells are depolarized for about 1/2 of the time; the Purkinje muscle fiber has a typical plateau action potential, with each depolarization lasting from 100 to 600 msec. The cardiac action potential is initiated by a depolarization, then positive feedback increases the sodium conductance above threshold (about −60 mV). This causes a brief "fast Na^+ current" of about 600 $\mu A\ cm^{-2}$, which is replaced by a slower Na^+ and Ca^{2+} current. Depolarization inactivates the K^+ channels and decreases g_K, so the membrane E_m quickly repolarizes to about −10 to −30 mV. A progressive activation of X_1 K^+ channels (since E_m is in their activation range) provides sufficient current flow ($I_{K(X_1)}$) to eventually repolarize the E_m to about −90 mV. This E_m activates the K_2 K^+ channels and the repolarization is stabilized. However, the K_2 channels slowly inactivate, and this slowly depolarizes E_m to threshold, initiating another action potential. A continual influx of Na^+ and efflux of K^+ during the long depolarized plateau would require considerable energy expenditure by the Na^+-K^+ pump to reestablish the normal ion concentration gradients. This is avoided by the low density of most ionic channels, which restricts the current flow to 1 to 10 $\mu A\ cm^{-2}$ (although the Na^+ channels pass up to 1 to 2 mA for the brief periods during which they are open).

Inward rectifying K^+ channels are also present in other cells. Some egg membranes have them to minimize K^+ efflux during the long depolarization after fertilization that prevents additional sperm from entering the fertilized egg. The electric organ of the electric eel has inward rectifying K^+ channels that allow the maximum development of Na^+ current to shock the eel's prey. In frog skeletal muscle, these K^+ channels may prevent excessive hyperpolarization of the cell membrane by very active electrogenic Na^+-K^+ pumps.

Calcium channels. Ca^{2+} channels were accidentally discovered in crab leg muscle cells, which have Ca^{2+}-driven action potentials rather than the typical Na^+-driven action potential (Fatt and Katz 1951). The absence of Na^+ in the external ringers actually increased the magnitude of the action potential in the crab leg muscle cell! An action potential can be driven by changes in Ca^{2+} rather than Na^+ permeability and flux, since the calcium equilibrium potential is positive, like the sodium equilibrium potential. For example, in the crustacean skeletal muscle either Ca^{2+} or the similar ions Ba^{2+} or Sr^{2+} are required for an action potential to occur normally, but Na^+ is not; the action potential is a "Ca^{2+} spike" and not a "Na^+ spike" (Fatt and Ginsborg 1958).

Ca^{2+} channels are present in virtually every type of excitable cell. They support a Ca^{2+} action potential in some cells (arthropod, molluskan, tunicate, and nematode muscle). In other cells, they

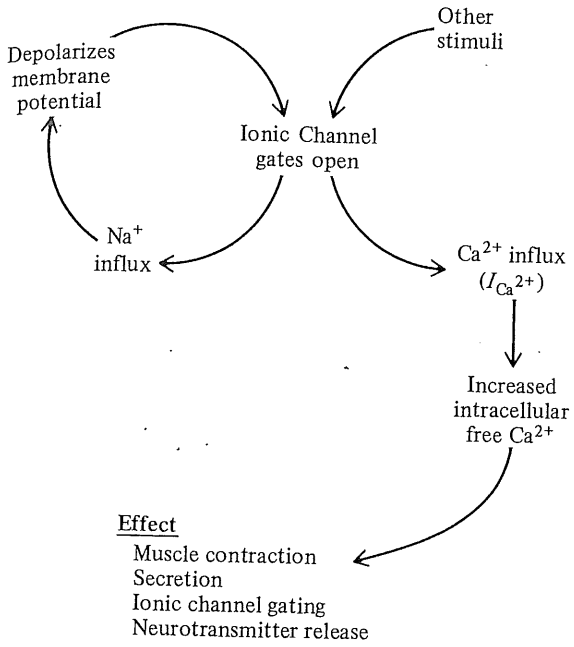

FIGURE 6–18 Membrane calcium channels are activated by strong depolarization (e.g., an action potential) and the low-current influx of Ca^{2+} (I_{Ca}) dramatically increases the normally low intracellular concentration ($< 10^{-7}$ M) by perhaps 20 ×. The increase in intracellular Ca^{2+} concentration is the signal initiating a number of important biological processes in different cells, from muscle contraction to secretion.

allow influx of Ca^{2+} into the cell to induce some nonelectrical event (e.g., muscle contraction, glandular secretion, vesicle exocytosis; Figure 6–18).

Ca^{2+} channels are activated by depolarization. They usually require a greater depolarization to open than do Na^+ channels. Their inactivation is slow and incomplete if the stimulus depolarization is maintained. The intracellular Ca^{2+} concentration is normally very low (e.g., 10^{-7} M) and so the Ca^{2+} influx can easily increase the intracellular concentration by 20 × or more during a single depolarization. The level of the intracellular Ca^{2+} is buffered to low levels by special Ca^{2+}-binding proteins (e.g., calmodulin, troponin) that are very sensitive to Ca^{2+} concentration changes of the order of 10^{-7} to 10^{-6} M. In muscle cells, the increased Ca^{2+} concentration due to influx from either the extracellular fluid or intracellular membranous vesicles (the sarcoplasmic reticulum) stimulates shortening of the muscle sarcomere units. In nonmuscle cells, the Ca^{2+}-calmodulin complex has effects on the intracellular cytoskeleton, hence intracellular motility (e.g., mitotic movement, ciliary and flagellar movement). The release of neurotransmitter at chemical synapses is a consequence of Ca^{2+} influx through Ca^{2+} channels. Ca^{2+} influx affects many hormone systems, including the adrenergic system. For example, the effect of epinephrine on cardiac muscle to enhance the force of contraction is due in part to an increased Ca^{2+} current. Thus, gating of the Ca^{2+} channels by various hormones and other molecules can modify cellular function.

Chloride channels. Chloride is the most abundant anion of body fluids and there are some physiological roles for Cl^- channels. However, Cl^- is generally distributed across animal cell membranes in equilibrium with the resting E_m, i.e., $E_{Cl} = E_m$. Chloride channels therefore stabilize the E_m against depolarization (like K^+ channels). In many cells, such as vertebrate twitch muscle, the g_{Cl} is up to 10 × higher than g_K, and much higher than g_{Na}, and so the Cl^- channels play a "background" role in stabilizing the resting E_m. Some animal cells have voltage-dependent Cl^- channels (i.e., are rectified) but their role is unclear. The slow action potentials of the giant algae *Nitella* and *Chara* are thought to be due to the regenerative opening of Cl^- channels in response to a depolarizing current (i.e., analogous to the Na^+-driven action potential of animal cells) and repolarization due to a delayed increase in g_K. The ionic distributions across these algal cell membranes must be very different from those across animal cells in order for Cl^- flux to initiate an action potential (Nobel 1983); E_{Cl} is about +99 mV and the resting E_m is about −138 mV. It is possible that the increase in g_{Cl} is not actually voltage dependent but due to influx of Ca^{2+} due to voltage-dependent Ca^{2+} channels (Lunevsky et al. 1983).

Role of the Na^+-K^+ Pump. The Na^+-K^+ pump of excitable cell membranes (and also all other cells) exchanges Na^+ for K^+ across the cell membrane. The typical Na^+-K^+ pump exchanges 3 Na^+ for 2 K^+ per ATP hydrolyzed. It is electrogenic and contributes to the resting cell membrane potential. For example, injection of Na^+ into a snail neuron causes a rapid hyperpolarization due to the action of the Na^+-K^+ pump in pumping Na^+ out of the cell in a 3:2 exchange for K^+, thus reinforcing the normal −90 mV resting E_m. This hyperpolarization is blocked by ouabain (a cardiac glycoside that selectively blocks the Na^+-K^+ pump) and by removal of extracellular K^+, indicating that hyperpolarization is due to Na^+-K^+ exchange. The membrane potential of neurons of the gastropod mollusk *Anisodoris* can be separated by experiments at differing temperature into two components: one determined by ionic permeability and ionic concentration differ-

ences, and one due to the electrogenic pump (Marmor and Gorman 1970). In frog nerves, the E_m can become even more negative than E_K when there is a high rate of Na^+-K^+ exchange, presumably because of the electrogenic nature of the pump.

The Na^+-K^+ pump is not normally important in producing or maintaining the resting E_m, at least directly. For example, metabolic inhibitors, which block the Na^+-K^+ pump, have little or no immediate effect on E_m, and blocked cells can sustain many action potentials. However, blocked cells exhibit a slow, progressive decline in E_m towards 0 mV because of the slow dissipation of the Na^+, K^+, and other ion gradients. Thus, the Na^+-K^+ pump is essential as the ultimate mechanism for establishment of the ion concentration gradients on which the resting E_m and action potentials are dependent but is of little direct consequence to E_m and action potentials.

Properties of Action Potentials

There are a number of general properties of action potentials, such as threshold, shape, and frequency, that merit further discussion. The properties of membranes, enzymes, and protein channels are also influenced by the physical environment; two important physical parameters of the environment that can dramatically influence the electrical characteristics of membranes are temperature and pressure.

Temperature has a marked effect on excitable cell membranes. One minor effect is the influence of temperature on the mobility of ions and the establishment of a membrane potential by diffusion gradients as calculated by the Goldman-Hodgkin-Katz equation. This is a weak effect; increasing the temperature by 10° C increases the E_m by only 3 to 5%, i.e., the Q_{10} is about 1.035. Temperature affects the activity of important membrane enzymes. For example, the Na^+-K^+ pump of neurons of the mollusk *Anisodoris* is temperature dependent and so its electrogenic contribution to the resting membrane potential increases at elevated temperature.

Ion channel conductance is temperature dependent; Q_{10} values are generally about 1.3, but can range from 1.0 to 2.5. For example, an Arrhenius plot of conductance (g; pSiemens) as a function of 1/T yields a linear inverse relationship at T > 6° C with a Q_{10} of about 1.2, but a sharp transition at about 6° C to a more negative slope with Q_{10} about 7.2 (Figure 6–19). The activation energy for ion movement through the channels increases dramatically from about 25.6 kJ $mole^{-1}$ at T > 6° C to 194.6 kJ $mole^{-1}$ at T < 6° C. There is a similar temperature

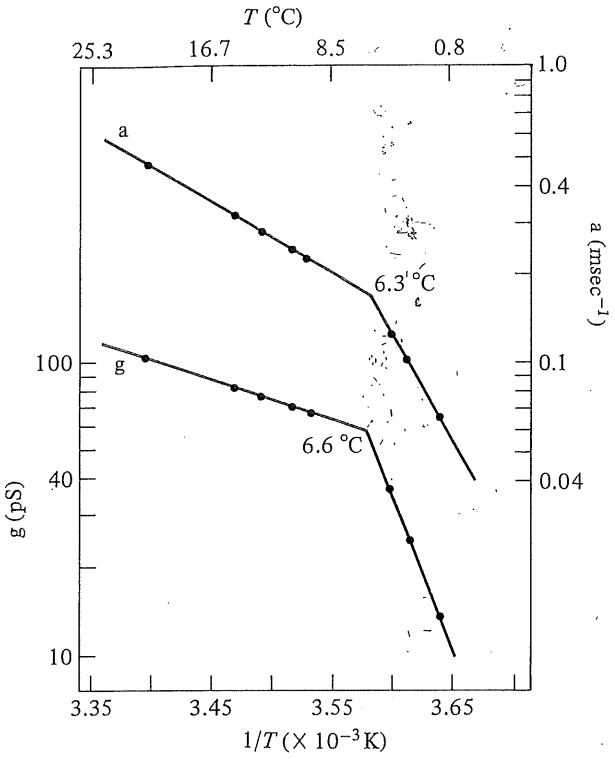

FIGURE 6–19 Effect of temperature on conductance and ion channel closing. *(Modified from Anderson, Cull-Candy, and Miledi 1977.)*

dependence of the rate of ion channel closing (a, $msec^{-1}$), also with a transition temperature of about 6° C. The activation energy increases from 47.7 kJ $mole^{-1}$ (Q_{10} = 1.8) to 139.3 kJ $mole^{-1}$ (Q_{10} = 6.3). These temperature-dependent properties of ion channels are possibly due to a change in the membrane fluidity, i.e., there is a solid-liquid phase transition at 6° C or a conformational change in the receptor-ion channel protein. Various ion channels can respond differently to a temperature change, and so the ratio of conductances of two ions can alter at differing temperatures.

Hydrostatic pressure has a similar effect on ionic mobility as lowered temperature. There is, in fact, a formal relationship between temperature and pressure effects

$$K_p/K_0 = e^{-P\Delta V^*/RT} \qquad (6.13)$$

where K_p is the reaction rate constant at pressure P, K_0 is the rate at standard pressure (0.1 MPa), and ΔV^* is the volume change of reactants as they are activated. Hydrostatic pressure often does not affect the resting E_m or threshold, although prolonged high pressure depolarizes the resting E_m of

a crustacean axon by 10 to 15 mV, possibly due to effects on the electrogenic pump.

High pressure prolongs the duration of an action potential and decreases the rate of depolarization and repolarization. Vertebrate cardiac muscle has a decreased excitability at high pressure, a lower conduction velocity of action potentials, and increased action potential duration. Hydrostatic pressure can also affect the membrane current during an action potential. For example, a pressure of 20 MPa slightly diminishes the delayed K^+ current and especially the Na^+ current across a squid giant axon during an action potential. This is probably because the gating properties of the ion channels are altered, rather than because of a change in the number of open ion channels during an action potential.

High pressure generally has a lesser effect on excitable membranes of deep-sea fish than shallow-water fish. For example, high pressure decreases the amplitude of action potentials in axons of shallow-water fish but not deep-sea fish. The action potential amplitude for the shallow-water cod (*Gadus*) is reduced at 31 MPa to about 30% of the normal value at 0.1 MPa, whereas there is no effect at 42 MPa for the deep-sea *Bathysaurus* and *Coryphaenoides*. *Mora*, a fish of intermediate depth, has an intermediate depression of action potential amplitude. The duration, threshold, and absolute refractory period increase for axons of all species regardless of normal depth. The conduction velocity decreases for all species regardless of depth, although the effect is less for the deep-sea fish.

Threshold. A depolarization must reach a certain, critical level before the feedback cycle between depolarization and increase in g_{Na} becomes positive. This critical depolarization level is the **threshold** (Figure 6–20A). A subthreshold depolarization fails to reach threshold and does not elicit an action potential. A suprathreshold depolarization exceeds threshold and will elicit an action potential. In general, a faster rate of depolarization will cause a more rapid attainment of threshold and action potential initiation.

All-or-None Response. Normally, all action potentials of a given neuron are exactly equivalent in shape, i.e., have the same duration and amplitude. The effect of membrane depolarization is "all-or-none"; there is an action potential if E_m reaches threshold ("all"), but no action potential if threshold is not reached ("none").

There are some other exceptions to the all-or-none form of an action potential. One is the reduction in amplitude of action potentials that occurs in the relative refractory period, soon after a previous action potential (see below). A second example is the experimental manipulation of the external environment, e.g., replacing the extracellular Na^+ with choline diminishes the amplitude of the action potential because E_{Na} is reduced; application of small doses of tetrodotoxin also diminishes the action potential amplitude because some Na^+ channels are blocked.

Latency. The **latency** is the time period between the onset of the stimulus current and the peak of the ensuing action potential. Latency decreases with increasing current strength because the depolarization to threshold occurs faster.

Strength-Duration Relationship. A stimulating current must be of at least a minimal value to depolarize a cell membrane to threshold, but both the strength and the duration of the stimulus determine whether threshold is reached (Figure 6–20B). A short duration of a high-intensity current might have the same threshold action as a longer duration of a lower-intensity current. The inverse relationship between stimulus strength and duration is of the general form

$$E_{th} = \frac{a}{t} + b \qquad (6.14)$$

where E_{th} is the threshold voltage, t is the stimulus duration (msec), and a is a constant. The other constant, b, is the **rheobase**; it is the lowest current that will initiate an action potential. The **chronaxie** is the minimum required stimulus duration when the current is 2 × rheobase. Rheobase and chronaxie define the shape of the strength-duration relationship.

Accommodation. A constant depolarizing or hyperpolarizing current can modify the kinetics of Na^+ and K^+ channels and alter the threshold. A maintained depolarization causes the threshold to rise towards 0 mV. A slowly increasing depolarizing current may not initiate an action potential even though it may rise to an intensity much greater than threshold for a rapidly rising stimulating current because accommodation occurs faster than the current intensity rises. A maintained hyperpolarization causes the threshold to decrease further from 0 mV. The threshold may even fall below the normal resting E_m, so that an action potential is initiated when the hyperpolarizing current is removed because the return to resting E_m passes the lowered threshold; this is anodal block excitation.

Refractory Period. It is not possible to elicit a second action potential for a brief period after an

action potential (Figure 6–20C). This short period is called the absolute refractory period. It occurs because all of the Na^+ channels are inactivated, and cannot be activated; they are refractory to depolarization. As some Na^+ channels become capable of activation, another depolarizing stimulus may initiate a second action potential, but its amplitude will be less than the normal amplitude because

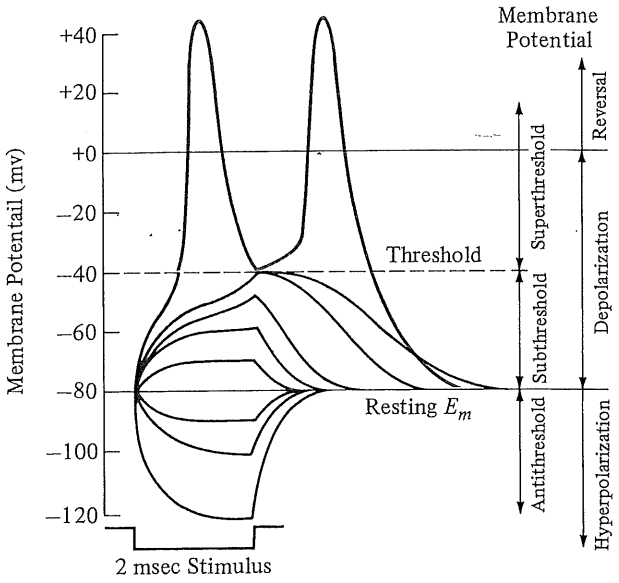

A

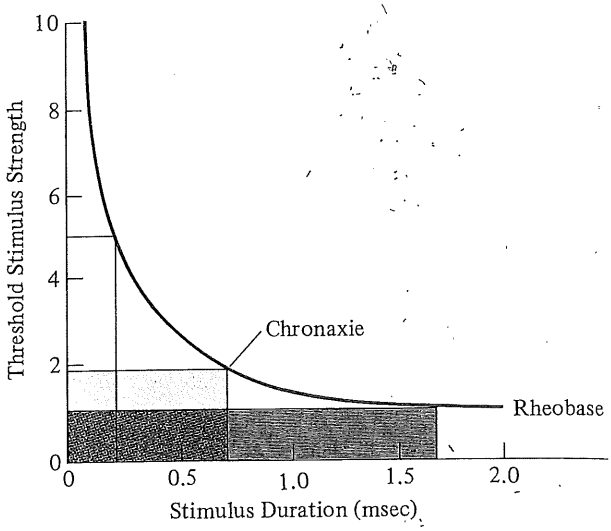

B

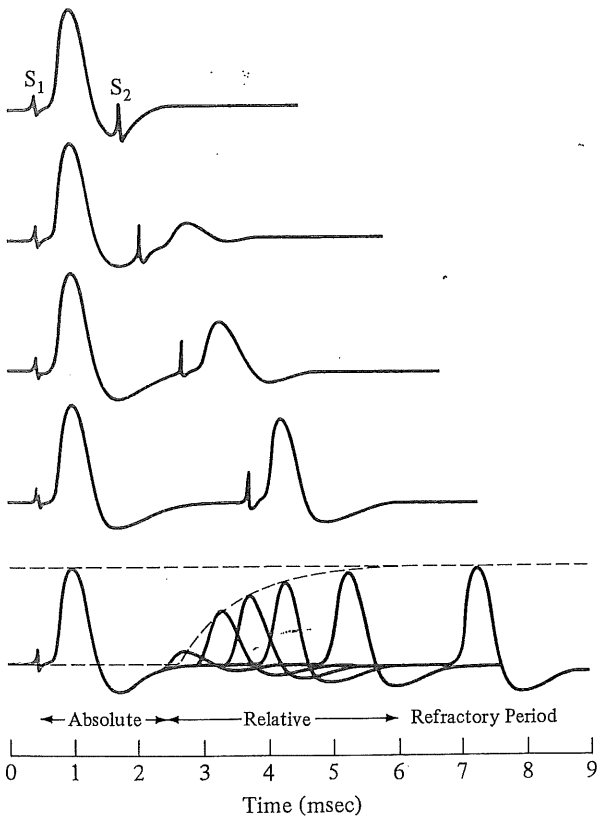

C

FIGURE 6–20 **(A)** A local depolarization only initiates an action potential if it reaches or exceeds the threshold value ($E_{threshold}$). Hyperpolarizing changes are antithreshold; no action potential is initiated. Depolarizing changes can be subthreshold (no action potential elicited) or superthreshold (action potential elicited). Depolarizations that increase the E_m above zero (reversal) are typically superthreshold and elicit an action potential. **(B)** Effect of strength and duration of a stimulating current on the threshold stimulation. Three combinations of strength and duration that elicit threshold are shown. The rheobase (minimum voltage at long duration) and chronaxie (pulse duration at a voltage of 2 × rheobase) are indicated. **(C)** The absolute refractory of an isolated whole nerve is the period after an initial stimulus (S_1) during which a second stimulus (S_2) fails to elicit a second action potential; the relative refractory period is that during which the second stimulus fails to elicit an action potential of normal amplitude. *(From Katz 1966.)*

not all of the Na^+ channels can be activated; some are still inactivated and refractory. This second action potential, which occurs in the relative refractory period, has a lower than normal amplitude. A progressively more normal amplitude action potential occurs as the duration between successive stimuli is increased because the second stimulus occurs when more and more Na^+ channels are capable of being activated. Eventually, the delay is sufficient that the second stimulus elicits a normal action potential.

Axonal Propagation

Excitable cell membranes not only sustain an action potential, but also allow its spread, or **propagation**. The spread of an action potential along a nerve cell axon well illustrates the mechanism of propagation. The axon is an elongate process of a neuron extending a variable distance from the cell body. A fairly typical multipolar neuron with a long axon is shown in Figure 6–21. An action potential is initiated at the axon hillock, where the axon extends from the cell soma. The action potential propagates along the length of the axon until it reaches the terminal synapse.

An axon can be represented by a sequence of equivalent membrane electrical circuits (Figure 6–22A), just as we have previously used an R_mC_m equivalent circuit to represent the cell membrane except that we must also consider the external resistance to electrical flow (through the extracellular fluid, R_o) and the internal resistance to electrical flow (through the cytoplasm of the axon, R_i).

There is both a passive spread of electrical depolarization along the equivalent circuit of resistors and capacitors, as well as a regenerative spread of an action potential. The passive electrical spread is similar to the conduction of electricity through wires, resistors, and capacitors; it is **electrotonic spread**. The extent of passive electrotonic spread is determined by the values of the membrane resistances and capacitances. These values determine the cable properties of the axon, i.e., how the axon would act if it were a passive electrical cable. Some

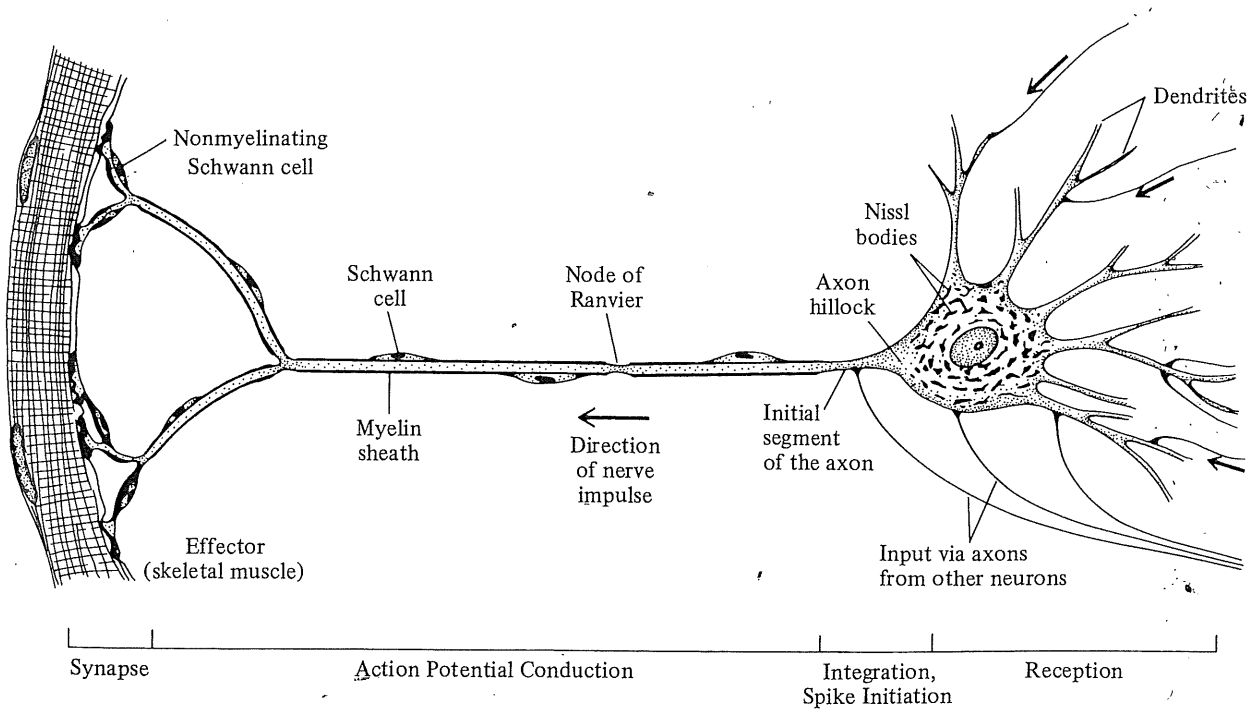

FIGURE 6–21 Schematic representation of a multipolar neuron showing the many dendritic afferents where sensory information is received, the axon hillock where this information is integrated to initiate action potential spikes, the axon conducting portion, and the terminal portion where neurotransmitter is released at the effector cell. *(Drawing from Fawcett, D. W. (1986) after Bunge from Bailey's Textbook of Histology 16th ed.)*

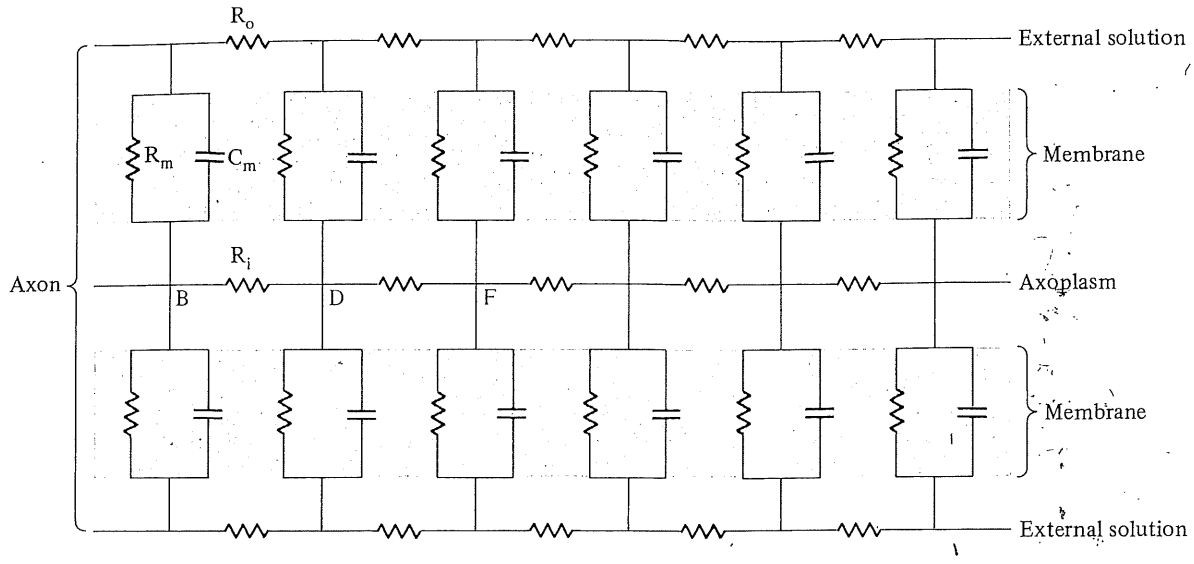

A

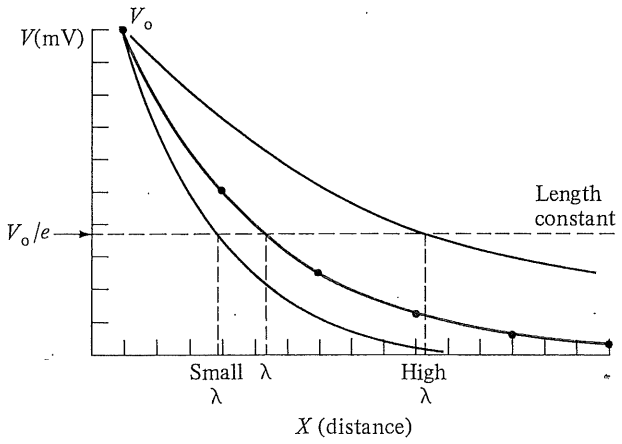

B

FIGURE 6–22 **(A)** Electrical circuit analog for the axon of neuronal cells. **(B)** Electronic spread of an applied electrical potential in the electrical circuit analog of an axon. The voltage (E) declines to 36.7% of the applied voltage (E_o) at a distance equal to the length constant (λ). *(Modified from Aidley 1989.)*

typical cable property values for R_i, R_o, R_m, and C_m are summarized in Table 6–9. The current flow due to a voltage E_o applied between R_i and R_o through a cable network transiently charges the membrane capacitors, then is a sustained, smaller current through the successive R_mC_m circuits for as long as E_o is applied. The voltage (E_x) measured at a point x along the axon decreases exponentially as a function of distance from where E_o is applied (Figure 6–22B).

$$E_x = E_o e^{-x/\lambda} \qquad (6.15a)$$

The constant λ, the length constant, determines how quickly the voltage E_x decreases with distance from E_o. If $x = \lambda$, then $E_x = 0.368\ E_o$, i.e., the length constant is the distance at which E_x is decreased (or attenuated) to 37% of E_o. The value of the length constant is determined by the values of R_i, R_o, and R_m

$$\lambda = \sqrt{R_m/(R_i + R_o)} = \sqrt{R_m/R_l} \qquad (6.15b)$$

where R_l is the summed longitudinal resistance of the axon "cable" ($R_i + R_o$). If R_m is high, then the E_o will electrotonically spread over a long distance because little current will flow through the membrane. If R_i and R_o are high, then E_o will not spread as far along the cable.

An axon shows exactly the same electrotonic spread as the equivalent circuit, although this is only apparent if the depolarization is subthreshold or the initiation of an action potential is blocked, for example by local cooling (Figure 6–23). The length constant for the axon illustrated in Figure 6–23 is about 0.6 mm.

TABLE 6–9

Cable properties of cell membranes at a temperature of about 20° C. *(Data from Katz 1966; Hays, Lang, and Gainer 1968; Rall 1977.)*

Cell	Dia μ	Length Constant λ mm	Time Constant τ msec	Capacitance $\mu F\ cm^{-2}$	RESISTANCE		
					Membrane $\Omega\ cm^2$	Cytoplasm Ω cm	Extracellular Ω cm
Marine worm nerve	560	5.4	0.9	0.75	1200	57	—
Squid nerve	500	5	0.7	1	700	30	22
Lobster nerve	75	2.5	2	1	2000	60	22
Crab nerve	30	2.5	5	1	5000	60	22
Crab muscle	334	1.6	14.5	37	465	157	—

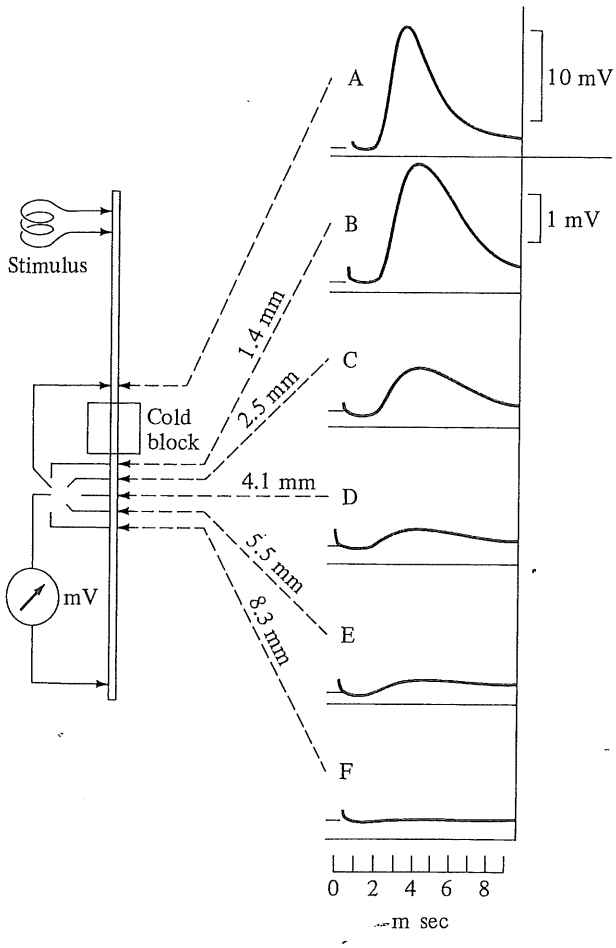

FIGURE 6–23 Electronic spread is readily observed for an axon with action potential propagation blocked by cold. There is an exponential decrease in voltage amplitude with distance from the block. The length constant is about 0.6 mm (distance for attenuation of voltage to 36.7% of E_o). *(Modified from Hodgkin 1937.)*

The velocity of electrotonic spread is extremely rapid, as is electrical current flow in conducting wires and electrolyte solutions. This is why Johannes Muller declared in the late 1830s that the velocity of action potential propagation would never be accurately measured. However, within a couple of decades one of his students, von Helmholtz, had measured the velocity of an action potential as 3 10^3 cm sec^{-1}. Action potential propagation is clearly much slower than electrotonic spread. It is also a regenerative process; the voltage amplitude of an action potential at any point, x, is identical, i.e., a -90 to $+50$ mV signal, in contrast to the exponential voltage decline with x observed for electrotonic spread.

An action potential occurring at any particular point on an axon induces a local current flow, an inward Na^+ current followed by an outward K^+ current (Figure 6–24). There is also an electrotonic spread of current forward (and also backward) relative to the direction of propagation. This depolarizes the axon membrane to threshold, and a new action potential is initiated at a point ahead of the present action potential. Another action potential is induced further in front by electrotonic current spread. There actually is a smooth forward progression of the action potential, rather than a jumping motion as depicted for convenience in Figure 6–24.

Action potentials only travel in one direction along an axon from the neuron soma towards the axonal tip. This one-way propagation is not an inherent property of the axon membrane or action potential propagation mechanism. This can be readily demonstrated experimentally; an axon stimulated in the middle will propagate an action potential in each direction. An action potential traveling in the "correct" direction, from neuron soma to axon terminus, is described as **orthodromic**, whereas an

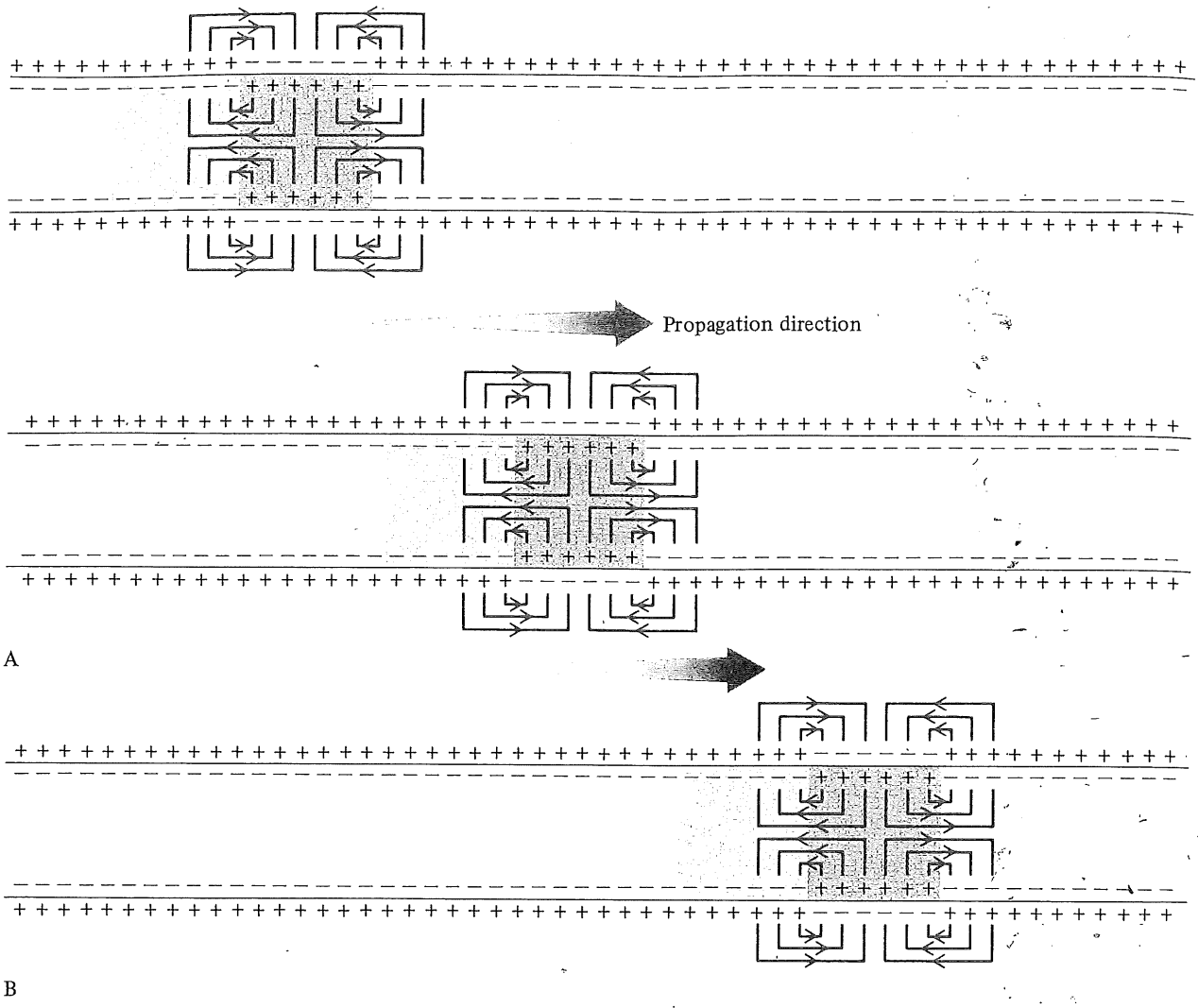

FIGURE 6–24 Local current flow during the propagation of an action potential along an axon. Arrows indicate direction of conventional current flow (i.e., flow of positive charges). The region of action potential depolarization is shown by dark color; the refractory portion is indicated by intermediate color. The one-way direction of propagation is maintained by the refractory period of the membrane after an action potential has occurred.

action potential traveling in the abnormal direction is **antidromic**. An action potential doesn't suddenly reverse direction as it spreads along an axon because the membrane where the action potential has just occurred is refractory; the Na^+ channels are inactivated and there is an outward K^+ current that hyperpolarizes the membrane, counteracting any electrotonic depolarization. In front of the action potential there is no repolarizing K^+ current and the Na^+ channels are not refractory.

The velocity of propagation of a regenerative action potential is much less than that of electrotonic spread because the membrane capacitance discharges at a finite rate and because complex protein configurational changes must occur. These processes are extremely slow compared to electrotonic spread, and so the action potential velocity is much less. The velocity of an action potential depends in part on the rate at which the membrane ahead of the action potential depolarizes to threshold. This in turn depends on the cable properties of the axon and the actual threshold level. The longitudinal resistance of the axoplasm (R_i) depends on both the intrinsic, or specific, resistance of the axoplasm (about 60 Ω cm for most axons) and the cross-sectional area of the axon (πa^2, where a is the axon radius). A 25 μ radius axon would have an internal resistance of about $3\ 10^6\ \Omega\ cm^{-1}$, whereas a 100 μ

radius axon would have a lower resistance of about $2\ 10^5\ \Omega\ cm^{-1}$. The lower internal resistance might be expected to increase conduction velocity. The theoretical relationship between propagation velocity (V) and fiber diameter (D), if all other cable constants remain the same, is as follows.

$$V \propto \sqrt{D} \qquad (6.16)$$

One way to increase the conduction velocity is to increase axon diameter, although there clearly is a practical upper limit to the velocity that can be attained in this manner without the axon becoming impossibly large. Nevertheless, many invertebrates and lower vertebrates have giant axons that have high conduction velocities (Table 6–10). The giant axons of the polychete *Myxicola* are up to 1 mm in diameter and conduct at 6 to 20 m sec^{-1}! The function of giant fibers is predominantly rapid behavioral reflexes for protection from predators; they trigger massive behavioral responses, such as body flexion (fish) or abdominal flexion (crayfish) rather than controlled, finely graded movement.

Giant axons have independently evolved many times, but there are three basic patterns (Dorsett 1980). First, paired giant axons run longitudinally along the nerve cord with the cell bodies located in the central nervous system, e.g., Mauthner cells of fish, giant fibers of the polychete *Protula*, and cockroach giant axons. Second, segmental giant neurons form junctions with adjacent neurons to act as a single functional unit that can conduct in either direction, e.g., median and lateral giant fibers of the earthworm and lateral giant fibers of crayfish. The junctions between the giant fibers of the earthworm slow down the conduction velocity to about 8 m sec^{-1} from 25 m sec^{-1}, and there is a slight reduction of the action potential amplitude across the gap junction. Third, a large number of axons from different neurons fuse to form a single giant fiber, e.g., the median giant fiber of the polychete *Nereis* and the giant axon of squid. Giant axons are not always a suitable solution for maximizing conduction velocity. For example, it would be very cumbersome for the optic nerve of vertebrates to contain giant fibers, and the spinal cord would assume huge dimensions if all of its nerve fibers were giant axons.

Many vertebrate axons and some invertebrate axons are covered with a series of insulating sleeves and intervening, uninsulated nodes. Special **Schwann sheath cells** surround the axons to form the insulation. The arrangement of the Schwann cells ranges from one Schwann cell per axon, to many axons per Schwann cell, to many Schwann cells per axon (Figure 6–25A). The Schwann cell membrane of many axons becomes repeatedly wound round the axon, forming a thick layer of cell membrane (Figure 6–25B). The thick lipid sheath of myelin is interrupted by gaps between the adjacent Schwann sheath cells, called the **nodes of Ranvier**. This arrangement of Schwann sheath cells, myelin, and nodes of Ranvier of vertebrate axons (Figure 6–25C) is closely paralleled by the myelination of some invertebrate axons, such as those of the prawn *Palaemonetes* (Figure 6–25D). The presence of a myelin sheath considerably alters the electrical properties of the axon (Rall 1977). There is an additional capacitance and resistance of the myelin sheath ($0.004\ \mu F\ cm^{-2}$; $0.01\ 10^6\ \Omega\ cm^2$) compared to the internodal membrane ($5\ \mu F\ cm^{-2}$; $15\ \Omega\ cm^2$).

Myelination of axons is an alternative means of increasing conduction velocity. The conduction velocity of myelinated axons is very high because of the important role of electrotonic spread. Consider the effect of covering an axon with a series of insulating sleeves to increase R_m and λ, but leaving "nodes" where the axon membrane is exposed to the extracellular fluid (Figure 6–26A). The inward Na^+ current due to an action potential occurring at a node cannot exit from the axon except at the adjacent nodes because of the insulation; the current therefore rapidly spreads electrotonically from one node to the next. There is then a time delay as the membrane capacitance discharges and the Na^+

TABLE 6–10

Diameter (μ) and conduction velocity for giant axons of various invertebrates and vertebrates. Hydrozoa *(Nanomia, Aglantha)*, polychete worms *(Nereis, Myxicola)*, cockroach *(Periplaneta)*, crayfish *(Cambarus)*, lobster *(Homarus)*, squid *(Loligo)*, oligochete *(Lumbricus)*, cyclostome *(Enterosphenus)*, teleost *(Cyprinus)*. *(Data from Dorsett 1980).*

	Dia (μ)	Velocity (m sec^{-1})
Nereis Paramedial	9	2.5
Aglantha ring	35	2.6
Nanomia stolon	30	3
Aglantha motor giant	40	4
Nereis Median	18	4.5
Nereis Lateral	35	5
Enterosphenus Muller cell	50	5
Lumbricus lateral	60	11.3
Periplaneta giant fiber	40	12
Cambarus laterals	150	15
Homarus median	125	18
Myxicola	1000	20
Lumbricus median	90	25
Loligo third order giant fiber	450	30
Cyprinus Mauthner	65	55

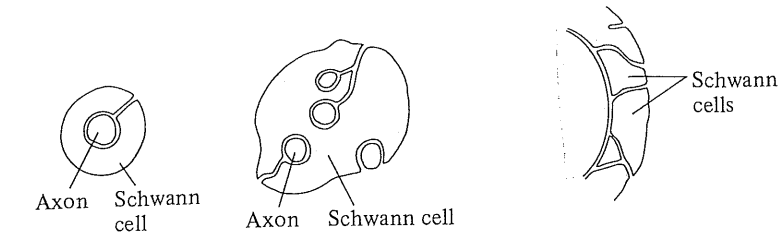

A Schwann cells

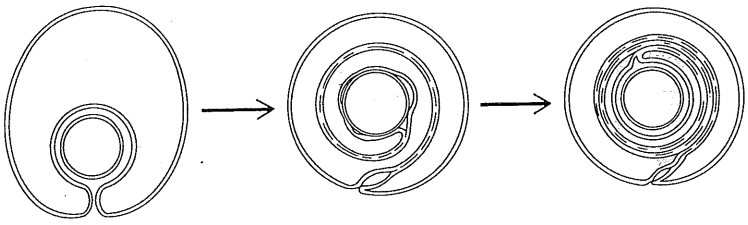

B Myelination

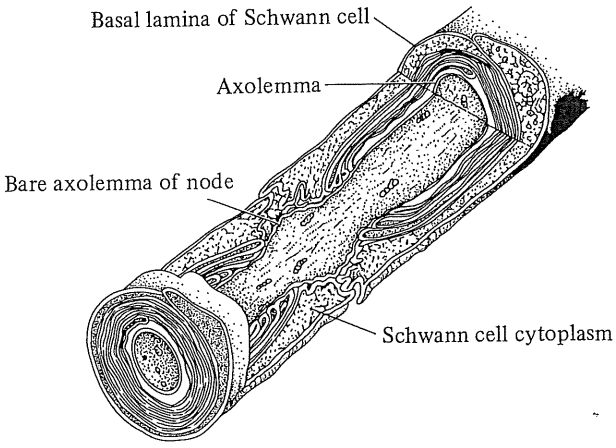

C Vertebrate Myelinated Axon

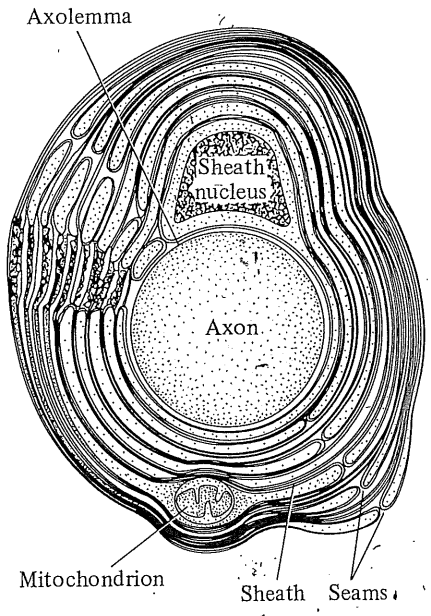

D Invertebrate Myelinated Axon

FIGURE 6–25 **(A)** Various arrangements of Schwann sheath cells around a single or multiple axons, and multiple Schwann cells around a giant axon. **(B)** The myelin sheath of myelinated axons is formed by an encircling extension of the inner Schwann cell membrane. **(C)** The myelin sheath of a vertebrate myelinated axon is surrounded by multiple membrane layers of the Schwann sheath cells, with Nodes of Ranvier between adjacent Schwann cells. **(D)** Cross section of a myelinated axon from an invertebrate (a prawn) is superficially similar to the myelin sheath of a vertebrate axon. *(From Aidley 1989; Fawcett 1986; Huesner and Doggenweiler 1966.)*

channels open, as occurs in naked axons, but then the inward Na^+ current rapidly spreads electrotonically to the next node. The net effect is an overall higher conduction velocity than for a naked axon of the same diameter because the action potential jumps from node to node at high velocity. This jumping propagation is **saltation** or **saltatory conduction**. A second advantage to saltatory conduction is the energy economy resulting from having only a small portion of the axon membrane actually supporting an action potential. The I_{Na} and I_K are smaller and the Na^+-K^+ pump doesn't expend as much ATP to restore the normal ionic concentration differences, as if the whole axon membrane sustained an action potential.

The action potential conduction velocity (V) of a myelinated axon depends on its diameter (D) (Figure 6–26B). There is a fairly linear relationship between

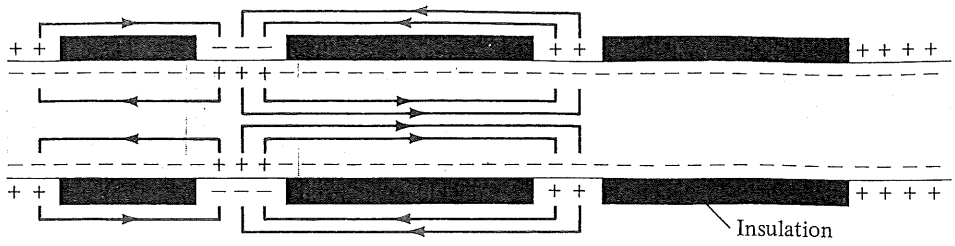

A

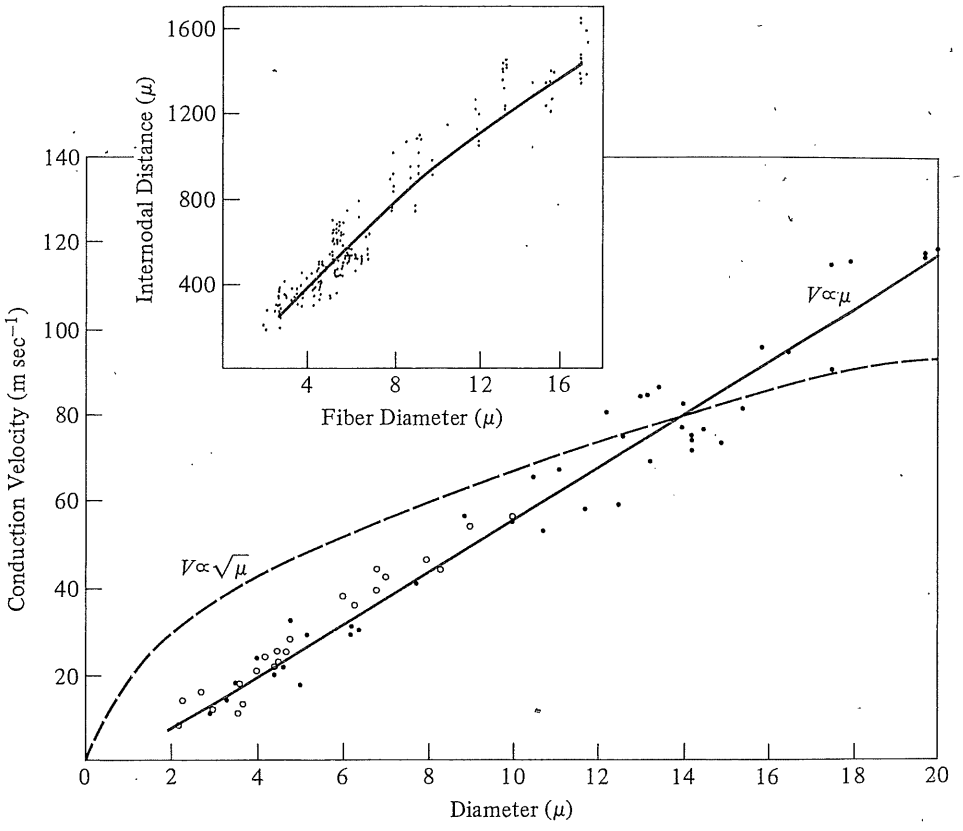

B

FIGURE 6–26 **(A)** Local current flow in an axon covered with discontinuous insulation. Current travels electrotonically along the axon to the node between insulating layers, rather than through the axon membrane where it is covered with the insulator. **(B)** Essentially there is a linear relationship between the fiber diameter (μ) and conduction velocity (V) for vertebrate (cat) myelinated axons rather than a square root relationship (dashed line). This linear relationship is due to the linear relationship between internode distance and fiber diameter (inset). *(Modified from Hursh 1939.)*

conduction velocity and diameter because the internode distance is correlated with the axon diameter. There is a minimum theoretical diameter, about 1 μ, below which myelinated axons have a slower propagation than nonmyelinated axons (Rushton 1951). This corresponds well with the observed minimum diameter of unmyelinated axons found in peripheral nerves of mammals, but smaller myelinated axons (about 0.2 μ diameter) are found in the mammalian central nervous system.

The peripheral nerves of animals contain many different axons of varying diameter and presence/absence of myelination. Consequently, the axons of these compounds vary in conduction velocity. This

is readily apparent from recording the **compound action potential** of a compound nerve, such as the frog sciatic. The action potentials, recorded at a distance from the point of stimulation, are separated into discrete classes of action potentials, depending on the characteristic conduction velocity (i.e., axon diameter and myelination). The large, myelinated Aα axons have the highest conduction velocity ($4.2\ 10^3$ cm sec^{-1}) and their action potentials are recorded first (Figure 6–27). The unmyelinated C axons have the lowest conduction velocity ($4\text{-}5\ 10^1$ cm sec^{-1}) and their action potentials are recorded considerably after the Aα axon action potentials. The Aβ, Aγ, Aδ, and B axons have intermediate diameters and conduction velocities.

Sloths, especially the three-toed sloth (*Bradypus tridactylus*), are renowned for their slow motion movements; but is their "slothfulness" physiological or motivational, i.e., would sloths move more rapidly if appropriately motivated? Their axonal conduction velocity (6 to 35 m sec^{-1}), action potential duration (2 to 3 msec for skeletal muscle membrane), and synaptic delay (about 2 to 3 msec for skeletal muscle membrane) are a little slower than are found in other mammals, but not enough to explain their slothfulness (Enger and Bullock 1965). A slow muscle contraction velocity is probably the reason for the slowness of sloths (see Chapter 9).

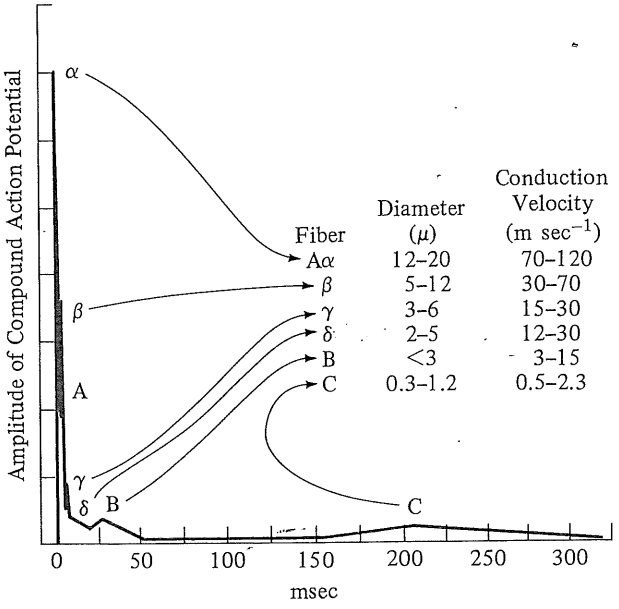

FIGURE 6–27 Hypothetical compound action potential recorded from a peripheral compound nerve shows the peaks for different-sized nerve fibers. *(Modified from Ganong 1969.)*

Many neurons that lack axons, or have short axons, are nonspiking, or local circuit, neurons. They do not sustain action potentials; rather, they rely on electrotonic spread because only short distances are involved and the electrical signal remains sufficiently great to elicit the appropriate response. These small cells also tend to have a high membrane resistance to minimize the attenuation of the electrotonic spread. Local neurons are found in the vertebrate retina and barnacle eye, the vertebrate and insect central nervous systems, and the stomatogastric ganglion of crustaceans. Electrotonic spread also occurs in the invaginated muscle cell membrane, called the t-tubule system.

Synaptic Transmission

Action potentials are transmitted from one cell to another. There are essentially two different mechanisms for transfer of electrical information from one cell (the presynaptic cell) to the next (the postsynaptic cell): (1) electrical synapses and (2) chemical synapses (Figure 6–28). In electrical synapses, the action potential jumps electrotonically from the presynaptic cell membrane to the postsynaptic cell membrane. Electrical synapses are more simple in principle, but are less common, than chemical synapses. The more common chemical synapse involves release of a special chemical, a neurotransmitter, from the presynaptic cell. The neurotransmitter has an electrical effect at the postsynaptic membrane, often depolarizing the membrane and initiating an action potential.

Electrical Synapses

Electrical synapses have a very specific anatomical organization and specialized membrane properties to electronically transmit an action potential from the presynaptic membrane to the postsynaptic membrane without so much attenuation that the postsynaptic cell fails to be depolarized to threshold (Katz 1966). The presynaptic membrane at an electrical synapse is closely apposed to the postsynaptic membrane to form a **gap junction** (Figure 6–29A). These gap junctions are composed of numerous **connexons** that allow direct movement of ions and small molecules from the presynaptic cell into the postsynaptic cell (Figure 6–29B). The connexons allow passage of small molecules (up to a molecular weight of about 800). The permeability of the connexon can be regulated, perhaps by the intracellular Ca^{2+} concentration. The electrical connection usually allows current flow in either direction, but this

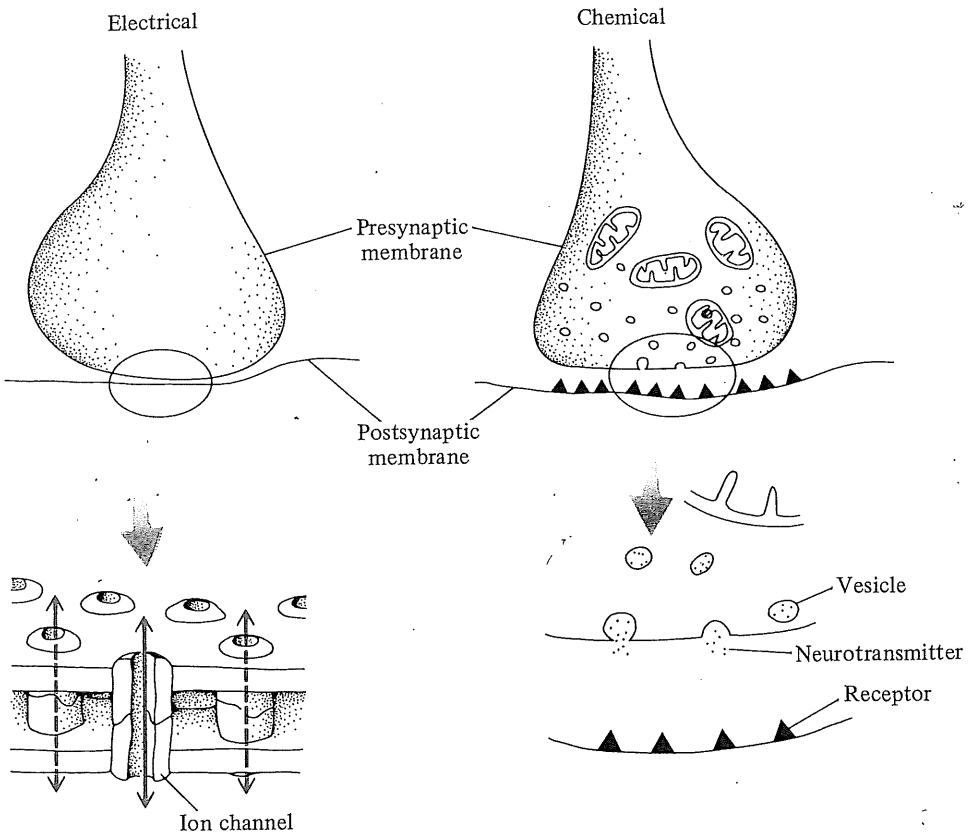

FIGURE 6–28 Comparison of an electrical synapse with gap junctions for electrical continuity between adjacent cells (left) and a chemical synapse where neurotransmitter is released from vesicles in the presynaptic terminal and binds to a receptor on the postsynaptic membrane (right). *(Gap junction from Loewenstein 1976.)*

is not always so. Preferential current flow in one direction is **rectification**.

Electrical junctions between neurons rely on local currents from the presynaptic membrane to the postsynaptic membrane (see Supplement 6–2, page 251). Sufficient current must flow from the first cell to depolarize the second cell to threshold. It is unlikely that an action potential in a small diameter axon could generate sufficient current flow to depolarize to threshold a large postsynaptic neuron with a high membrane area and low input resistance. Thus, an axon could probably not initiate an action potential across, for example, a neuromuscular junction (from a small neuron end terminal to a very large muscle cell). This limitation of electrical transmission is most likely one reason for the relative rarity of electrical synapses compared with the widespread occurrence of chemical synapses. Electrical synapses also do not allow complex signal integration.

The direct electrical coupling of neurons is often observed when there is a requirement for the close synchronization of effector organs (Bennett 1966). Examples are the cells of the lobster heart, the electric organ of mormyrid fish, the sound production muscle of toadfish, and the escape response of some invertebrates (e.g., cockroachs and crayfish) and vertebrates (e.g., fish).

The "tail-flick" escape response of the crayfish (Figure 6–30) involves giant axons in the nerve cord; they are giant to maximize conduction velocity. These axons stimulate large motor axons that innervate the abdominal musculature. There is an almost immediate depolarization of the giant motor fiber when the lateral giant fiber is stimulated. There is virtually no time delay, or latency, in transmission of electrical depolarization from the presynaptic to postsynaptic neuron. A small "kink" in the postsynaptic depolarization indicates the point at which the depolarization of the postsynaptic mem-

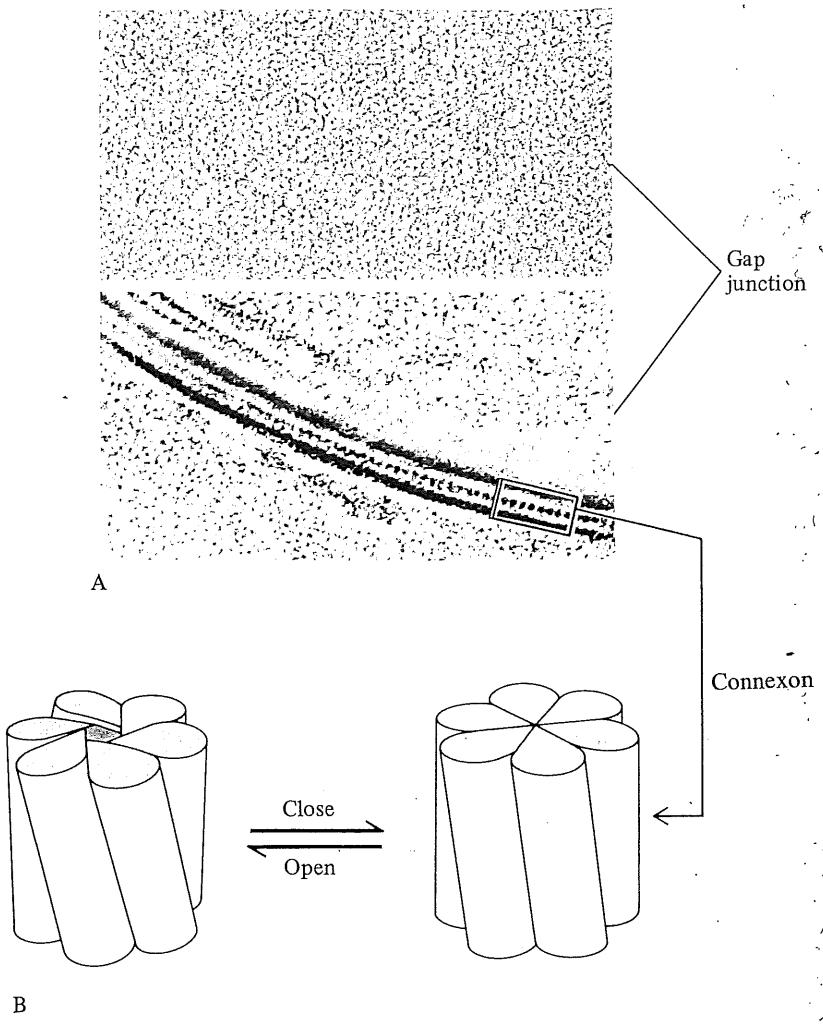

FIGURE 6–29 **(A)** Electron micrographs of the gap junction region viewed from a perpendicular direction (upper) and a parallel direction (lower). The connections appear as hexagonal units from above and as bridges connecting the two cell membranes from the side. **(B)** A schematic model of the six subunits of a connection suggest a mechanism for opening and closing of the connexon pore by a sliding and rotation of the subunits. *(From Unwin and Zampighi 1980.)*

brane reaches threshold. The normal direction of synaptic transmission is from the presynaptic membrane to the postsynaptic membrane (i.e., orthodromic). If the giant motor axon is stimulated, then little depolarization spreads to the lateral giant axons, i.e., there is little antidromic spread of the depolarization. This is a rectified electrical synapse.

Some electrical synapses are inhibitory. Many fish, when startled, rapidly flex their bodies by a massive synchronous contraction of lateral muscles on one side, followed by a tail flip. This startle response involves two large interneurons, the Mauthner fibers, with cell bodies in the brain and spinal axons that innervate the lateral musculature. It obviously is important that only muscles on one side of the body contract during the startle reflex, and so there must be rapid inhibition of one Mauthner cell when the other is active. There appears to be a hyperpolarizing and inhibitory potential near the axon hillock of a Mauthner cell when the other is firing (Furukawa and Furshpan 1963).

Chemical Synapses

Chemical synapses connect sensory cells to neurons, neurons to other neurons, and neurons to effector cells. They have a more complex structure than the simple gap junctions of electrical synapses.

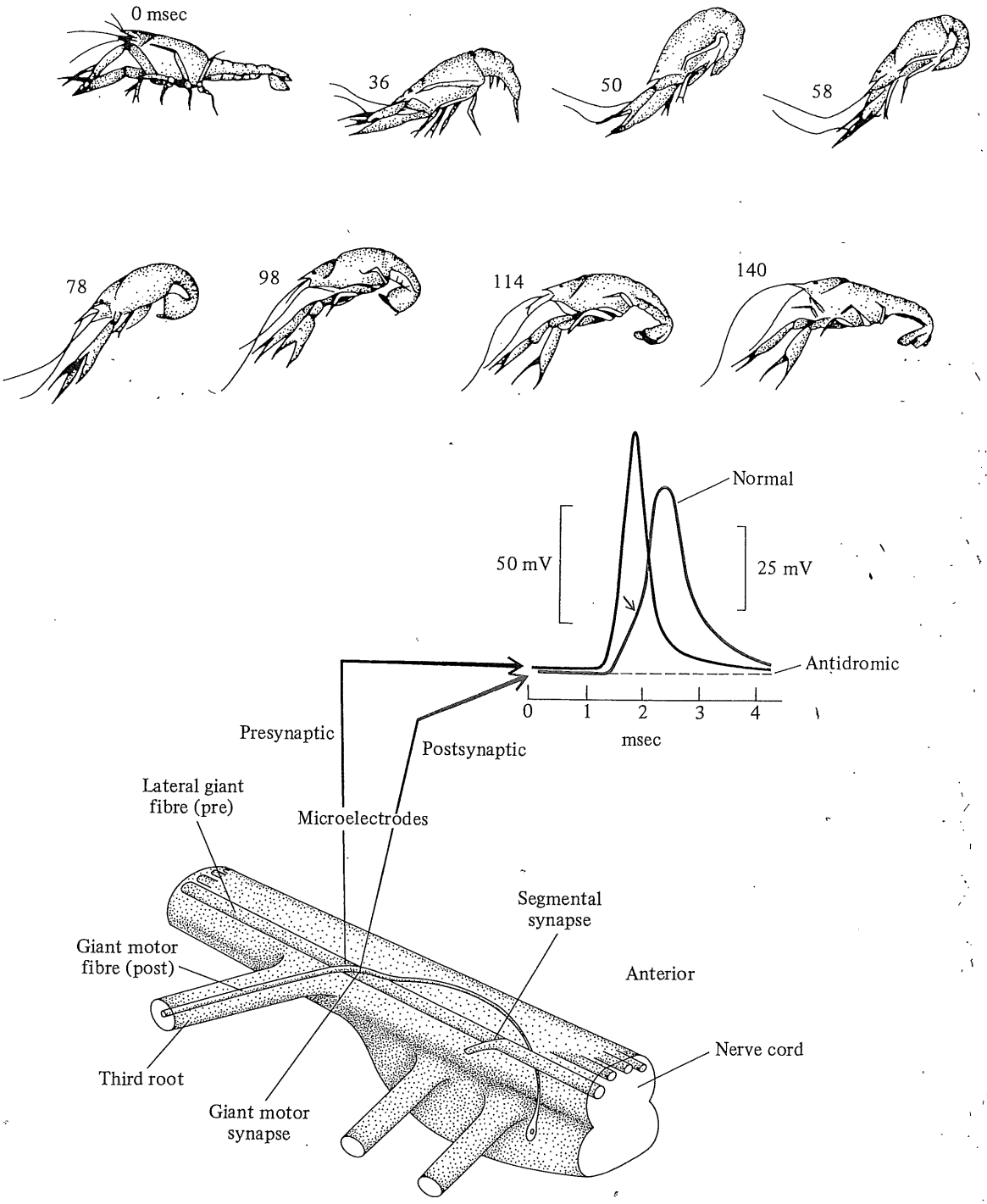

FIGURE 6–30 The "tail-flick" startle response of the crayfish (top panel) is controlled by lateral giant axons that innervate the tail flexor muscles via large motor fibers. The diagrammatic representation of part of the abdominal nerve cord of the crayfish shows the course of one motor axon from the cell body in the ventral nerve cord to the third ganglionic root on the other side of the nerve cord. The electrical synapse of the motor axon with the giant lateral axon is shown (not shown are additional electrical synapses between the motor axon and two medial giant axons). The recording microelectrodes are shown in the giant lateral axon and the motor axon. The normal stimulation of the giant fiber results in an extremely rapid depolarization of the motor axon; the postsynaptic potential initiates an action potential at the point indicated with an arrow. Antidromic stimulation of the motor axon results in a negligible (about 0.3 mV) depolarization of the lateral giant axon indicating that this electrical synapse is capable of considerable rectification. *(From Wine and Krasne 1982; Furshpan and Potter 1959.)*

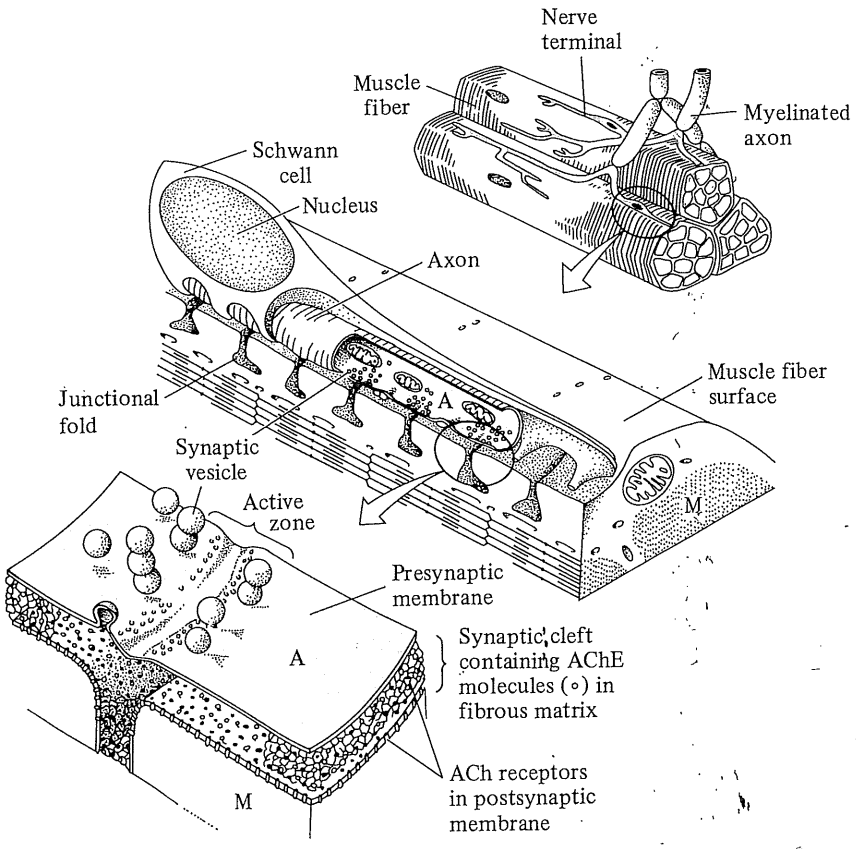

FIGURE 6–31 Representation of the end plate of a typical neuromuscular junction. Branches of the innervating axon form multiple end plates on one or more muscle cells; each axonal branch has an incomplete Schwann cell sheath. The synaptic vesicles are located in the axon terminal and are concentrated at synaptic junctional folds of the postsynaptic membrane, where neurotransmitter (acetylcholine) receptors are abundant. The extracellular matrix of the synaptic cleft contains acetylcholinesterase. *(From Hille 1984.)*

The neuromuscular junction is a typical example of a chemical synapse (Figure 6–31) between a presynaptic neuron membrane and a postsynaptic muscle cell membrane. The synaptic portion of the muscle cell membrane is the **end plate**. The axon terminal characteristically contains many mitochondria and synaptic vesicles, small membrane-bound vesicles about 40 nm diameter containing 1 to 5 10^4 molecules of neurotransmitter. There is a well-defined space, the synaptic cleft, between the presynaptic and postsynaptic membranes. This cleft is filled with mucopolysaccharide that attaches to the pre- and postsynaptic membranes.

The basic sequence of events during chemical synaptic transmission (Figure 6–32) is:

(A) the presynaptic action potential depolarizes the presynaptic membrane;
(B) the increased Ca^{2+} permeability of the depolarized presynaptic membrane allows Ca^{2+} influx into the axon terminal;
(C) the elevated intracellular Ca^{2+} concentration causes the release of neurotransmitter from synaptic vesicles into the synaptic cleft;
(D) neurotransmitter molecules diffuse across the synaptic cleft to the postsynaptic membrane, and they reversibly bind to specific receptors on the postsynaptic membrane;
(E) the receptor-neurotransmitter complex increases the permeability of the postsynaptic membrane to ions (e.g., Na^+, Ca^{2+}, Cl^-) and depolarizes or hyperpolarizes the end plate; and
(F) the end plate potential spreads electrotonically and initiates an action potential that propagates along the postsynaptic membrane, and the neurotransmitter is removed from the synaptic cleft by uptake into the presynaptic terminal and by enzymatic hydrolysis in the synaptic cleft.

Let us now examine some of these steps in greater detail.

Transmitter Release. Ca^{2+} has a central role in neurotransmitter release. There is a strong correlation between the postsynaptic depolarization and presynaptic intracellular Ca^{2+} concentration. A low extracellular Ca^{2+} concentration, presence of competing ions such as Mg^{2+} and La^{2+}, or depolarization of the E_m to E_{Ca} reduce neurotransmitter release,

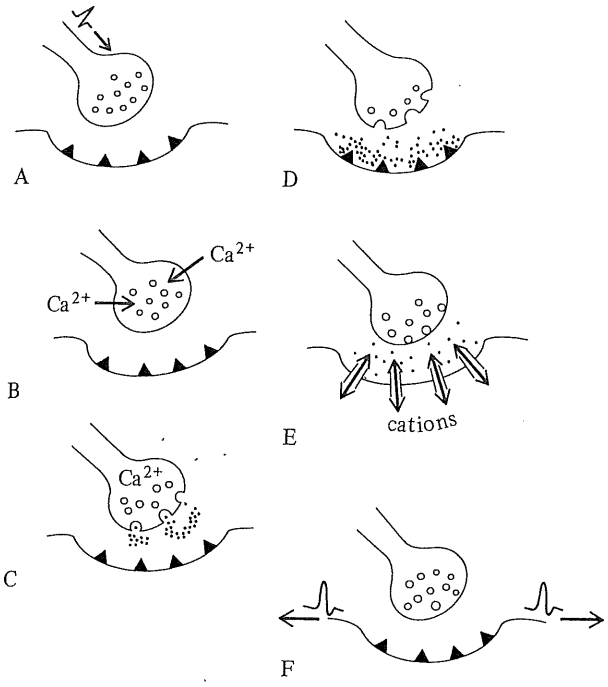

FIGURE 6–32 Representation of the sequence of events that occurs at a chemical synapse from an action potential reaching the axon terminal to initiation of a subsequent action potential on the postsynaptic membrane of a typical motor end plate. **(A)** Action potential reaches the presynaptic axon terminal. **(B)** Depolarization of axon terminal allows Ca^{2+} influx. **(C)** Increased intracellular Ca^{2+} concentration causes synaptic vesicles to release neurotransmitter into the synaptic cleft, by exocytosis. **(D)** Neurotransmitter diffuses to postsynaptic membrane. **(E)** Neurotransmitter combines with specific receptors on the postsynaptic membrane and opens fairly nonspecific cation channels. **(F)** Local current flow through cation channels depolarizes the postsynaptic membrane and the postsynaptic potential spreads electrotonically to the adjacent postsynaptic cell membrane and depolarizes it to threshold; an action potential is initiated and propagates over the postsynaptic cell membrane. The neurotransmitter is removed from the synaptic cleft and the cation channels close.

whereas microinjection of Ca^{2+} into the presynaptic terminal elicits additional neurotransmitter release.

The intracellular Ca^{2+} is required for the synaptic vesicle to fuse with the presynaptic membrane and release its contents (about 1 to 5 10^4 neurotransmitter molecules and about 1/5 as many ATP molecules) by exocytosis. The Ca^{2+} probably forms some intermediate, Ca"X" (or perhaps Ca_4"X"). There appear to be 2 to 4 Ca^{2+} per active site because the rate of neurotransmitter release is proportional to $(Ca^{2+})^n$, where n varies from 2 to 4 (Dodge and Rahamimoff 1967). The Ca^{2+} may activate a protein complex in the presynaptic terminal resembling actin and myosin of muscle cells. Brain presynaptic terminals contain two such proteins: neurin (associated with the presynaptic membrane) and stenin (associated with the synaptic vesicles) that may be involved in exocytotic neurotransmitter release.

There is considerable evidence for the quantal release of vesicles containing neurotransmitter, i.e., the release of the contents of 1 synaptic vesicle, or 2 vesicles, or 3, or 4, etc. (see Supplement 6–3, page 252). That the entire contents of a vesicle is released is not surprising, nor is the observation that either 1, 2, 3, 4, etc. vesicles release their contents at a time. This property of quantum release enabled the estimation of the number of neurotransmitter molecules per vesicle to be about 1 to 6 10^4.

Receptor Binding. The neuromuscular junction is a typical example of a chemical synapse. The postsynaptic membrane in the immediate vicinity of the synapse, the **motor end plate**, has proteinaceous receptors that specifically bind the neurotransmitter, acetylcholine (ACh). Each acetylcholine receptor has an ionic channel (Figure 6–33). The conductance of the motor end plate would increase linearly with (ACh) if only one ACh was required to bind to the receptor and open each channel. However, the conductance is proportional to $(ACh)^2$, suggesting that two ACh molecules are needed to open each ionic channel. The activation sequence for the receptor (R) by ACh would be something like the following.

$$R \overset{ACh}{\rightleftharpoons} R\text{-}ACh \overset{ACh}{\rightleftharpoons} R\text{-}ACh_2 \rightleftharpoons R\text{-}ACh_2^* \quad (6.17)$$

Only the activated $R\text{-}ACh_2^*$ complex opens the ionic channel. Once activated, the receptor becomes desensitized for a variable period of time during which the ionic channel remains closed even in the presence of ACh. The desensitized state may last briefly (fast desensitized state) or for seconds or more (slow desensitized state). The ACh-ionic channel can be specifically and irreversibly blocked by α-bungarotoxin (BuTX), which is one component of the venom of the krait, a highly venomous cobra snake. d-Tubocurarine, the active ingredient of curare, inhibits the action of ACh. It competitively binds to the ACh receptor but doesn't open the ionic channel. (Curare is a poison used by some South American Indians; it is a crude mixture of various plant extracts.)

The end plate ACh-ionic channel, when activated and open, is relatively unselective to cations. Any

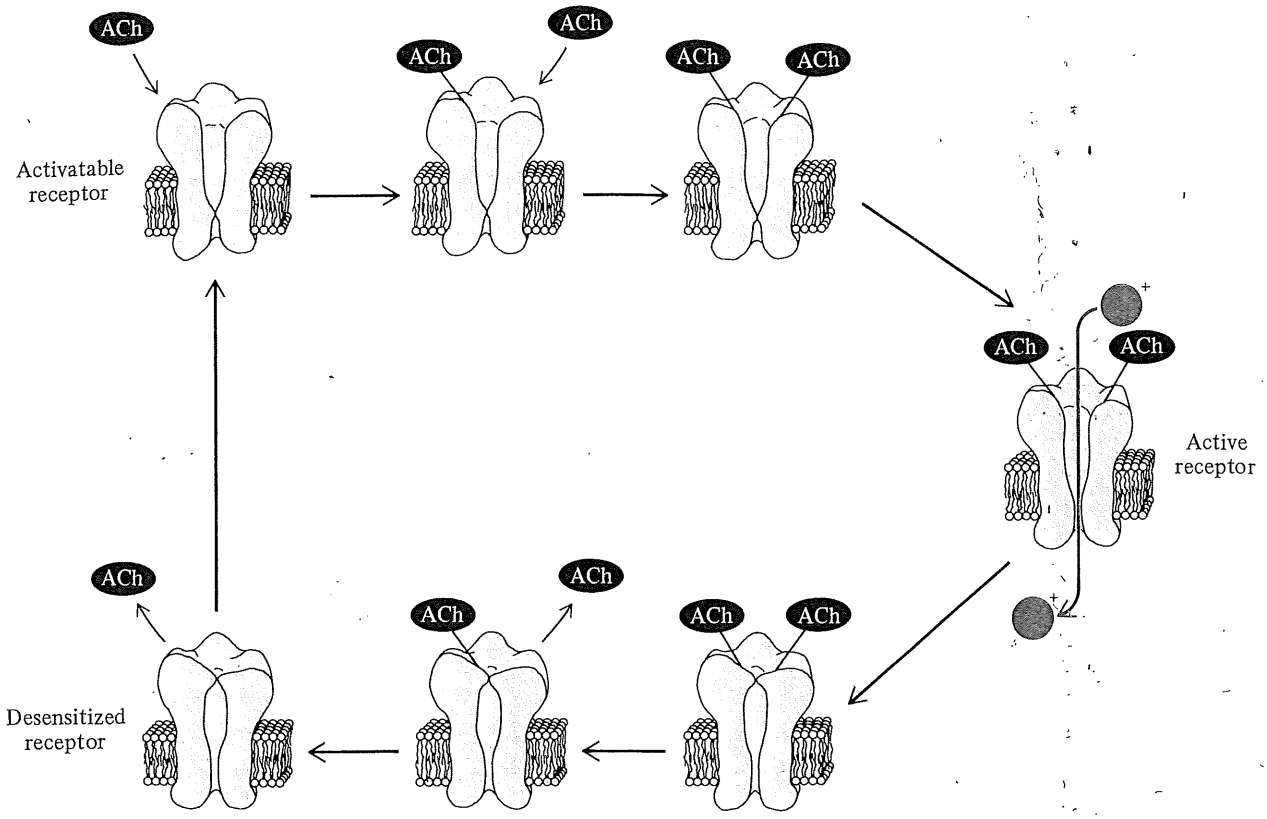

FIGURE 6–33 There is a complex series of reactions between the neurotransmitter acetylcholine and its receptor. This schematic diagram of these reactions shows the main cycle of activation, with two ACh molecules binding to a receptor and activating it, opening a cation channel through the membrane and allowing Na^+ influx. The ACh-receptor complex becomes inactivated and the ion channel closes, the ACh molecules detach from the receptor, and the receptor is temporarily desensitized to further binding of ACh and opening of the cation channel. *(From Montal, Anholt, and Labarca 1986.)*

monovalent and divalent cations are permeable if they can fit through a 0.65 × 0.65 nm pore. This includes not only the alkali metals (Li^+, Na^+, K^+, Rb^+, Cs^+, Fr^+) and alkaline earth metals (Be^{2+}, Mg^{2+}, Ca^{2+}, Sr^{2+}, Ba^{2+}, Ra^{2+}) but also various organic cations such as choline (Table 6–11). The channel rejects anions. It is this relatively unselective permeability to cations that results in the reversal potential of the end plate being different from the equilibrium potential of either K^+, Na^+, or Ca^{2+} (see below).

The synaptic cleft of the neuromuscular junction contains high concentrations of an enzyme that hydrolyzes ACh, **acetylcholinesterase** (ChE). The ChE rapidly removes ACh by hydrolysis; it can hydrolyze 10^{-14} mole ACh (6 10^9 molecules) in 5 msec.

Inhibitory synapses have anion channels, of relatively unselective permeability, e.g., glycine and GABA channels (Table 6–11).

End Plate Potentials. The **end plate potential** (EPP) is the electrical depolarization of the postsynaptic end plate. This membrane cannot sustain a regenerative action potential; it can only electrotonically propagate a depolarization. The remainder of the postsynaptic membrane can, however, propagate a regenerative action potential.

The separate recording of end plate potentials and action potentials at the postsynaptic membrane of a skeletal muscle cell can be accomplished by recording at different distances from the end plate, and by administering curare to reversibly block the action potentials (Figure 6–34A). At a considerable distance from the end plate, only the regenerative action potential is observed with low curare levels. Nearer the end plate, however, the regenerative action potential is recorded at low enough levels of curare to still allow depolarization to threshold, but at higher curare levels only subthreshold depolarizations due to electrotonic spread of the end plate

TABLE 6–11

Relative permeability of excitatory end plate ion channels to different ions in frog skeletal muscle in response to acetylcholine activation, and two inhibitory neuron ion channels of the mouse spinal cord that respond to the inhibitory neurotransmitters glycine and GABA.

Channels Neurotransmitter Permeability Ratio	Excitatory ACh P/P_{Na}		Inhibitory Glycine P/P_{Cl}	Inhibitory GABA P/P_{Cl}
Tl^+	2.51	SCN^-	7.0	7.3
NH_4^+	1.79	I^-	1.8	2.8
K^+	1.11	NO_3^-	1.9	2.1
Na^+	1.0	Br^-	1.4	1.5
Li^+	0.87	Cl^-	1.0	1.0
Trimethylamine	0.36	$Formate^-$	0.33	0.50
Ca^{2+}	0.22	HCO_3^-	0.11	0.18
$Acetate^-$	<0.01	$Acetate^-$	0.035	0.08
$Choline^+$	<0.15	F^-	0.025	0.02
Cl^-	<0.01	K^+	<0.05	<0.05

potential are observed. There is an exponential decrease in the amplitude of the end plate potential with distance from the end plate and an increasing time delay to peak depolarization, as would be expected for electrotonic spread (Figure 6–34B).

Small fluctuations in the end plate potential can be measured even in the absence of any stimulation of the presynaptic membrane. These spontaneous miniature end plate potentials have the typical shape of normal end plate potentials evoked by stimulation of the presynaptic neuron, but are of much smaller magnitude (typically 1 to 1.5 mV) than the normal end plate potentials (about 50 mV). These miniEPPs reflect the spontaneous release of one, or a few, synaptic vesicles. Neurotransmitter is released in a quantum fashion, i.e., one vesicle releases neurotransmitter, or two vesicles, or three vesicles, etc. (see Supplement 6–3, page 252). Exogenous administration of about 6000 molecules of ACh depolarizes the motor end plate by about 1 mV. An average miniEPP thus reflects the release of about 10000 molecules of ACh, and this must therefore be

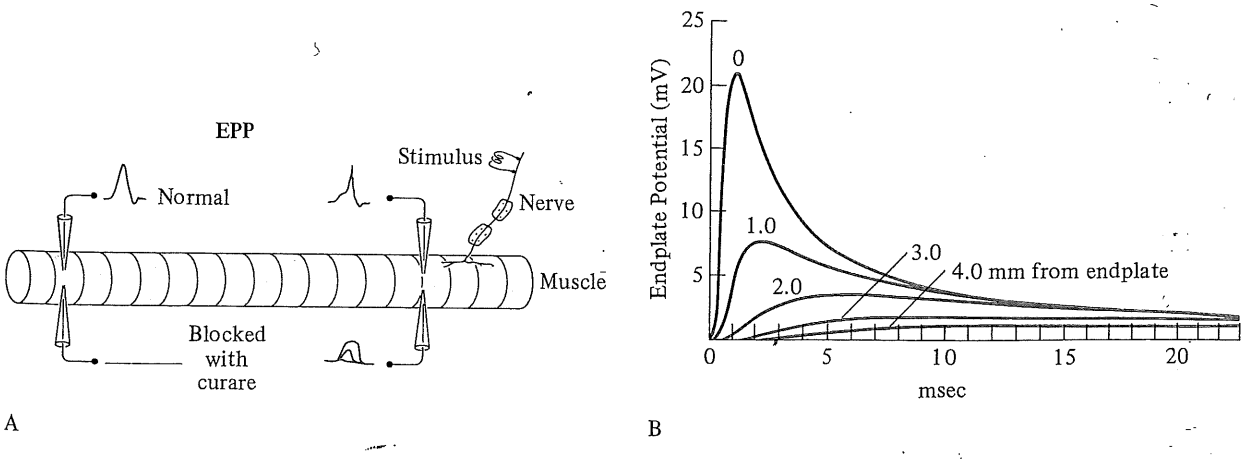

FIGURE 6–34 **(A)** Procedure shown in diagrammatic fashion for recording end plate potentials and action potentials of the postsynaptic membrane of a neuromuscular junction. Application of different levels of curare reversibly inactivates the postsynaptic membrane cation channels from opening, decreasing the amplitude of the end plate potential below threshold and inhibiting action potential initiation. **(B)** End plate potentials recorded at different distances from the end plate show electrotonic spread. The end plate potential amplitude diminishes with distance from the end plate, and the time delay increases. *(Modified from Katz 1966; Fatt and Katz 1951.)*

the number of neurotransmitter molecules in each synaptic vesicle (Kuffler and Yoshikami 1975).

The end plate does not sustain an action potential, and so the E_m will not rise to the action potential peak of +40 to 50 mV. The peak voltage of an end plate potential depends on the ion permeabilities of the ACh-receptor ion channel. This channel is relatively unspecific for cations (Table 6–11). There is a K^+ flux, and the I_K would hyperpolarize the E_m. Likewise, there are Na^+ and Ca^{2+} fluxes that depolarize the E_m. The E_m does not approach the equilibrium potential of any specific ion (e.g., E_K, E_{Na}, E_{Ca}) but approaches a potential determined by the relative permeabilities of all cations. This potential, called the **reversal potential** (E_{rev}) can be calculated from the Goldman-Hodgkin-Katz equation. For example, E_{rev} for the ACh-receptor ion channel can be estimated for mammalian skeletal muscle from the relative permeabilities of the channel to K^+, Na^+, and Ca^{2+} (Table 6–11) and the transmembrane ion concentrations (Table 6–5, page 208), considering only K^+, Na^+, and Ca^{2+} as follows.

$$E_{rev} = \frac{RT}{F} \ln \frac{[Na^+]_o P_{Na} + [K^+]_o P_K + [Ca^{2+}]_o^{\frac{1}{2}} P_{Ca}}{[Na^+]_i P_{Na} + [K^+]_i P_K + [Ca^{2+}]_i^{\frac{1}{2}} P_{Ca}}$$

$$= 58 \log_{10} \frac{(145)(1.0) + (4.0)(1.11) + (1.5)^{\frac{1}{2}}(0.22)}{(12)(1.0) + (155)(1.11) + (10^{-7})^{\frac{1}{2}}(0.22)}$$

$$= -5.2 \text{ mV} \qquad (6.18)$$

The normal E_m is depolarized toward E_{rev} when ACh is released at the motor end plate, although it doesn't necessarily reach E_{rev} if there is insufficient current flow. The E_m returns to normal when the ACh is removed by hydrolysis (Figure 6–35). If the E_m of the endplate is experimentally clamped to a more negative value, e.g., −50 mV, then the addition of ACh will cause a depolarization that will move E_m closer to E_{rev}. However, if the E_m is clamped to a value more positive than E_{rev}, e.g., +20 mV, then addition of ACh will hyperpolarize the E_m towards the E_{rev}. The direction of change in E_m is now opposite, or reversed, to the normal direction of change; this is why it is called the reversal potential.

The reversal potential is not the same for all postsynaptic ionic channels. E_{rev} depends on the nature of the transmitter and the specific properties of the ionic channels. Values for E_{rev} vary for different neurotransmitters/ionic channels from a hyperpolarizing −105 mV to a highly depolarizing +6 mV (Table 6–12). This variation in E_{rev} reflects the specific permeabilities of the ionic channel for various ions, either cations or anions. For example, the effects of different ratios of P_{Na} to P_K are shown in Figure 6–35.

Whether the effect of neurotransmitter release at a chemical synapse is excitatory or inhibitory is not an inherent property of the particular neurotransmitter. For example, acetylcholine can be excitatory at some synapses (e.g., the neuromuscular motor end plate) but inhibitory at other synapses (e.g., parasympathetic synapses in the heart).

Synaptic Delay. Depolarization of a presynaptic membrane is followed virtually instantaneously by a depolarization of the postsynaptic membrane at an electrical synapse; any small time delay could be ascribed to the cable constant properties of the membranes involved. In contrast, there is a considerable delay at a chemical synapse between

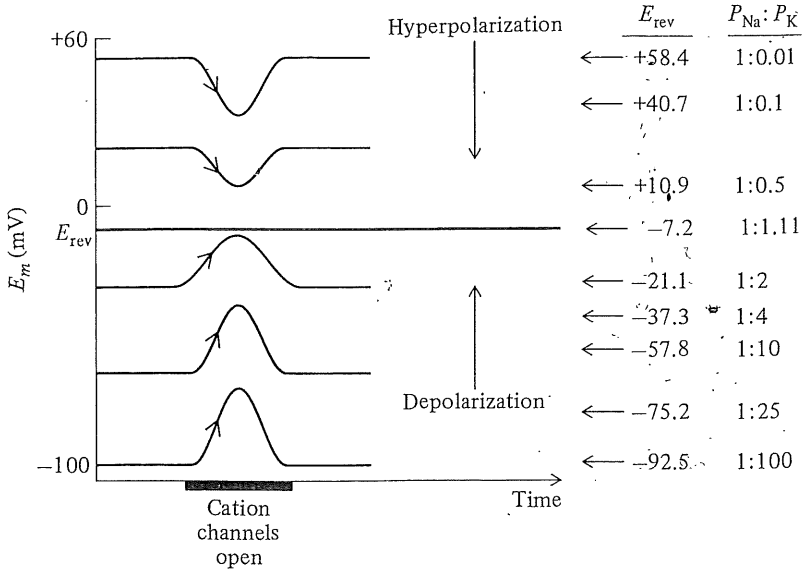

FIGURE 6–35 Reversal potential (E_{rev}) of a membrane clamped at varying membrane potentials is the potential towards which depolarization ($E_m < E_{rev}$) or hyperpolarization ($E_m > E_{rev}$) occurs when the cation channels are opened. The E_{rev} (−7.2 mV) shown in this example is for frog skeletal muscle end plate with a 1.0:1.11 ratio of P_{Na}:P_K. Different values of E_{rev} are shown for varying ratios of P_{Na}:P_K on the right. E values are calculated at 25° C using the short version of the Goldman-Hodgkin-Katz equation

$$E_{rev} = 59.16 \log_{10} \frac{[K^+]_o P_{K:Na} + [Na^+]_o}{[K^+]_i P_{K:Na} + [Na^+]_i}$$

TABLE 6–12

Summary of various end plate channels with differing receptors and electrical responses to neurotransmitters because of differences in ionic conductance changes and reversal potentials. *(Adapted from Hille 1984.)*

End Plate	Receptor	Response	Conductance Change	E_{rev}
Crayfish leg	Glutamate	EPSP	Cations	+ 6 mV
Frog skeletal muscle	ACh[1]	EPP	Cations	−5 mV
Aplysia buccal ganglion cell	ACh	Rapid IPSP	Anions	−60 mV
Crayfish leg	GABA	IPSP	Anions	−72 mV
Frog sympathetic ganglion cell	ACh[2]	Slow EPP	K^+	−86 mV
Mudpuppy parasympathetic ganglion cell	ACh[2]	Slow IPSP	K^+	−105 mV

[1] Nicotinic.
[2] Muscarinic.

electrical activity arriving at the presynaptic terminal and the regenerative action potential propagating away from the postsynaptic membrane. Considering the complex sequence of events involved in chemical synaptic transmission (A–F listed on page 234), it is not surprising that there is a time delay, especially as some events involve physical movement of synaptic vesicles and protein conformational changes. Any disadvantage of a time delay is apparently compensated for by the one-way transmission across synapses and the capacity for complex integration of numerous inputs.

The pre- and postsynaptic depolarizations of a frog-toe neuromuscular junction show considerable variability in the magnitude of the EPP (as expected reflecting the quantum release of synaptic vesicles) and also a considerable variability in the synaptic time delay, from 0.5 msec to 2.0 msec or even more. Why is there such a long synaptic delay, and why is it so variable? The time for diffusion of neurotransmitter from the synaptic cleft to the receptors can be estimated to be about 0.05 msec, i.e., it is insignificant. Postsynaptic depolarization begins within about 0.15 msec of the addition of neurotransmitter to the postsynaptic membrane, and so this is not the major time delay. The major portion of the synaptic time delay is most likely the opening of Ca^{2+} channels and the release of neurotransmitter from the presynaptic terminal. Probably the movement of the vesicles to the membrane and exocytosis is the major, variable time delay in chemical synaptic transmission.

Neurotransmitters. Identification of a substance as a neurotransmitter is often difficult. The criteria for probable identification of a substance as a neurotransmitter include: (1) it must be released from the presynaptic terminal during action potential transmission, (2) it must elicit the normal postsynaptic depolarization, and (3) the effect of the substance must be blocked by the same agents that block synaptic transmission. There are many different neurotransmitters, which fall into four general categories: (1) acetylcholine, (2) biogenic amines, (3) amino acids, and (4) peptides.

Acetylcholine is the neurotransmitter at the vertebrate neuromuscular junction; we have already examined in detail this neuromuscular junction as a typical example of a chemical synapse. ACh is also the neurotransmitter at the preganglionic synapse of the sympathetic and parasympathetic nervous system and the neurotransmitter at the postganglionic synapse of the parasympathetic nervous system (and also rarely at the postganglionic synapse of the sympathetic nervous system; see Chapter 8). The structure of ACh and the dynamics of its release, hydrolysis, and resynthesis are shown in Figure 6–36A. Not all ACh receptors are identical. For example, the vertebrate postganglionic parasympathetic ACh receptor (and the less common cholinergic sympathetic receptor) is stimulated by muscarine (derived from the mushroom *Amanita muscaria*); it is a **muscarinic** ACh receptor. In contrast, the preganglionic parasympathetic and sympathetic synapses, and the neuromuscular end plate are unaffected by muscarine but are stimulated by nicotine; these are **nicotinic** ACh receptors. The muscarinic and nicotinic receptors respond to different structural aspects of the same ACh molecule. Muscarine and nicotine compete with ACh for the receptor site, but muscarinic and nicotinic receptors have different inhibitors and potentiators.

The catecholamines, epinephrine (adrenaline), norepinephrine (noradrenaline), and dopamine con-

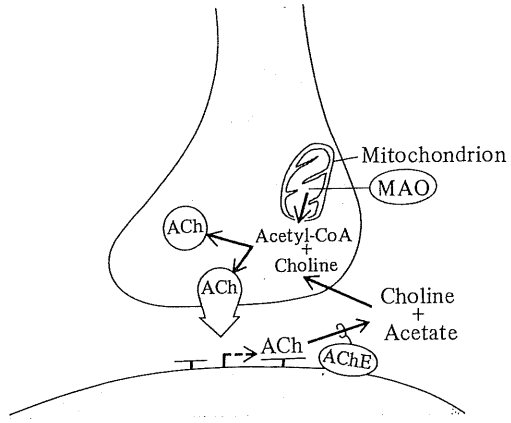

A Acetylcholine synapse

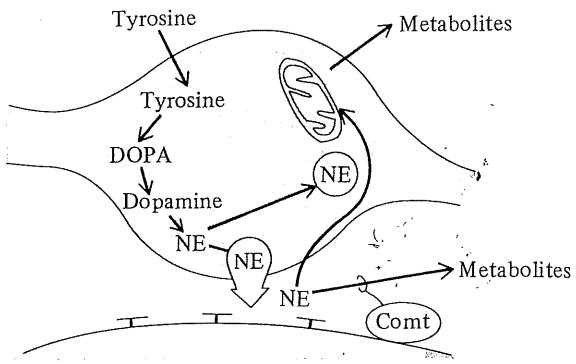

B Norepinephrine synapse

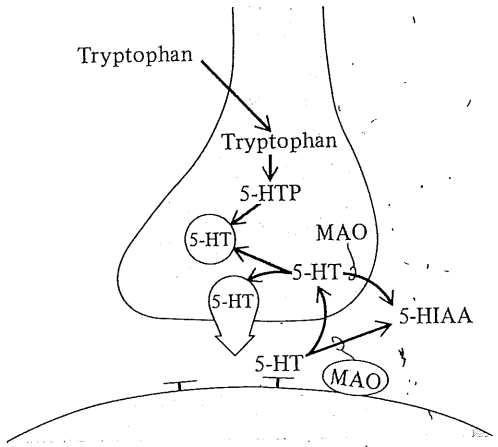

C 5-HT Synapse

FIGURE 6–36 **(A)** Dynamics of acetylcholine (ACh) release at a neuromuscular junction showing release, receptor binding, hydrolysis by acetylcholine esterase (ChE), and recycling of choline and acetate into the presynaptic nerve terminal. **(B)** Dynamics of norepinephrine synthesis, release, and recycling at a postganglionic axon swelling. The enzymes for norepinephrine hydrolysis (MAO, monoamine oxidase; COMT, catechol-o-methyl transferase are located intracellularly, not in the synaptic cleft). **(C)** Dynamics of a 5-hydroxytryptaminergic (5-HT) synapse showing synthesis, release, and recycling.

tain an amine and a catechol group (a benzene ring with two adjacent hydroxyl groups). They are closely associated by their common synthetic pathway from phenylalanine. Norepinephrine is the neurotransmitter of the postganglionic sympathetic synapse for most vertebrates (epinephrine is the transmitter in some, such as amphibians). Epinephrine and norepinephrine are also circulating hormones, released from the adrenal medulla. The pharmacology of catecholamine receptors is even more complex than that of ACh receptors. There are α- and β-type norepinephrine and epinephrine receptors and even subclasses of β receptor, e.g., β_1 and β_2 receptors. The dynamic cycle of norepinephrine release, hydrolysis, and resynthesis is summarized in Figure 6–36B. The catechols are enzymatically inactivated by monoamine oxidase (MAO; located within the mitochondria) and catechol-o-methyltransferase (COMT; in the cytoplasm). Both MAO and COMT are intracellular enzymes and therefore are not the primary means of inactivating catecholamines after release into the synaptic cleft. The catechols are removed from the synaptic cleft mainly by reincorporation into presynaptic vesicles or by diffusion into the general circulation.

Serotonin (5-hydroxytryptamine or 5-HT) is also an amine neurotransmitter, but it does not contain a catechol group. It is synthesized from the amino acid tryptophan (Figure 6–36C). The nervous systems of many mollusks contain 5-HT, and it is probably the neurotransmitter of the molluskan catch muscle synapse. It is also found in high levels in the central nervous system of vertebrates. There are at least three subtypes of 5-HT receptors: 5-HT_1, 5-HT_2, and 5-HT_3. These receptors for amine neurotransmitters are generally thought to transduce their effects via GTP binding proteins, but the 5-HT_3 receptor is also the actual ion channel (Derkach, Suprenant, and North 1989). Histamine is a neurotransmitter in arthropod photoreceptors (Hardie 1989).

A number of amino acids are known, or are suspected, to be neurotransmitters. Glutamate,

aspartate, glycine and cysteic acid, and GABA (γ-aminobutyric acid) may be neurotransmitters at various synapses in different animals.

A wide variety of neuropeptides have been putatively identified as neurotransmitters, although they can also be neuromodulators or hormones. The first neuropeptide identified as a neurotransmitter, Substance P, has acetylcholine-like effects but is not blocked by ACh antagonists. Other noteworthy neuropeptides that may act as neurotransmitters are antidiuretic hormone (ADH), oxytocin, angiotensin II, LH-releasing hormone, and cholecystokinin. Endorphins and enkephalins are neuropeptides that bind at opioid receptors on the surface membranes of some neurons. Met-enkephalin, leu-enkephalin, β-endorphin, and other related opioid peptides are generally thought to be the natural messengers that bind to opioid receptors in animal tissues to which morphine (a plant opioid) also binds (Kosterlitz 1985). These opioid receptors probably only coincidentally bind exogenous narcotic opiates (opium, morphine, heroin) although endogenous morphine is present in animal tissues (especially the brain) at low levels. There are three opioid receptors: μ, γ, and κ receptors. Morphine binds very selectively at low K_m to μ-receptors (selectivity index = 0.98; $K_m = 0.56\ nM^{-1}$), whereas β-endorphin and met-enkephalin have lower selectivity (0.52 and 0.09, respectively). Naloxone is a competitive inhibitor of opioid receptors, and thus interferes with the actions of exogenous and endogenous endorphins and enkephalins.

The classical concept of chemical synaptic transmission is the release of a single neurotransmitter that binds to a specific receptor on the postsynaptic membrane (i.e., Figure 6–37A). This simple concept has recently been elaborated in a number of ways. There may be a number of different receptors on the postsynaptic membrane that have different responses on synaptic transmission, e.g., α and β receptors (Figure 6–37B). In addition, there may be receptors for the neurotransmitter on the presynaptic membrane that influence subsequent synaptic transmission (Figure 6–37C). Many synapses have multiple neurotransmitters, i.e., there may be two or more neurotransmitters coexisting in the presynaptic terminal in the same vesicles or different vesicles (Figure 6–37D).

Many neuropeptides are found at the same synapse with some of the "more classical" neurotransmitters (e.g., norepinephrine, ACh, GABA; Table 6–13) or with other neuropeptides at synapses that lack a "classical" neurotransmitter (e.g., the hypothalamic neurosecretory cells of the paraventricular and supraoptic nuclei of the vertebrate central

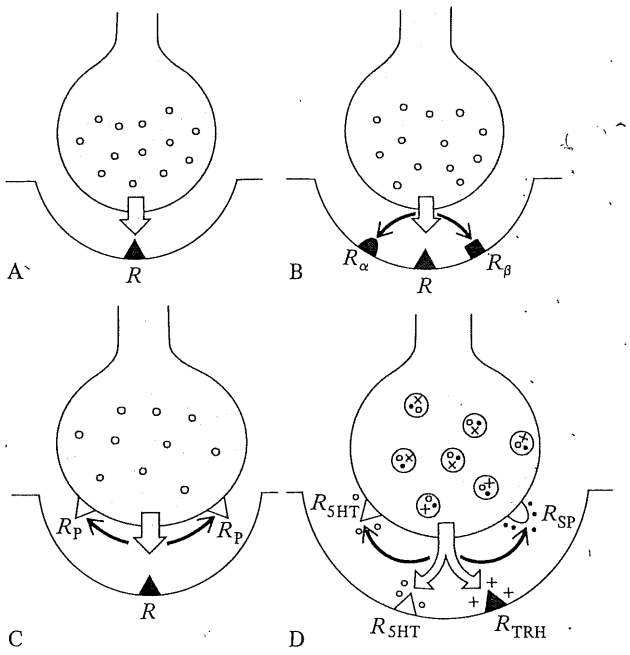

FIGURE 6–37 Representation of current concepts for chemical synaptic transmission. **(A)** Classical view of neurotransmitter release and binding to postsynaptic receptor (R). **(B)** There may be additional types of postsynaptic receptors for the same neurotransmitter that have different effects on the postsynaptic membrane (R_α and R_β). **(C)** There may be presynaptic receptors for the neurotransmitter that influence subsequent release of neurotransmitter (R_p). **(D)** There may be multiple neurotransmitters released at a single synapse with both postsynaptic and presynaptic receptors. Shown is a 5-HT neuron synapse in the ventral spinal cord that also contains thyroxin-releasing hormone (TRH) and Substance P. The smaller vesicles (about 50 nm dia) only contain 5-HT, whereas larger vesicles (about 100 nm dia) contain all three messengers. 5-HT acts on both postsynaptic excitatory receptors and presynaptic inhibitory receptors. TRH may act on a postsynaptic excitatory receptor (similar to the 5-HT receptor). Substance P may block the presynaptic inhibitory receptor of 5-HT. *(Modified from Hokfelt et al. 1986.)*

nervous system). Some neuron terminals contain more than one classical neurotransmitter (e.g., GABA and 5-HT, or GABA and dopamine can occur in the same presynaptic terminal). In some instances, ATP has been considered to be a neurotransmitter since it is often present in presynaptic vesicles (e.g., with ACh or norepinephrine). The functional role of multiple messengers at chemical synapses is not clear at present, but there are many possibilities. Multiple messenger systems may

TABLE 6–13

Coexistence of classical neurotransmitters and peptides in the central nervous system (based on immunohistochemical evidence). *(Modified from Hokfelt et al. 1986.)*

Classical	Peptide Neurotransmitter
Dopamine	CCK[1], neurotensin
Norepinephrine	Enkephalin, NPY[2], vasopressin
Epinephrine	CCK, Substance P, neurotensin, NPY
5-HT	CCK, enkephalin, Substance P, TRH[3]
ACh	Enkephalin, Substance P
GABA	CCK, enkephalin, NPY
Glycine	Neurotensin

[1] CCK = cholecystokinin.
[2] NPY = neuropeptide Y.
[3] TRH = thyrotropin releasing hormone.

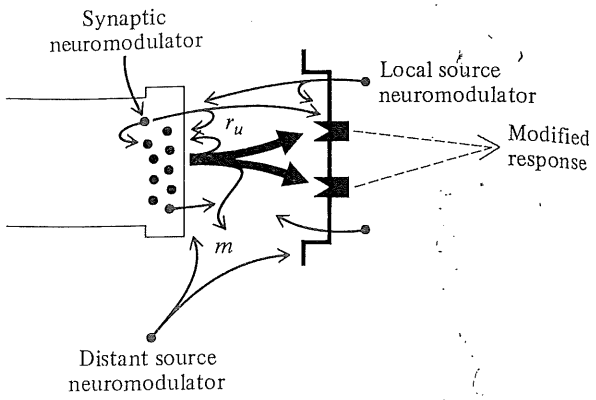

FIGURE 6–38 The presence of a neuromodulator (●) produces a modified synaptic response to transmission at a chemical synapse. The neuromodulator can be released from the synapse, from a local source (e.g., the postsynaptic cell), or from a distant sourse. The possible mechanisms for action of neuromodulator may be on the synaptic vesicles, on vesicular release of neurotransmitter (●), on the interaction of the neurotransmitter with its receptor (◣), on reuptake (r_u) of the neurotransmitter, or on the metabolic removal (m) of the neurotransmitter. *(Modified from Gorski 1983.)*

increase the capacity for complexity of information transfer. Multiple receptor systems on the postsynaptic membrane can have different effects on transmission properties if they have different reversal potentials; receptors, or multiple receptors on the presynaptic membrane, could also have different effects on subsequent synaptic transmission. The neuropeptides may not be involved with the transmission of action potentials *per se*, but may have other roles, e.g., growth (trophic) effects, induction of long-term changes in synaptic function (neuromodulation; see below), etc.

A variety of neurotransmitters and neuropeptides act as **neuromodulators** because they alter, or modify, the functioning of synapses (Figure 6–38). For example, serotonin, GABA, norepinephrine, and octopamine are neurotransmitters that are thought to be such modulating agents; several opiates and enkephalins are also thought to be modulating agents. These neuromodulating agents that alter synaptic transmission may be released at that synapse or may be released from a different synapse, i.e., they have a heterosynaptic effect. Their action may be to change the Ca^{2+} influx into the presynaptic terminal, thereby influencing synaptic vesicle release of neurotransmitter.

Synaptic Agonists and Antagonists. Modification of any of the sequential processes of synaptic transmission can block or potentiate transmission. Chemicals agents, or drugs, that have the same effect as a neurotransmitter are **agonists** (or mimetics), whereas chemicals that reduce or prevent synaptic transmission are **antagonists** (or lytics).

Agonists often mimic the neurotransmitter at the receptor site. For example, choline, carbachol, succinylcholine, nicotine, and muscarine are all agonists of acetylcholine; part of their chemical structure mimics that of ACh, hence they mimic ACh at the receptor site (Figure 6–39). Agonistic effects can occur by mechanisms other than mimicking the neurotransmitters at the receptor. For example, the venom of the black widow spider causes massive release of ACh from the presynaptic vesicles, thereby mimicking normal ACh synaptic transmission (this is followed by a block in transmission because synaptic vesicles are depleted by the action of the venom). A number of drugs (eserine, neostigmine) and organophosphates (e.g., diisopropylphosphofluoridate) inhibit acetylcholine esterase, thereby potentiating the effect of normally released ACh.

Antagonists may competitively or noncompetitively inhibit the neurotransmitter at the receptor site. Curare, a crude mixture of various plant alkaloids, including d-tubocurarine, competitively blocks ACh at the receptor. α-bungarotoxin, a polypeptide from the venom of the krait *Bungarus multicinctus*, noncompetitively binds to the ACh receptor. Hemicholinium prevents synthesis of ACh. Botulinum toxin (produced by the bacterium

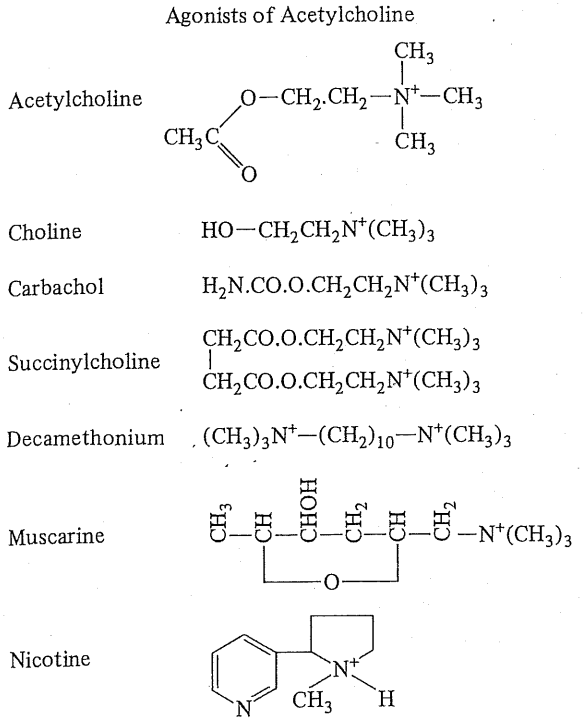

FIGURE 6–39 Chemical structure of acetylcholine compared with that of a variety of agonists.

Clostridium botulinum) prevents the release of ACh from presynaptic vesicles.

Cone shells (*Conus*) have a potent venom that they inject into their prey (fish) to rapidly immobilize them. The venom contains a variety of toxic peptides, called conotoxins (Olivera et al. 1987). These are small polypeptides (13 to 29 amino acids), are strongly basic, and are highly cross-linked. They act at various steps in neuromuscular transmission. The ω-conotoxin prevents the voltage-dependent influx of Ca^{2+} into the presynaptic terminal, α-conotoxins inhibit the ACh receptor, and μ-conotoxins directly inhibit the postsynaptic (muscle cell) action potential.

Neural Integration

Synapses integrate incoming action potentials, often in exceedingly complex fashions. A single neuron can have hundreds, or even thousands, of presynaptic terminals. This immense amount of incoming information is integrated at the axon hillock (where the axon extends from the cell soma) to generate the efferent information (action potentials) that travel along its axon. Effector cells generally do not integrate information by having numerous presynaptic terminals, but simply respond to the presence or absence of afferent information from a single neuron. For example, most types of muscle cell have a single, or a few, excitatory motor end plates. However, some effector cells (e.g., invertebrate striated muscle) are innervated by two or even more types of neurons, which are excitatory and inhibitory.

The α motoneuron of the vertebrate spinal cord has been well studied with respect to neural integration. The cell body, which is located in the ventral horn of the spinal cord, receives thousands of excitatory and inhibitory synapses, the net integration of which determines its rate of action potential firing. The axon extends from the spinal cord to innervate a peripheral skeletal muscle cell. The action potentials that arise in the neuron are initiated at its axon hillock. This membrane region has a lower threshold and therefore a greater sensitivity to depolarization than the rest of the cell.

An excitatory synaptic event increases the likelihood of an action potential being initiated at the axon hillock, i.e., the reversal potential is more positive than the threshold. However, the depolarization of a single synapse generally does not even approach the reversal potential because of the low number of postsynaptic ionic channels opened. The stimulation of a single presynaptic terminal will release a few synaptic vesicles of neurotransmitter and depolarize the axon hillock membrane by only a mV or so towards the reversal potential; this is an **excitatory postsynaptic potential** (EPSP). This is in marked contrast to the neuromuscular junction previously described where presynaptic stimulation typically released 200 or so synaptic vesicles and depolarized the end plate membrane by about 40 to 60 mV. The small depolarization of the postsynaptic membrane by a single presynaptic terminal is analagous to the mini-end plate potentials of the neuromuscular junction end plate. Postsynaptic currents spread electrotonically from the dendrites in accord with the cable properties of the cell membrane. Depolarizing currents from different synapses are attenuated to varying extents when they reach the axon hillock. For example, a long, slender dendrite will have greater attenuation of its EPSP than would a short, thick dendrite or a synapse nearer the axon hillock. Some incoming action potentials are thus more important than others.

A large number of presynaptic terminals must be depolarized before the axon hillock of a neuron is sufficiently depolarized to initiate an action poten-

tial. The activity of one presynaptic terminal is added to the depolarizations of other presynaptic terminals; this is **spatial summation**, a summation of different stimuli occurring at different places (Figure 6–40A). Alternatively, the sequential activity of two presynaptic terminals will add, or superimpose, the depolarization of the second to that of the first; this is **temporal summation** (Figure 6–40B).

An **inhibitory postsynaptic potential** (IPSP) has a reversal potential that is more negative than threshold. The IPSP will hyperpolarize the E_m if the reversal potential is more negative than E_m. A postsynaptic potential with E_{rev} equal to resting E_m will cause no change in E_m. If the reversal potential lies between threshold and E_m, then the membrane depolarizes but the IPSP will reduce the depolarizing effect of a simultaneous EPSP and inhibit an action potential that might have been initiated had the IPSP not occurred (Figure 6–40C). The neurotransmitter GABA causes postsynaptic inhibition because its receptor-gated, postsynaptic membrane channels allow Cl^- flow. Consequently, GABA-activated receptors stabilize E_m close to the resting value and are inhibitory because E_{Cl} is similar to resting E_m. Inhibitory postsynaptic potentials are also summed (actually, subtracted) with EPSPs at the axon hillock.

Some GABA Cl^- channels are also permeable to HCO_3^- (see Table 6–11, page 237). The large size of HCO_3^- ions suggests that these HCO_3^--permeable Cl^- channels are about 0.52 nm diameter. There is a substantial electrochemical force driving HCO_3^- out of the cell (Kaila and Voipio 1987). The intracellular and extracellular HCO_3^- concentrations are about 15 to 20 mM in crayfish and mammalian neurons, and so the resting E_m of about −90 mV is a large outward driving force for HCO_3^-. The E_{rev} for HCO_3^- is about 0 mV; the E_{rev} for the GABA-activated Cl^-/HCO_3^- channels is about 10 to 15 mV more positive than E_{Cl}. Some glycine-activated Cl^- channels are also permeable to HCO_3^-. An outward flux of HCO_3^- could increase the intracellular pH and modify the sensitivity of ion channels and even alter intracellular ion concentrations.

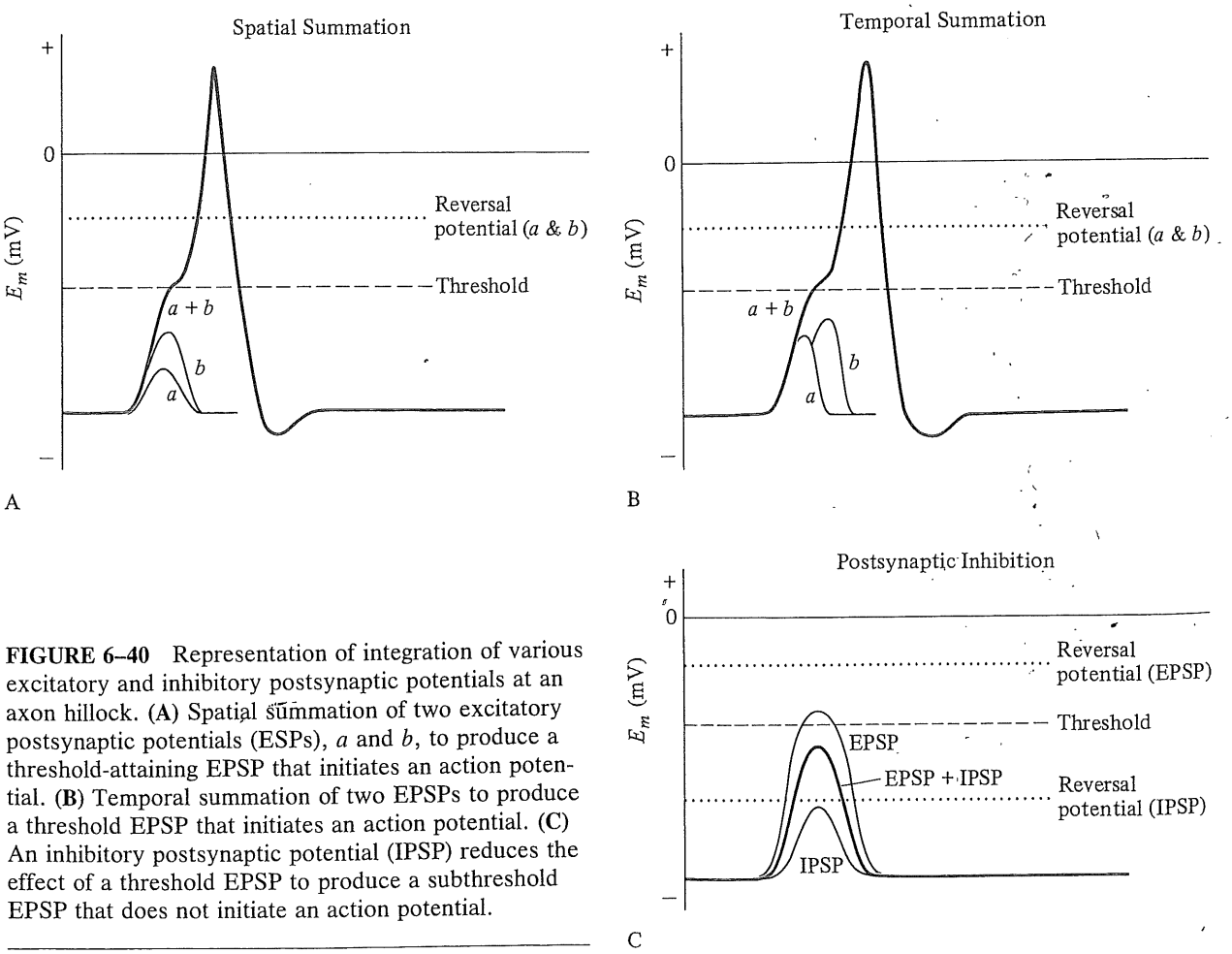

FIGURE 6–40 Representation of integration of various excitatory and inhibitory postsynaptic potentials at an axon hillock. **(A)** Spatial summation of two excitatory postsynaptic potentials (ESPs), *a* and *b*, to produce a threshold-attaining EPSP that initiates an action potential. **(B)** Temporal summation of two EPSPs to produce a threshold EPSP that initiates an action potential. **(C)** An inhibitory postsynaptic potential (IPSP) reduces the effect of a threshold EPSP to produce a subthreshold EPSP that does not initiate an action potential.

The summation and inhibition processes described so far occur at the postsynaptic membrane; they are **postsynaptic excitation** and **postsynaptic inhibition**. In contrast, **presynaptic inhibition** occurs when an inhibitory nerve terminal synapses with an excitatory nerve terminal, and activity of the inhibitory nerve terminal diminishes the amount of transmitter released at the excitatory synapse. There are many examples of presynaptic inhibition, but a particularly interesting one is the crustacean striated muscle fiber, which has not only an excitatory innervating axon but also an inhibitory innervating axon; this is a relatively uncommon example of multiple innervation of an effector cell (Figure 6–41A). The inhibitory axons responsible for postsynaptic inhibition also send collateral branches that terminate on the excitatory innervating axons; this occurs at both the muscle and within the central nervous system. The presynaptic inhibitory synapse appears to increase the permeability of the excitatory presynaptic membrane to K^+ and/or Cl^-, thereby decreasing the magnitude of the action potential spike, of Ca^{2+} influx, and of neurotransmitter release. There is therefore a reduced postsynaptic potential. About 16 quantum units of postsynaptic current can be measured for a crustacean striated muscle fiber in response to stimulation of the excitatory neuron; this is reduced to almost zero by presynaptic inhibition (Figure 6–41B). Presynaptic inhibition occurs in the vertebrate and invertebrate central nervous systems, as well as the crustacean striated muscle fiber.

The effect of a postsynaptic depolarization depends not only on the cable properties but also on the recent history of synaptic activity. There can be temporary functional alterations in synaptic transmission dependent upon its prior activity. Facilitation, depression, and post-tetanic potentiation are examples of such use-dependent changes in synaptic function.

Facilitation occurs when the effect of a presynaptic stimulus is enhanced by another presynaptic stimulus, i.e., the effect of the second stimulus is greater than the effect of the first, and the sum of the two is greater than twice the first stimulus (Figure 6–42). Facilitation occurs because some calcium ions that entered the nerve terminal during the first stimulus are still present during the second; the intracellular $[Ca^{2+}]$ is therefore greater for the second stimulus and so more neurotransmitter is released (neurotransmitter release is proportional to $[Ca^{2+}]^n$ where n is 2 to 4).

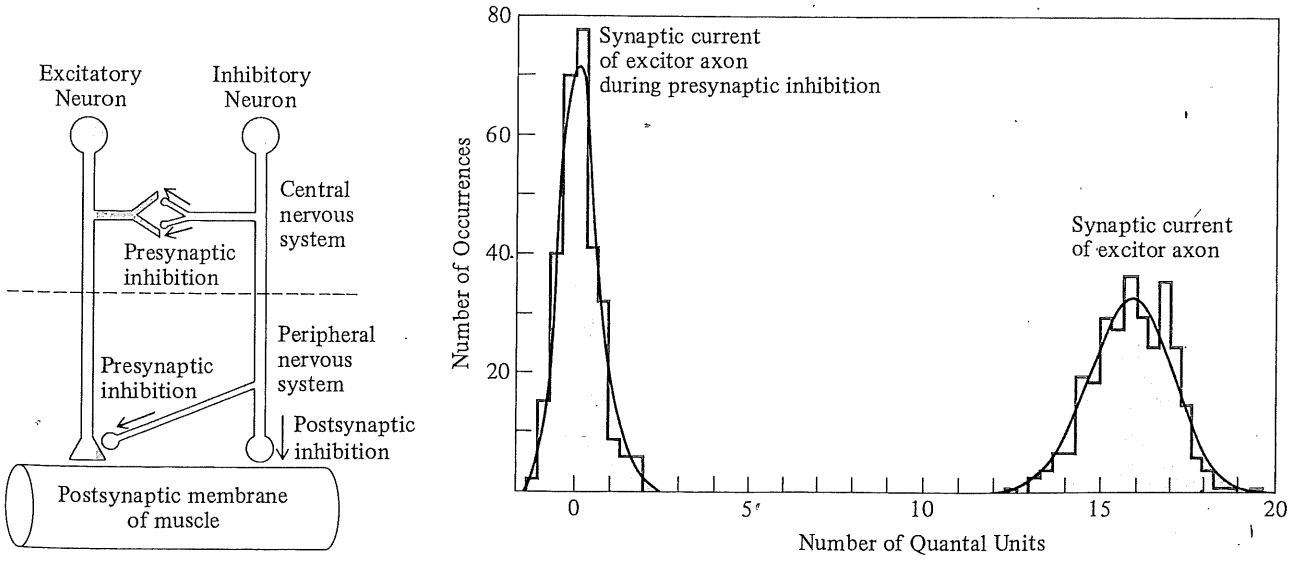

FIGURE 6–41 **(A)** Organization of the neuromuscular excitator and inhibitor neurons of the crayfish claw. The excitator muscle that opens the claw is presynaptically inhibited at both the muscle fiber synapse and within the central nervous system. **(B)** Recording from synapses of the crab leg muscle neuromuscular junction indicates that stimulation of the excitatory nerve causes release of about 16 quanta of neurotransmitter (with a high probability of release; $P = 0.99$). The probability of quantum release is markedly decreased by presynaptic inhibition ($P = 0.16$) and far fewer quanta are released. *(From Tse and Atwood 1986.)*

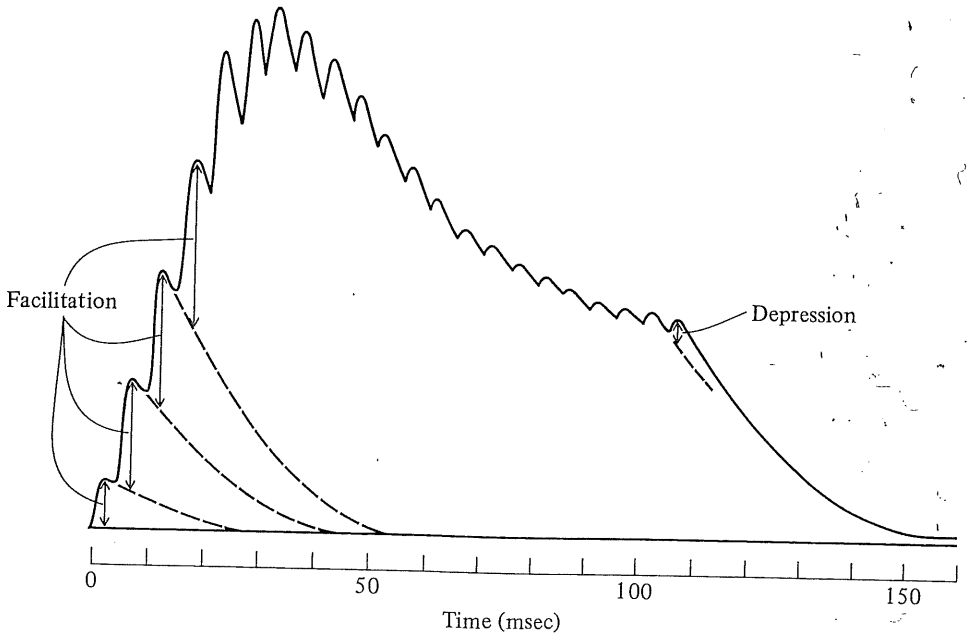

FIGURE 6–42 Repetitive stimulation initially causes a facilitation of the response (vertical bar with arrowheads) but eventually causes depression of the response to each individual stimulus. *(From Katz 1966.)*

Synaptic depression is the decrease in magnitude of the postsynaptic potential that occurs with repeated stimulation of the synapse because of depletion of synaptic vesicles in the presynaptic terminal. Fewer synaptic vesicles fuse with the presynaptic membrane, less neurotransmitter is released, and the postsynaptic potential is correspondingly reduced. Depression does not occur during magnesium block (elevated extracellular [Mg^{2+}]) because the Mg^{2+} diminishes the rate of neurotransmitter

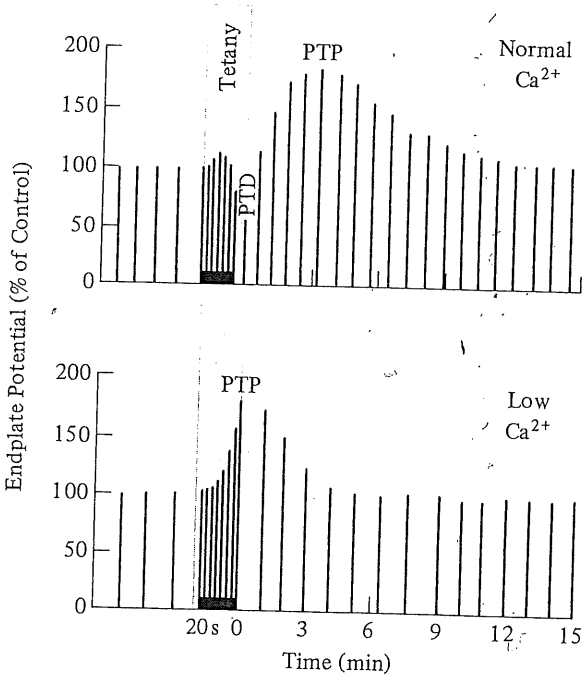

FIGURE 6–43 Tetanic stimulation of the frog neuromuscular junction normally results in post-tetanic depression, followed by post-tetanic potentiation at slower stimulation rate. The post-tetanic depression (PTD) is due to synaptic vesicle depletion, and post-tetanic potentiation (PTP) is due to residual elevation of intracellular Ca^{2+} concentration and reformation of synaptic vesicles. With low extracellular Ca^{2+} ($^1/_{12}$ normal), there is no post-tetanic depression (since synaptic vesicles are not depleted) but post-tetanic potentiation occurs sooner because of the residual intracellular Ca^{2+}. *(Modified from Rosethal 1969.)*

release and synaptic vesicles are not depleted by repetitive stimulation.

Post-tetanic potentiation occurs after repetitive high-frequency stimulation of a presynaptic terminal (Figure 6–43). The postsynaptic potential declines with repetitive stimulation due to synaptic vesicle depletion. After the tetanic stimulation is removed, there is a delayed increase in the postsynaptic potential which greatly exceeds that of the control postsynaptic potential (by about 2 ×). This post-tetanic potentiation of the postsynaptic potential is probably due to residual Ca^{2+} ions in the presynaptic terminal that augment release of the neurotransmitter once it is again present in synaptic vesicles. If this experiment is repeated with a low external $[Ca^{2+}]$, there is a smaller postsynaptic potential because the intracellular $[Ca^{2+}]$ is lower, there is no synaptic depression because there has not been any depletion of synaptic vesicles, and there is an immediate (not delayed) post-tetanic potentiation because of the residual Ca^{2+} in the presynaptic terminal.

Summary

Cells have an outer cell membrane (plasmalemma) and a complex array of inner membrane structures. Membranes are responsible for control of entry of solutes into and out of cells, and the compartmentalism of the cell into regions of specialized structure and function. Membranes are lipid bilayers and associated proteins that are often enzymes, transport mechanisms, or ion channels. Solute permeation of membranes can be passive diffusional exchange, due to lipid solubility or exchange through pores; passive transport by a facilitated diffusion carrier; or active transport by an energy-requiring carrier mechanism.

There generally is an electrical potential across biological membranes (resting membrane potential, E_m). A Donnan effect and electrogenic pumps contribute to the E_m, but the most important source of biopotentials is ionic equilibrium potentials. The ionic equilibrium potential (E_{eq}) for a particular ion species depends on its concentration difference across the membrane; its magnitude is calculated by the Nernst equation. The membrane potential is determined by the relative mobility, permeability, and concentration differences for each ion species between the inside and outside of the cell membrane; its magnitude is calculated by the Hodgkin-Huxley-Katz equation. The normal, resting E_m is approximately equal to the K^+ equilibrium potential, about −90 mV (inside relative to outside).

Action potentials are rapid, transient changes in E_m (about 1 msec duration) from the K^+ equilibrium potential (−90 mV) to about the Na^+ equilibrium potential (+60 mV). The action potential is initiated by depolarization of the E_m to a critical threshold value, and a consequent positive feedback increase in membrane Na^+ permeability. The Na^+ permeability is voltage dependent and increases with depolarization; the increase in Na^+ permeability then depolarizes the membrane further, initiating a positive-feedback cycle of continued depolarization. The action potential is terminated by an automatic decrease in membrane Na^+ permeability and by a transient increase in K^+ permeability that hyperpolarizes the membrane.

Action potentials are induced in excitable membranes by a depolarization to threshold. They are (generally) all-or-none transient increases in E_m, i.e., either an action potential occurs in response to depolarization or it doesn't. Information is conveyed by the rate of action potential firing, not by their shape or amplitude. There is an inverse relationship between the depolarization intensity and duration required to initiate an action potential, and there is a minimum depolarization voltage (rheobase) required to elicit an action potential. There is a latency period between the depolarizing stimulus and the action potential. Excitable membranes have an absolute refractory period during which they are unresponsive to successive depolarizing stimuli and cannot sustain an action potential. This is followed by the relative refractory period in which an action potential of reduced amplitude can be initiated.

Excitable membranes, such as neuron axons, can propagate an action potential at a velocity dependent on their cable properties, i.e., membrane capacitance and resistance. The conduction velocity for unmyelinated axons is proportional to the square root of the diameter. Many invertebrates and vertebrates have giant axons that provide rapid conduction of important reflexive information (e.g., predator escape responses). Myelination of axons by Schwann sheath cells also increases the conduction velocity by making action potentials saltate between adjacent nodes (lacking the myelin sheath). The conduction velocity of myelinated axons is proportional to internodal distance and axon diameter.

Electrical activity is transmitted between excitable cells at synapses. Electrical synapses allow rapid coupling of neurons for highly synchronized responses. Chemical synapses have a more complex structure and functioning. A specific chemical messenger, the neurotransmitter, is released from vesicles in the presynaptic terminus. The neurotransmitter diffuses to the postsynaptic membrane

and binds to specific postsynaptic receptors. Activation of the receptors modifies the permeability of relatively nonspecific anion and cation channels, which causes depolarization or hyperpolarization of the postsynaptic membrane. Depolarization of the postsynaptic membrane to threshold will elicit an action potential in the postsynaptic cell. Chemical synapses allow complex integration of information of the synapse and unidirectional information transfer.

Supplement 6–1

Hodgkin-Huxley Model of Action Potentials

Changes in ionic conductance and E_m during an action potential were elegantly measured and analyzed by Hodgkin and Huxley in the 1950s using voltage clamp experiments. Their results illustrate the basic principles of action potential generation and the relationships between E_m, ionic conductance, and ionic currents.

In a representative experiment, the resting membrane potential of a squid giant axon was depolarized and clamped to about −60 mV; the membrane potential was then rapidly depolarized and held at 0 mV. There was a transient inward current of about 2 mA followed by a maintained, outward current of about 2 mA. A different current signal was recorded if the experiment was repeated with the axon in a fluid bath with a low Na^+ and high K^+ concentration rather than normal squid Ringers because there could be no current due to Na^+ movement. The difference between these two current signals, normal and low Na^+, represents the Na^+ current (I_{Na}) that flows during the action potential. If all of the external Na^+ were replaced with choline [an impermeant cation, $HOCH_2CH_2N^+(CH_3)_3$], then there is actually a small outward Na^+ current when the Na^+ permeability increases because of Na^+ efflux. The potassium current could also be readily determined during an action potential by similar experimental manipulations. The Na^+ and K^+ conductances during an action potential were calculated from the currents, I_{Na} and I_K, as

$$I_{Na} = g_{Na}(E_m - E_{Na})$$
$$I_K = g_K(E_m - E_K)$$

The data for g_{Na}, g_K, I_{Na}, and I_K at a variety of voltage-clamped values of E_m were used to formulate a mathematical model of the membrane potential, current flow, and permeability changes that occur during an action potential. The changes in sodium conductance were analyzed as being due to two discrete events: Na^+ channel activation and inactivation. The activation event is due to opening of three channel gates (m) and inactivation by a single gate (h). The potassium conductance was analyzed as being activated by the opening of four n gates. The conductance of the Na^+ and K^+ channels is

$$g_{Na} = g_{Na,max}m^3h$$
$$g_K = g_{K,max}n^4$$

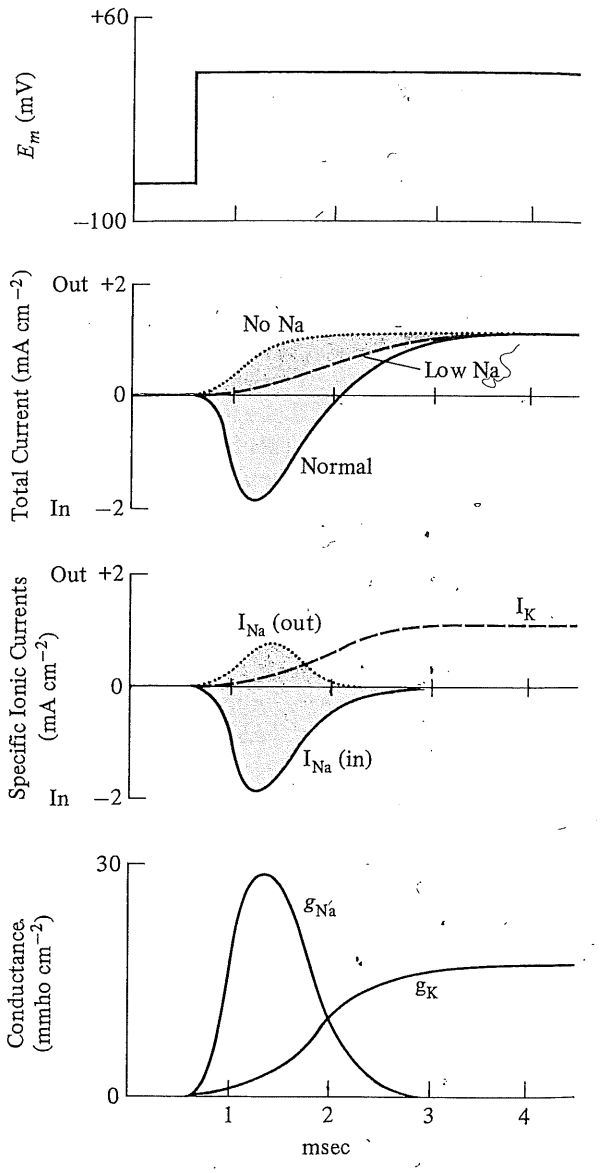

Currents during an action potential.

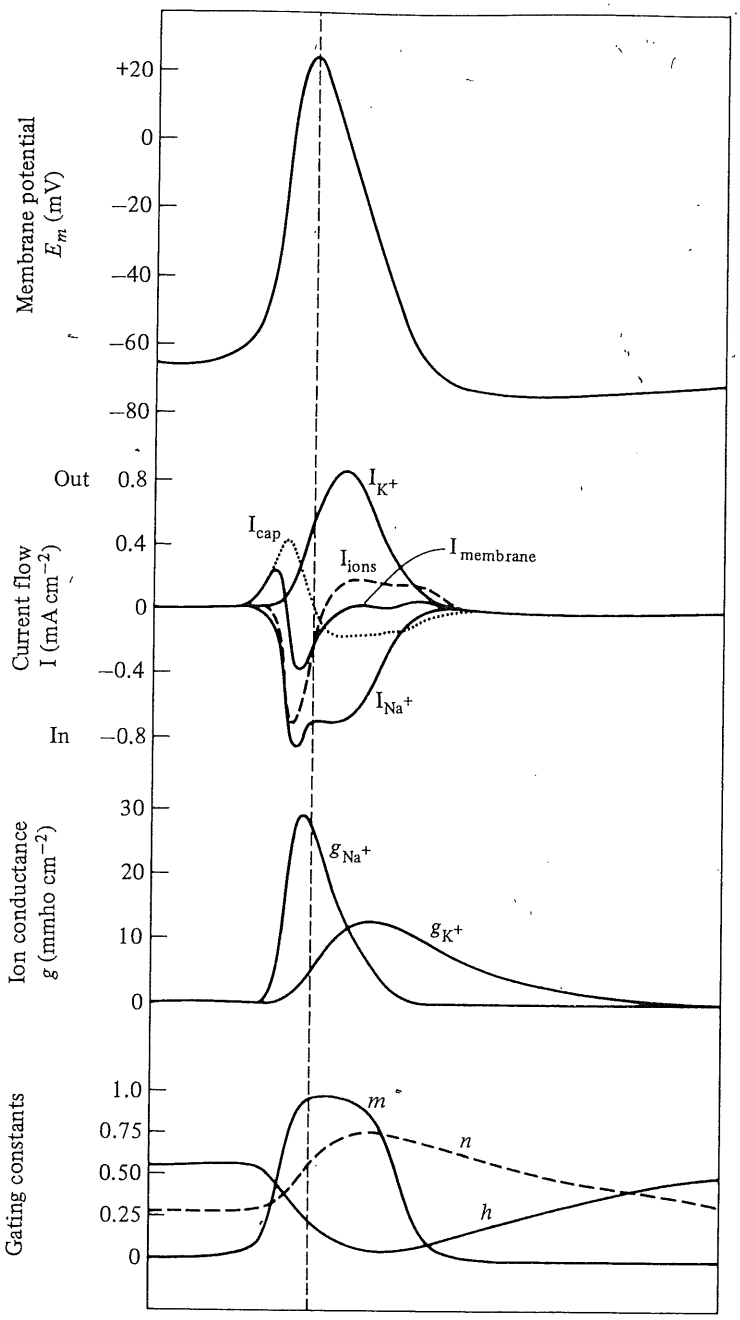

Action potential electrical events.

where $g_{Na,max}$ is the maximum Na^+ conductance and $g_{K,max}$ is the maximal K^+ conductance. The mathematical model enabled Hodgkin and Huxley to calculate g_{Na}, g_K, and E_m over time, from m, h, and n.

The variables m, h, and n can be imagined to be membrane-bound particles that form part of the Na^+ and K^+ channels, and change from closed to open and open to closed in an exponential fashion. If 3 m particles must each open to form a single Na^+ channel, then the transition from closed to open occurs in a sigmoidal (m^3) fashion since all subunits need to open for Na^+ flux; only the single h gate needs to close to prevent Na^+ movement through the Na^+ channel.

A major limitation of this model is that it describes the electrical events during an action potential, but not the mechanisms. Are there really m, h, and n gates in the cell membrane that collectively control the Na^+ and K^+ channels? The details of gating mechanisms for Na^+ and K^+ channels at the molecular level are still poorly understood, but models based on the empirical observations and original assumptions of Hodgkin and Huxley are still useful diagrammatic simplifications that at least enable us to visualize possible mechanisms. (*See Hodgkin and Huxley 1952a; Hodgkin and Huxley 1952b; Benzanilla, Rojas, and Taylor 1970; Aidley 1989; Hille 1984.*)

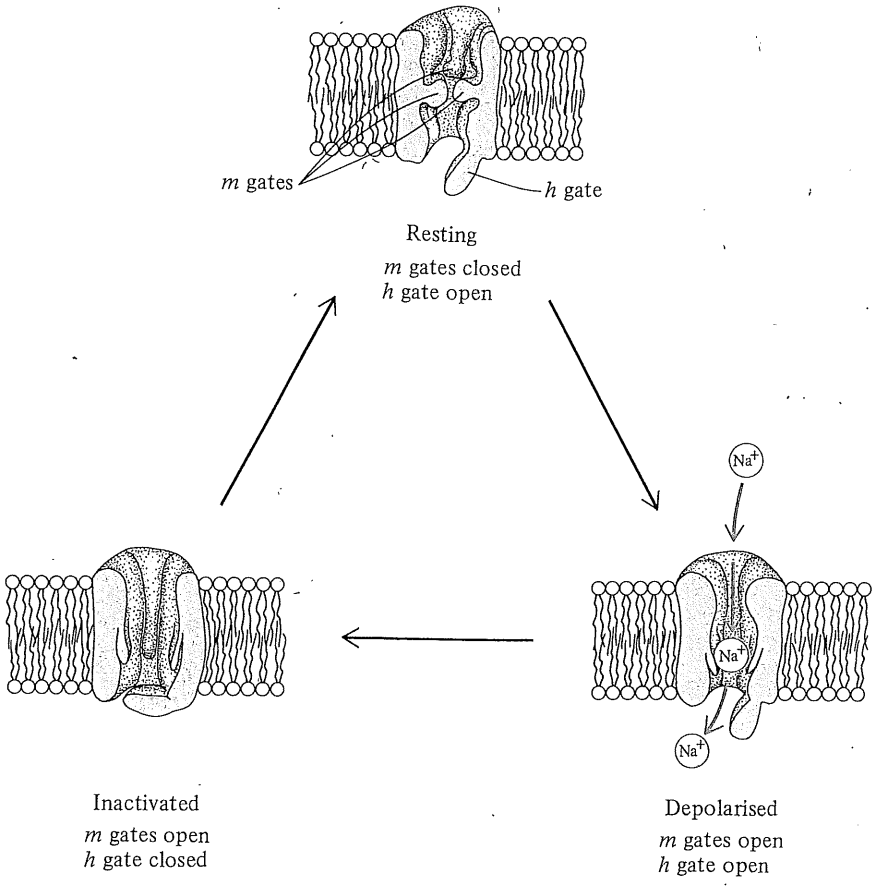

Supplement 6–2

Electrical Synapses

Signal transmission across an electrical synapse is difficult because of the high resistance of the intermembrane space to current flow. The typical action potential amplitude at the presynaptic membrane is about 140 mV (changing from −90 to +50 mV) and the depolarization of the postsynaptic membrane must reach about −70 mV to initiate an action potential. Thus, the 140 mV amplitude of the action potential can be reduced to about 20 mV and still result in propagation of an action potential, i.e., the attenuation can be 20/140 or 14%.

Let us consider electrical transmission across a typical 5μ radius axon with an area-specific membrane resistance (R_m) of 2000 Ω cm², membrane capacitance (C_m) of 1 μF cm^{-2}, and specific cytoplasmic resistance (R_i) of 200 Ω cm. An action potential traveling along this axon would be attenuated by current leakage through the cell membrane and eventually dissipate if there was not a regenerative membrane process. The overall resistance of the axon to current loss, the input impedance (Z), is about 2 10^7 Ω. Impedance is essentially the equivalent in an AC circuit of resistance in a DC circuit; it is a complex function of both the membrane and cytoplasmic resistances, axon radius (μ), and the frequency of the action potential signal (f; about 250 sec^{-1});

$$Z = \sqrt{\frac{R_m R_i}{2\pi^2\mu^2\sqrt{1 + (4\pi^2 f^2 R_m^2 C_m^2)}}}$$

There is little attenuation of the action potential along the axon, but there is extreme attenuation across the axon membrane. If we place a single membrane septum across the axon, then the high impedance will obviously reduce longitudinal spread along the axon, i.e., there will be

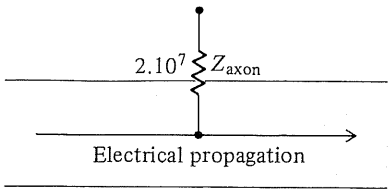

Attenuation = 0

Axon (5μ)

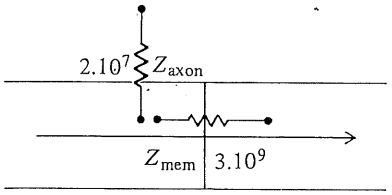

$$\text{Attenuation} = 100\frac{2.10^7}{3.10^9} = 0.7\%$$

Axon + single membrane

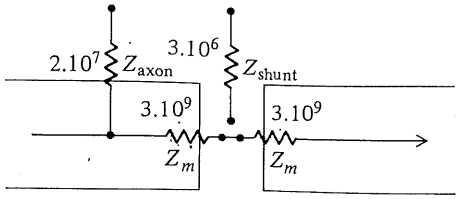

$$\text{Attenuation} = 100\frac{(2.10^7)(3.10^6)}{(3.10^9)(3.10^9)} = 0.0007\%$$

12 μ Extracellular Gap

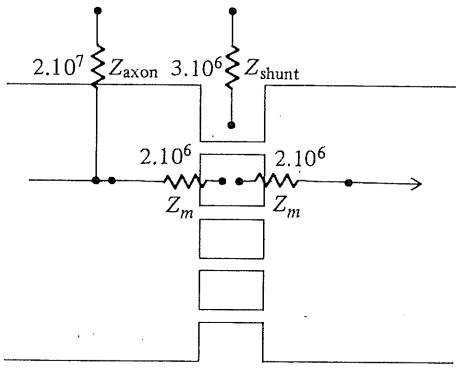

$$\text{Attenuation} = 100\frac{(2.10^7)(3.10^6)}{(2.10^6)(2.10^6)} = 15\%$$

Gap + cross bridges

Extracellular gap and cross-bridge electrical synapses.

greater attenuation. The attenuation can be calculated from the ratio of radial to longitudinal impedance, i.e., attenuation = $(2\ 10^7)/(3\ 10^9) = 0.007 = 0.7\%$. This extent of attenuation would never allow propagation of an action potential across the membrane septum. Electrotonic transmission is made even more difficult by adding a second membrane septum and having a 10 nm gap of extracellular fluid between the two septa, i.e., a realistic electrical synapse. There is now a radial loss of current via the extracellular fluid, which we shall label as a shunt impedance (Z_{shunt}). The overall attenuation at such a synapse reduces the presynaptic depolarization to about 0.0007% at the postsynaptic membrane, which is too small for transmission of an action potential.

An electrical synapse must have a specific anatomical organization and special membrane properties to be able to pass action potentials. Increasing the axon diameter facilitates electrical transmission since Z_m is decreased in proportion to the increase in cross-section area. Increasing the radius from 5 to 150 μ increases the attenuation to 7%, which is closer to the required value of 14%. Thus, giant axons are better able to have electrical synapses. A few electrical cross-bridges between adjacent axons facilitate electrical transmission by decreasing the resistance at the junction. Only about 1 pore per μ^2 (1/10,000 of the cross-section area of the gap) will decrease the membrane resistance to a value (e.g., $2\ 10^6\ \Omega$) such that signal attenuation is greater than 14%. (*See Katz 1966.*)

Supplement 6–3

Quantal Release of Neurotransmitter Vesicles

The quantal nature of neurotransmitter release from the presynaptic terminus of chemical synapses has been demonstrated by a statistical analysis of the amplitudes of miniature end plate potentials (miniEPPs). Not all synaptic vesicles contain exactly the same number of neurotransmitter molecules, and so not all miniEPPs have exactly the same amplitude; rather, there is a normal distribution of miniEPP amplitudes. The amplitude of EPPs elicited by presynaptic neural stimulation of a frog skeletal muscle end plate showed a distribution that was

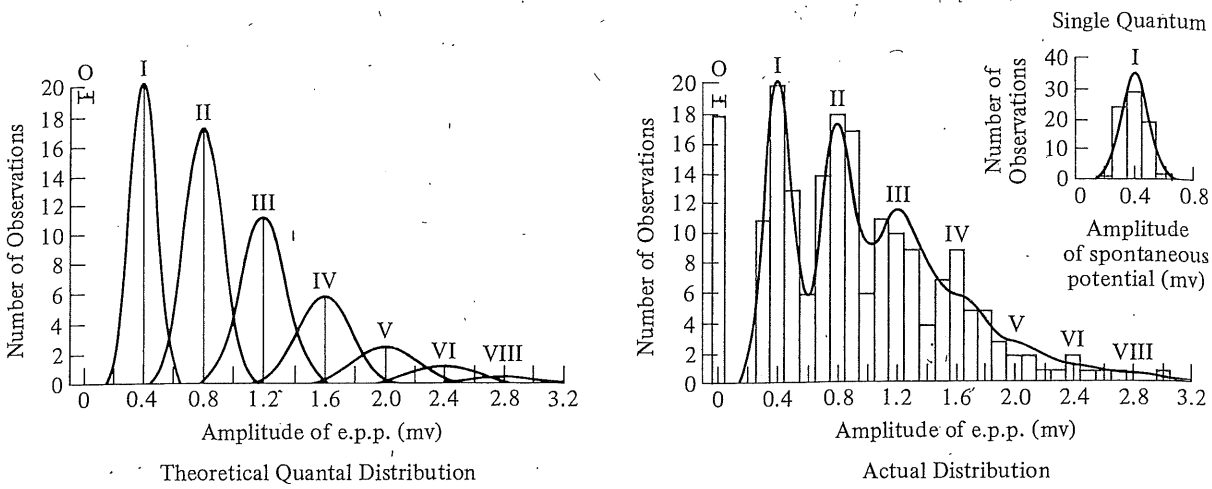

Theoretical and actual quantal distributions. *(From Boyd and Martin 1956.)*

consistent with the predicted distribution based on (1) a normal distribution of miniEPP amplitudes, and (2) by assuming quantal release of neurotransmitter, i.e., 1 vesicle, or 2 vesicles, or 3, etc. In this experiment, the neuromuscular junction was partially blocked by a high external Mg^{2+} concentration to decrease the number of vesicles released per stimulation. In fact, the majority of stimuli did not elicit an EPP equivalent to a normal miniEPP (i.e., were "failures"; $n = 0$). (*See Boyd and Martin 1956; del Castillo and Katz 1954.*)

Recommended Reading

Aidley, D. J. 1989. *The physiology of excitable cells*. Cambridge: Cambridge University Press.

Bennett, M. V. L. 1966. Physiology of electrotonic junctions. *Ann. N. Y. Acad. Sci.* 137:509–39.

Bryant, H. J., and J. E. Blankenship. 1979. Action potentials in single axons: Effects of hyperbaric air and hydrostatic pressure. *J. Appl. Physiol.* 47:561–67.

Cooper, J. R., F. E. Bloom, and R. Roth. 1986. *The biochemistry of neuropharmacology*. New York: Oxford University Press.

Diamond, J. M., and E. M. Wright. 1969. Biological membranes: The physical basis of ion and non-electrolyte selectivity. *Ann. Rev. Physiol.* 31:581–646.

Dorsett, D. A. 1980. Design and function of giant fibre systems. *TINS* 3:205–8.

Finean, J. B., R. Coleman, and R. H. Mitchell. 1978. *Membranes and their cellular functions*. Oxford: Blackwell.

Hall, Z., J. G. Hildebrand, and E. Kravitz. 1974. *The chemistry of synaptic transmission*. Newton: Chiron.

Harper, A. A., et al. 1987. The pressure tolerance of deep sea fish axons: Results of Challenger cruise 6B/85. *Comp. Biochem. Physiol.* 88A:647–53.

Henderson, J. V., and D. L. Gilbert. 1975. Slowing of ionic current in the voltage-clamped squid axon by helium pressure. *Nature* 258:351–52.

Hille, B. 1982. Membrane excitability: Action potential and ionic channels. In *Physics and biophysics*, edited by T. C. Ruch and H. D. Patton, vol. IV, 68–100. Philadelphia: Saunders.

Hille, B. 1984. *Ionic channels of excitable membranes*. Sunderland: Sinauer Assoc.

Hodgkin, A. L. 1958. Ionic movements and electrical activity in giant nerve fibers. *Proc. Royal Soc. Lond. B.* 148:1–37.

Hodgkin, A. L. 1964. *The conduction of the nervous impulse*. Springfield: Thomas.

Hokfelt T., B. Everitt, B. Meister, T. Melander, M. Schalling, O. Johansen, J. M. Lundberg, A-L. Hulting, S. Werner, C. Cuello, H. Hemmings, C. Ouimet, I. Walaas, P. Greengard, and M. Goldstein. 1986. Neurons with multiple messengers with special reference to neuroendocrine systems. *Rec. Prog. Hormone Res.* 42:1–70.

Kandell, E. R., and J. H. Schwartz. 1985. *Principles of neural science*. New York: Elsevier.

Katz, B. 1966. *Nerve, muscle, and synapse*. New York: McGraw-Hill.

Kravitz, E. A., and J. E. Treherne. 1980. *Neurotransmission, neurotransmitters and neuromodulators*. Cambridge: Cambridge University Press.

Lockwood, A. P. M. 1978. *The membranes of animal cells*. London: Edward Arnold.

MacDonald, A. G., and A. R. Cossins. 1985. The theory of homeoviscous adaptation of membranes applied to deep-sea animals. In "Physiological adaptations of marine animals," edited by M. S. Laverack. *Symp. Soc. Exp. Biol.* 39:301–22.

Moore, J. W., and T. Narahashi. 1967. Tetrodotoxin's highly selective blockage of an ionic channel. *Fed. Proc.* 26:1655–63.

Rall, W. 1977. Core conductor theory and cable properties of neurons. In *Nervous system: Handbook of physiology*, edited by J. M. Brookhart and V. B. Mountcastle, sect. 1, vol. 1, pt. 1. Bethesda: Am. Physiol. Soc.

Sha'afi, R. I. 1981. Permeability for water and other polar molecules. In *Membrane transport*, edited by S. L. Bonting and J. J. H. H. M. de Pont, 29–60. Amsterdam: Elsevier/North Holland Biomedical Press.

Singer, S. J., and G. Nicholson. 1972. The fluid mosaic model of the structure of cell membranes. *Science* 175:720–31.

West, I. C. 1983. *The biochemistry of membrane transport*. London: Chapman & Hall.